UNIVERSIDADE D
COIMBRA

Filipe João Abrantes Soares da Conceição

NEW HYBRID MODULATION TECHNIQUES FOR FUTURE GENERATIONS OF COMMUNICATIONS

Dissertação no âmbito do Mestrado Integrado em Engenharia Electrotécnica e de Computadores, ramo de especialização em Telecomunicações orientada pelo Professor Doutor Marco Alexandre Cravo Gomes e pelo Professor Doutor Vitor Manuel Mendes da Silva e apresentada à Faculdade de Ciências e Tecnologia da Universidade de Coimbra no Departamento de Engenharia Electrotécnica e de Computadores.

Julho de 2019

UNIVERSIDADE D
COIMBRA

New Hybrid Modulation Techniques for Future Generations of Communications

Filipe João Abrantes Soares da Conceição

Dissertação para obtenção do Grau de Mestre em
Engenharia Electrotécnica e de Computadores

Orientador: Doutor Marco Alexandre Cravo Gomes
Co-Orientador: Doutor Vitor Manuel Mendes da Silva

Júri

Presidente: Doutora Maria do Carmo Raposo de Medeiros
Co-Orientador: Doutor Vitor Manuel Mendes da Silva
Vogal: Doutora Lúcia Maria dos Reis Albuquerque Martins

Julho de 2019

If at first the idea is not absurd, then there is no hope for it

- Albert Einstein

Agradecimentos

Gostaria de agradecer ao professor Marco Gomes pelo privilégio da sua orientação, pela sua dedicação, motivação, capacidade de trabalho, amizade e pelo seu incentivo para a relização deste projeto.

Ao professor Vitor Silva pela sua experiência, disponibilidade, esforço e apoio na elaboração deste trabalho, assim como pela sua capacidade de resolver problemas.

Ao professor Rui Dinis pelas suas sugestões e pela ajuda prestada durante a realização da presente dissertação.

Ao Instituto de Telecomunicações por todos os meios disponibilizados e pelo ambiente de trabalho descontraído e profissional que se vive.

À FCT/MEC e, quando aplicável, ao Fundo Europeu de Desenvolvimento Regional (FEDER), Programa Operacional Competitividade e Internacionalização (COMPETE 2020) e Programa Operacional Regional de Lisboa e Apoio Financeiro ao Público Nacional (FCT) (OE) por ter financiado em parte este trabalho no âmbito dos projetos UID/EEA/ 50008/2019, MASSIVE5G (POCI-01-0145-FEDER-030588) e PES3N (2018-SAICT-45-2017-POCI-01-0145-FEDER-030629).

Sinto também uma eterna gratidão aos meus pais e ao meu irmão pelo seu esforço, dedicação e pela constante disponibilidade de me acompanharem ao longo deste percurso académico e me ajudarem a atingir os meus objetivos.

A todos os meus amigos e colegas que, de uma forma direta ou indireta, me apoiaram para a elaboração do presente estudo.

A todos,
Muito Obrigado

Abstract

The future generations of mobile communications, known as 5th generation (5G) and post-5G, have ambitious requirements, which include very high data transfer rates, high spectral and power requirements, as well as transmission flexibility under conditions of adverse channels and at variable rates.

The orthogonal frequency division multiplexing (OFDM) technique has been, since the 3rd generation (3G) of wireless communications, the preferred waveform of choice since it presents interesting advantages, such as the easy implementation based on the fast fourier transform (FFT) and its inverse fast fourier transform (IFFT) algorithms, and the fact that efficient equalization in the frequency domain can be performed. In addition, OFDM is a robust technique when transmitting through dispersive channels. However, one of the drawbacks inherent to the use this technique is associated with its limited spectral efficiency, due to the high amplitude of its spectrum outside the allocated bandwidth. In this way, the objective of this work is the study of new hybrid modulation techniques, namely, time interleaved block windowed burst orthogonal frequency division multiplexing (TIBWB-OFDM) that allows increasing spectral and power efficiency, adapted to diverse mobile environments that translate into time dispersive (TD) channels and frequency dispersive (FD) channels. This is considered a hybrid technique since it combines features related to single-carrier (SC) and multi-carrier (MC) transmission. The TIBWB-OFDM waveform enables to achieve greater confinement in the signal spectrum that improves with the increase of the window roll-off since the out of band (OOB) radiation drops. However, the TIBWB-OFDM blocks length grows in time domain, which corresponds to a decrease on the transmission rate, limiting the increase in the spectral efficiency of the system. Furthermore, the windowing operation is responsible for the reduction in the average power of the signal, which, in turn, depends on the value of the window roll-off. As a consequence, the peak-to-average power ratio (PAPR) of the TIBWB-OFDM signal tends to grow as the roll-off increases. Therefore, this work proposes an alternative method concerning the TIBWB-OFDM symbol construction by allowing a partial overlap between ad-

jacent windowed OFDM-based symbols in order to reduce PAPR. Moreover, the new waveform helps to improve the spectral efficiency at the expense of introduced interference between the signal's blocks, that deteriorate the bit error rate (BER) performances, which, in turn, depends on the value of the window roll-off. In order to compensate the loss in BER, this work also proposes different TIBWB-OFDM receivers, iterative and non-iterative ones, with equalization at both frequency and time domains, able to cancel both TD channel constraints and interference between OFDM-based blocks of the TIBWB-OFDM waveform.

Keywords

Time Interleaved Block Windowed Burst OFDM with Windowing Time Overlapping (TIBWB-OFDM with WTO), Spectral Efficiency, Peak-to-Average Power Ratio (PAPR), Frequency Domain Equalization (FDE), Iterative Interference Cancellation - Time Domain Equalization (IIC-TDE)

Resumo

As próximas gerações de comunicações móveis, designada por 5ª geração (5G) e pós-5G, possuem requisitos ambiciosos, nos quais se destacam as muito elevadas taxas de transferência de dados, requisitos de elevada eficiência espetral e de potência e também flexibilidade de transmissão em condições de canais adversas e a taxas variáveis.

A técnica Orthogonal Frequency Division Multiplexing (OFDM) tem vindo a ser a mais utilizada pois apresenta vantagens interessantes, tais como, a fácil implementação baseada nos algoritmos da transformada de Fourier rápida (FFT) e a sua inversa (IFFT), e o facto de permitir uma igualização eficiente e de baixa complexidade no domínio da frequência. Para além disso, o OFDM apresenta-se como uma técnica robusta quando utilizada na transmissão de dados em canais dispersivos. No entanto, uma das desvantagens inerentes ao uso desta técnica está associada à sua eficiência espetral limitada, devido à elevada amplitude do seu espetro fora da banda útil de informação. Deste modo, o objetivo deste trabalho é o estudo de novas técnicas de modulação híbridas, nomeadamente, Time Interleaved Block Windowed Burst OFDM (TIBWB-OFDM) que permite aumentar a eficiência espetral e de potência, adaptadas a diversos ambientes móveis que se traduzem em canais dispersivos no tempo e na frequência. Esta é considerada uma técnica híbrida, pois combina características relativas a transmissão monoportadora e multiportadora. A forma de onda TIBWB-OFDM permite alcançar um maior confinamento no espetro de sinal que melhora com o aumento do *roll-off* da janela, uma vez que a amplitude do sinal fora da banda útil (*out of band* - OOB) diminui. No entanto, o comprimento dos blocos do sinal TIBWB-OFDM cresce temporalmente, correspondendo a uma diminuição da taxa de transmissão, limitando o aumento da eficiência espetral do sistema. Além disso, a operação de multiplicação pela janela é responsável pela redução da potência média do sinal, que, por sua vez, depende do valor do *roll-off* da janela. Como consequência, a relação entre a potência máxima e a potência média (*peak-to-average power ratio* - PAPR) do sinal TIBWB-OFDM tende a crescer à medida que o *roll-off* aumenta. Portanto, este trabalho propõe um

método alternativo relativo à construção do símbolo TIBWB-OFDM, permitindo uma sobreposição parcial entre os símbolos OFDM adjacentes para reduzir o PAPR. Para além disso, a nova forma de onda ajuda a melhorar a eficiência espetral em detrimento da interferência introduzida entre os blocos do sinal, que contribui para a degradação nas performances em termos da taxa de erros (*bit error rate* - BER), que, por sua vez, depende do *roll-off* da janela. Para compensar o aumento na taxa de erros, este trabalho também propõe diferentes recetores, iterativos e não-iterativos, da técnica TIBWB-OFDM, com igualização em ambos os domínios da frequência e tempo, capazes de cancelar tanto as restrições dos canais dispersivos no tempo e a interferência resultante entre os blocos baseados em OFDM da forma de onda TIBWB-OFDM.

Palavras Chave

Time Interleaved Block Windowed Burst OFDM with windowing time overlapping (TIBWB-OFDM with WTO), Eficiência Espetral, *Peak-to-Average-Power-Ratio* (PAPR), Igualização no Domínio da Frequência (FDE), Cancelamento Iterativo de Interferência - Igualização no Domínio do Tempo (IIC-TDE)

Contents

List of Figures

List of Acronyms

OFDM orthogonal frequency division multiplexing

BWB-OFDM block windowed burst orthogonal frequency division multiplexing

TIBWB-OFDM time interleaved block windowed burst orthogonal frequency division multiplexing

WTO windowing time overlapping

SEFDM spectrally efficient frequency division multiplexing

FBMC filter-bank multi-carrier

GFDM generalized frequency division multiplexing

RF radio frequency

LTE long term evolution

ISI inter-symbol interference

IBI inter-block interference

ICI inter-carrier interference

FFT fast fourier transform

IFFT inverse fast fourier transform

DFT discrete fourier transform

DTFT discrete time fourier transform

IDFT inverse discrete fourier transform

OOB out of band

CP cyclic prefix

FDE frequency domain equalization

PAPR peak-to-average power ratio

CCDF complementary cumulative distribution function

PSD power spectral density

SRRC square root raised cosine

RRC root raised cosine

ZP zero-pad

SC single-carrier

MC multi-carrier

S/P serial to parallel

P/S parallel to serial

MMSE minimum mean square error

ZF zero-forcing

PR perfect reconstruction

IB-DFE iterative block decision feedback equalization

IIC-TDE iterative interference cancellation time domain equalizer

LOS line of sight

FF feedforward

FB feedback

LLR log-likelihood ratio

MFB match filter bound

QPSK quadrature phase shift keying

AWGN additive white gaussian noise

LDPC low-density parity-check

BER bit error rate

TD time dispersive

FD frequency dispersive

SNR signal-to-noise ratio

OTFS orthogonal time frequency space

3GPP 3rd Generation Partnership Project

SISO single input single output

MIMO multiple input multiple output

MRC maximum ratio combining

EGC equal gain combining

CFO carrier frequency offset

USRP universal software radio peripheral

1

Introduction

Contents

The next generations of mobile communications, known as 5-th generation (5G) and post-5G [3, 4], have ambitious requirements [5–7], which highlight very high data transfer rates (up to 20 Gbit/s), high spectral and power efficiencies and flexibility brought by the need to efficiently transmit under adverse channel conditions and at varying rates. In order to support transmission of data in several scenarios, with different service qualities, delay requirements and different carrier frequencies, a new radio interface is being developed by 3rd Generation Partnership Project (3GPP) [8], in the scope of the 5G. The choice of the waveform for 5G New Radio culminated in the adoption of orthogonal frequency division multiplexing (OFDM) with the addition of cyclic prefix (CP) for the downlink and uplink transmissions, leaving open the possibility of using new waveform modulation types, as usually designated in the context of 5G. This brings the need for the development of new hybrid modulation techniques, as an alternative to OFDM, used in 4G, such as the recently proposed techniques, block windowed burst orthogonal frequency division multiplexing (BWB-OFDM), time interleaved block windowed burst orthogonal frequency division multiplexing (TIBWB-OFDM) [1, 9] and orthogonal time frequency space (OTFS) [10].

The Time Interleaved Block Windowed Burst Orthogonal Frequency Division Multiplexing (TIBWB-OFDM) has been disclosed as an OFDM-based technique able to offer an improved spectral confinement of the transmitted blocks, or, instead, higher transmission rates than conventional OFDM, along with better power efficiency. Also, it has the great advantage of being easily applied to multiple input multiple output (MIMO) and massive MIMO systems [6, 11]. On its basis, the TIBWB-OFDM technique consists into packing together several OFDM windowed blocks appended to single zero-pad (ZP) prefix, to deal with the duration of the impulse response of the mobile channel. The windowing operation allows better spectrum confinement and, consequently, increase the spectral efficiency. Furthermore, the use of a single ZP by a set of OFDM blocks allows a significant improvement in power efficiency when compared to conventional OFDM using a CP. Finally, the temporal interleaving operation creates a diversity effect in the spectrum that makes this modulation more robust and reliable when transmitting data through frequency selective channels (typical of multipath wireless channels). This technique is considered a hybrid technique, since it combines features associated to single-carrier (SC) and multi-carrier (MC) transmission systems, keeping in mind that, on the one hand, it can be considered a block-based single carrier technique with frequency domain equalization (FDE) on the receiver side and, on the other hand, it can be considered a simple MC OFDM system with a ZP on the transmission side.

Throughout this chapter, the motivations, the objectives and the contributions of this work will be introduced as well as the organization of the document.

1.1 Motivation

Future wireless communications systems are expected to bring improvements in the way data are transmitted and the waveforms are designed. Such improvements are related to higher data rate, lower latency, and flexibility brought by the need to transmit over hostile channel conditions, as well as higher spectral and power efficiency [12].

Orthogonal Frequency Division Multiplexing (OFDM) [13] has been, since the 3rd generation (3G) of wireless communications, the preferred waveform of choice, due to its robustness to inter-symbol interference (ISI) associated with multipath channels. OFDM is a MC technique that divides a high data rate stream into N parallel lower rate streams that, in turn, modulate N sub-carriers. OFDM presents other interesting advantages that make it so popular, such as the fact that the process of OFDM modulation and demodulation can be efficiently implemented by the inverse fast fourier transform (IFFT) operation and its inverse fast fourier transform (FFT), respectively. Besides, the orthogonality between sub-carriers is one of the main features of OFDM making it relatively robust to inter-carrier interference (ICI) and allowing a simple frequency domain equalization (FDE) [1]. The portion of the spectrum occupied by each stream is usually less than the coherence bandwidth of the frequency selective channel (also known as a time dispersive (TD) channel). This channel bandwidth represents frequency range where its response is approximately flat. Therefore, the ISI in each stream is neglected. In order to eliminate interference between the N symbol streams, it is necessary to add a cyclic prefix (CP) to each OFDM symbol, which must be longer than the duration of the impulse response of the transmission channel. The CP duration often represents 10% to 25% of the OFDM symbol period, and therefore the effective throughput of useful data and the spectral efficiency of CP-OFDM systems are reduced [1,9]. In fact, in order for a CP-OFDM system to achieve the same transmission rate of an OFDM system (without CP) the transmission rate of the useful data must be increased, which in turn increases the amount of spectrum used. Also, since the CP consists on an exact copy of final $N_g = N_{cp}$ samples of the current symbol, the power used to transmit the CP limits considerably the power efficiency of OFDM transceivers [9].

Besides the restricted spectral efficiency, time domain transmitted signals in an OFDM system can have high peak values since the instantaneous amplitude of each sub-carrier that form the OFDM symbol is added by the IFFT operation. As a

consequence, OFDM systems are known to have a high peak-to-average power ratio (PAPR) when compared to SC systems, which grows with an increasing number of sub-carriers. Thus, an OFDM system has a limited power efficiency and requires the use of a power amplifier with a considerable back-off to ensure a distortion-free linear signal amplification [9, 11].

This brought the need for the development of new techniques as alternatives to OFDM, with greater spectral and power efficiency. Recently, within the context of 5G, new waveforms alternative to conventional CP-OFDM have been the subject of many recent studies [6, 7], with several techniques being proposed as: filter-bank multi-carrier (FBMC) [14]; generalized frequency division multiplexing (GFDM) [15]; filtered-OFDM [16]; the non-orthogonal MC system termed spectrally efficient frequency division multiplexing (SEFDM) [17], which improves spectral efficiency by packing sub-carriers at frequency spacing below the symbol rate, intentionally creating inter-carrier interference (ICI); and more recently the Time-Interleaved Block Windowed Burst Orthogonal Frequency Division Multiplexing (TIBWB-OFDM) technique [9].

1.2 Objectives

Some of the solutions being proposed have drawbacks, such as the difficulty of extending FBMC to MIMO considered as a key enabling technology for 5G. The TIBWB-OFDM is already showed to be easily extendable to MIMO scenarios [11, 18].

Although the TIBWB-OFDM already tackles some of the disadvantages inherent to the use of the OFDM, this technique also presents several interesting challenges: the promised spectral and power efficiency increase proposed by the method is limited by the growth of the windowed OFDM-based blocks and also due to their juxtaposition. The initial OFDM-based sub-blocks, that form the TIBWB-OFDM mega-block are submitted to several operations, such as the cyclic extension and windowing with a square root raised cosine (SRRC) profile, followed by a time interleaving operation between the samples of the several OFDM component blocks that results in an increased sub-block's length. Since the blocks are juxtaposed this results in an increased mega-block length, which is proportional to the window roll-off. Consequently, the achieved spectral efficiency of this modulation technique is limited, by either, improving spectral confinement by reducing out of band (OOB) radiation when using a larger roll-off, or by improving symbol rate when conventional rectangular window is used since a sole ZP prefix is used per the group of packed OFDM-based blocks. Although the spectral confinement of the OFDM-

based blocks improves with the increase of the window roll-off, the block temporal extension is also verified which results in a temporal growth of the TIBWB-OFDM mega-block, corresponding to a reduction of the transmission rate. To keep transmission rate, in fact, the spectral occupancy must increase, thus limiting the spectral efficiency gains of the technique. Furthermore, conclusions drawn from this work are that the windowing operation is responsible for the decrease in the average power of the signal, which, in turn, depends on the value used for the roll-off. As a consequence, PAPR of the TIBWB-OFDM signal tends to grow as the roll-off increases.

Thus, this work proposes an alternative approach regarding the TIBWB-OFDM symbol construction by allowing a partial overlap between the adjacent windowed OFDM symbols, in time domain to keep transmission rate and spectrum occupancy. This new waveform would allow achieving a very high spectral efficiency since there is no temporal expansion of the TIBWB-OFDM block, permitting a spectrum saving when transmitting at a fixed rate. Furthermore, the overlapping operation creates a flatter waveform, diminishing the windowing attenuation effect and opposing the decrease in the average signal power and consequently decreasing the signal's PAPR. However, the overlapping operation introduces interference between the data transmitted in adjacent sub-blocks. Thus, time domain equalization algorithm must be developed acting as signal reconstruction methods. A forward and backward successive cancellation equalization method is proposed aiming to override the self-created interference resulting from this process, based on a sequential process. In this process, the data sent in the first symbol allows to partially recover the information that has been corrupted (superimposed) by the next symbol. In addition, the data sent in the last symbol allows partial retrieval of data that has been corrupted by the previous symbol. Furthermore, to improve robustness against TD channels time-interleaving of samples of the packed and TIBWB-OFDM with windowing time overlapping (WTO) based blocks is employed. Different embodiments of non-iterative and iterative receivers to cancel both channel impairments (at frequency domain) and interference resulting from the overlapping operation (at time domain) are proposed.

1.3 Dissertation Outline

This thesis is organized in five chapters. This chapter introduces the topic of the thesis, the motives that led to investigate and enhance the knowledge in this particular theme and describes the main goals proposed to achieve with this work. Chapter 2 introduces the concept and model of a typical wireless channel and also discusses

the differences between SC and MC transmission schemes, explaining why the MC approach is more efficient when transmitting through TD channels. This chapter also presents the concept of OFDM, discussing its advantages in regard to its efficient implementation and robustness in wireless transmission and its disadvantages, relative to the limited power and spectral efficiencies. By opposition as presenting a smaller PAPR and similar performance, block-based SC transmission with FDE (SC-FDE) is presented. Also, OFDM and block-based SC-FDE are both addressed, since TIBWB-OFDM can be seen as a hybrid technique, handled at transmitter as OFDM-based MC type, and at receiver as of SC type. This chapter also presents the concepts of the most common linear FDE algorithms. Chapter 3 presents the theory of the TIBWB-OFDM modulation technique, stressing the improvements towards typical CP-OFDM schemes. In this chapter, the chain of operations concerning the block formatting and unformatting are analyzed in the transmitter and receiver, respectively. Later, in the same chapter, the basic structure of a non-linear FDE algorithm, known as, iterative block decision feedback equalization (IB-DFE) is introduced, motivated by the fact that in the TIBWB-OFDM transceiver scheme, the received signal can be regarded as of a SC-FDE type, prompting the employment of this technique with the IB-DFE. In chapter 4, the new TIBWB-OFDM with WTO transceiver scheme is presented, leading to the proposal of an overlapping operation between the BWB-OFDM adjacent sub-blocks, in the transmitter, in order to compensate the temporal growth in the block's length and the degradation in the signal's PAPR, observed in the standard TIBWB-OFDM transmission scheme. In this chapter, the time domain equalization algorithms that try to cancel the interference, introduced by the overlapping operation, are also described in the receiver section. The PAPR issue is discussed for the new waveform and the performance of the new TIBWB-OFDM with WTO scheme is compared to the TIBWB-OFDM scheme while employing the minimum mean square error (MMSE) FDE and the Turbo-IB-DFE. Additionally, the performance of the new transmission scheme is also compared while employing the two versions (non-iterative and iterative) of the proposed time domain equalizers. This chapter ends with a review regarding the gain in spectral efficiency that can be achieved with this transmission scheme. Finally, chapter 5 concludes this thesis and presents some suggestions for future work.

1.4 Contributions and Publications

The research presented in this thesis was part of an ongoing research project whose objectives are to propose highly efficient waveform to 5G and beyond 5G, within which the TIBWB-OFDM technique was developed. One of the main con-

tributions of this work was the proposal of a new packing strategy for the TIBWB-OFDM technique that avoids the temporal expansion of OFDM-based blocks and the high PAPR typically observed in this transmission scheme due to the windowing operation. Aside this, efficient receivers have also been proposed.

In the context of this dissertation, some of the results have been published counting 1 Provisional Patent Application, 2 accepted publications at national conferences, and one international submission to the IEEE flagship conference GLOBECOM2019 (awaiting for decision). The list follows:

- Concerning the implementation and integration of the TIBWB-OFDM modulation technique within the long term evolution (LTE) resource grid structure a presentation [P1] was published at *26th RTCM Seminar*.

- In the conventional TIBWB-OFDM technique the PAPR reduction achieved by the single use of a ZP for multiple OFDM-based packed blocks, is rather limited, especially when higher root raised cosine (RRC) window roll-off are used to guarantee spectral efficiency. At *11th Conference on Telecommunications - ConfTele 2019* a paper [P2] was published proposing a new waveform that consists on a modification of the TIBWB-OFDM transmission technique by allowing a time domain overlap between the OFDM-based sub-blocks, improving both spectral and power efficiencies and keeping transmission rate and spectrum occupancy. In addition, in order to improve robustness against TD channels time-interleaving of samples of the packed and overlapped-OFDM-based blocks is employed. Although a PAPR reduction is achieved by the single use of a ZP for multiple OFDM-based packed blocks, the overall reduction achieved is limited. Therefore, this publication demonstrates that the PAPR values of TIBWB-OFDM with WTO can be contained due to the overlapping operation.

- The spectral efficiency of the new TIBWB-OFDM technique is improved at the expense of bit error rate (BER) performance since the time overlapping operation introduces interference in the transmitted signal. In order to improve the BER performance of the TIBWB-OFDM with WTO transmission scheme, a paper [P3] was submitted (awaiting for decision) at conference *WS-06: IEEE GLOBECOM 2019 Workshop on High Capacity Point-to-Point Wireless Communications (HCPtP 2019)* proposing the new packing strategy and a different TIBWB-OFDM receiver embodiment, consisting on non-iterative equalizers to cancel both channel impairments, at frequency domain, and interference resulting from the overlapping operation, at time domain.

- The BER performance improvement in behalf of the new non-iterative time domain equalization algorithms is limited. Therefore, along with the new window overlapping and time-interleaving transmission method, several embodiments of the TIBWB-OFDM with WTO receiver consisting, not only on non-iterative, but also on iterative equalizers at both time and frequency domains are considered at [P4].

Subsequently, a list of the submissions and publication resulting from the research process in the scope of the thesis is presented:

[P1] F. Conceição, M. Gomes, V. Silva, "Testbed implementation of TIBWB-OFDM within LTE frame structure", published at *26th RTCM Seminar* on January 24, 2019 (APPENDIX I),

[P2] F. Conceição, M. Gomes, V. Silva, R. Dinis, "Time Overlapping TIBWB-OFDM Symbols for Peak-To-Average Power Ratio Reduction", published at *11th Conference on Telecommunications - ConfTele 2019* on June 27, 2019 (APPENDIX II),

[P3] F. Conceição, M. Gomes, V. Silva, R. Dinis, "Highly efficient TIBWB-OFDM waveform for broadband wireless communications", submitted on *WS-06: IEEE GLOBECOM 2019 Workshop on High Capacity Point-to-Point Wireless Communications (HCPtP 2019)* (awaiting decision),

[P4] M. Gomes, V. Silva, F. Conceição, R. Dinis, Block Windowed Burst Orthogonal Frequency Division Multiplexing Transmission Method with Window Overlapping and Time-Interleaving, (PPP115602), June, 2019, (status pending).

2

Wireless Transmission and Single/Multi-Carrier Modulation Techniques

Contents

This chapter introduces the theoretical concepts regarding wireless transmission and the techniques that are used to modulate the data.

2.1 Wireless Channel

Wireless communication systems offer many advantages, such as mobility and easy access, however they are more limited than the wireline transmission systems, such as limited spectrum, capacity and service quality which affect the quality of received signals and the reliability of wireless systems.

In wireless mobile communications systems, the wireless radio channels are dynamic and time-varying, leading to the need of constant analysis and estimation of these channels, due to channel variations and user movement [19]. Besides, there is usually no direct line of sight (LOS) path between the mobile terminals and the base station. Thus, the electromagnetic waves that carry the information radio frequency (RF) signal over the air in RF bands encounter several obstacles, suffering phenomena of temporal dispersion, diffusion/scattering and multiple reflections [20]. This leads to path loss, shadowing and multipath fading.

The path loss or attenuation of a RF signal, in an obstruction-free , i.e. LOS, between the transmitter and receiver, is proportional to

$$P_r(d) \propto \left(\frac{\lambda}{4\pi d}\right)^2, \tag{2.1}$$

where $P_r(d)$ is the receiver signal power at a distance d from the transmitter and λ is the wavelength of the carrier signal. The path loss is a large-scale channel attenuation effect that represents the degree of signal power attenuation suffered from radio signals, propagating through free space, which increases at a rate that is inversely proportion to the square distance between the transmitter and the receiver [19]. A log-distance path loss can be modeled as

$$L = 10n\log_{10}\left(\frac{d}{d_{ref}}\right) + L_{ref}, \tag{2.2}$$

where n is the path loss exponent, that depends on the degree of obstruction and L_{ref} is the path loss value in free space for the reference distance d_{ref}.

In order to account with attenuation originating from obstacles and surrounding environments, measurements show that the actual signal loss at distance d is a random variable with log-normal distribution [19]. Therefore, shadowing describes the random and faster distance-based attenuation effects of the signal and is included on the path loss model. The total loss can be described as

$$L = 10n\log_{10}\left(\frac{d}{d_{ref}}\right) + L_{ref} + X, \tag{2.3}$$

where X is a normal-distributed random variable that represents the shadowing effect.

In addition to path loss and shadowing, which are large-scaled attenuation effects, there is also rapid channel fluctuations within a small region [19]. The transmitted signal travels through several paths during its transmission, reaching the receiver through these different paths with varied length. Hence, in a multipath channel, the arrival times of the different signal echos are, thus, spread in time and, thus, the baseband complex impulse response of a time-varying channel can be written as

$$h(\tau,t) = \sum_{r=1}^{R} \beta_r(t)\, e^{j\theta_r(t)}\, \delta(\tau - \tau_r), \tag{2.4}$$

where r is the path index from a total of R paths, $\beta_r(t)$ is the path gain, $\theta_r(t)$ is the phase shift, τ_r is the time delay of the r-th path and δ denotes the Dirac delta function.

This causes an effect called multipath fading. The several copies of the waves that carry the transmitted signal arrive at the receiver with random amplitudes, frequencies and phases and can be combined constructively and destructively, interfering with one another and causing the total received signal power to vary within a small region. The multipath fading can be modeled through the amplitude of the complex baseband channel, which has independent Gaussian-distributed real and imaginary parts with zero mean and equal variance, being Rayleigh-distributed in most cases, except when a stronger and dominant path (usually the LOS path) exists between the transmitter and the receiver, where it becomes Rician-distributed [19].

Thus, the scientific community has been developing transmission and modulation techniques that combat the effects suffered by the signals transmitted in wireless communication systems.

2.2 Single-carrier modulation techniques

In conventional SC modulation techniques, the transmission of a signal with symbol rate R_s requires the use of a bandwidth of at least $B = \frac{R_s}{2}$. Thus, when transmitting at high rates, the bandwidth occupied by the signal is also large. A wireless channel is regularly a frequency selective channel and has a coherence bandwidth, B_c. This bandwidth represents the frequency range where the frequency response of the channel is approximately flat. Therefore, high rate transmission scenarios through TD channels can be dangerous, especially when the coherence bandwidth of the channel, B_c, is much lower than B. In this case, the transmission of wire-

less signals usually suffers from frequency selective fading, i.e., different frequency components are faded differently by the channel, as opposed to flat-fading where all frequency components of the signal are equally faded by the channel. Therefore, the SC systems require complex equalization schemes to deal with ISI.

2.3 Multi-carrier modulation techniques

In order to deal with frequency selective fading parallel data transmission, also known as MC transmission, was proposed. In MC systems, a high rate stream of data is divided into N lower rates streams where independent data are modulated on different sub-channel, multiplexed in the frequency domain. The overall symbol rate remains the same as in the SC case, since, in this case, each parallel data stream has a symbol rate of R_s/N and, therefore, the overall symbol rate remains R_s.

However, due to the low rate streams, each sub-channel now occupies B/N, allowing only a small number of sub-channels to use the carriers that are affected by a deep fade [19]. Additionally, if the bandwidth occupied by each sub-channel is smaller than B_c each sub-carrier experiences frequency flat-fading. Nevertheless, a guard band is required between each adjacent sub-channel to eliminate any ICI.

2.4 Orthogonal Frequency Division Multiplexing

One of the most popular MC modulation methods is the OFDM technique. This section discusses its advantages and disadvantages.

2.4.1 Advantages of OFDM

The transmission technique that has been most used for wireless communications is OFDM, which can be described as multiplexing technique and a special case of MC transmission, forming the basis for 4G LTE wireless communication systems [21]. It was also chosen by 3GPP as the based modulation technique adopted by 5G New Radio [8], although space was left open for the introduction of new waveforms.

Frequency Selective Fading ISI and ICI immunity

An OFDM signal consists of N adjacent and orthogonal carriers spaced, at frequency domain, by $\Delta_f = \frac{1}{T_{sym}}$, where T_{sym} represents the duration of an OFDM symbol or OFDM signal. Following the same rule employed in MC transceivers, in an OFDM transmitter a high rate stream of data is divided into N lower rates streams through a serial to parallel (S/P) operation that are assigned to each of those carrier, creating an OFDM symbol. These values are put back into serial stream

with a parallel to serial (P/S) operation. The data rate per sub-carrier is reduced by a factor of N, which increases the sub-symbol time by N. Thus, if the symbol period is T_s for the source stream, the total period for the OFDM symbol/block is $T_{sym} = NT_s$. This reduces the effect of ISI because the symbols are substantially longer. [22].

Therefore, the principle of OFDM is to divide the transmission channel's bandwidth into narrowband sub-channels, associated with the orthogonal sub-carriers, transforming a broadband frequency selective channel into multiple narrowband flat-fading sub-channels, allowing one to consider a constant attenuation of each sub-channel, over its entire bandwidth. In other words, the number of carriers employed in an OFDM system should be adjusted in order to the bandwidth of each sub-channel is affected by flat-fading. This allows simplification in the equalization process at frequency domain (FDE) with only one equalization iteration per sub-carrier, in the receiver.

Each of the sub-carriers is individually modulated and simultaneously transmits data in an overlapping and parallel scheme, allowing a considerable gain in spectral efficiency, saving up to 50% of the used spectrum [19]. The overlapping approach cause interference between adjacent sub-channels. This interference is, however, *transparent* among sub-carriers, due to the fact that they are spectrally spaced from $\Delta_f = \frac{1}{T_{sym}}$. This orthogonality property shows that the power spectral density (PSD) peaks of each sub-carrier occur at a point at which the PSD of other sub-carriers is zero [22]. Since an OFDM receiver calculates the maximum spectrum values at those points, it can demodulate any individual sub-carrier free from interference from other sub-carriers [13]. Hence, OFDM is relatively robust to ICI. Additionally, since the information data are carried by orthogonal carriers, it can be retrieved by coherent detection, projecting the received signal onto the signal space, i.e. the sub-carriers, during its interval [23].

In order to avoid ISI between OFDM symbols, associated with multipath fading, this technique adds, also, to each OFDM symbol a cyclic extension of the symbol itself, called a CP, in which its duration is required to be greater than the impulse response of the TD transmission channel, which, in turn, is related to the delay spread. This allows transforming the linear convolution that occurs in the transmission channel, in a cyclic convolution at the level of the individual processing of each OFDM symbol. The total delay spread is typically defined as the difference between the arrival time of the earliest multipath component (typically the LOS component) and the arrival time of the latest multipath components and has a significant impact on the ISI. This ISI deteriorates the transmission at higher rates

because the distance between symbols (or bits) is smaller and the expansion of time due to multipath interferes with subsequent symbols (or bits) [22]. If the symbol duration is much larger than the delay spread, the ISI become irrelevant.

FFT/IFFT implementation

OFDM presents other interesting advantages, such as, the easy implementation of the transmitters based on IFFT algorithm and the receivers based on its inverse transform, i.e. the (FFT) algorithm, allowing an efficient and low complexity equalization in the frequency domain.

Conventionally, a MC transmitter consists on a set of modulators that modulate the data in a specific set of carriers. The modulator outputs are, then, combined into one signal [24]. The baseband complex-valued transmitted signal is given by

$$s(t) = \sum_{k=0}^{N-1} S_k e^{j2\pi f_k t}, 0 \leq t \leq T_{sym}, \tag{2.5}$$

where $S_k, k = 0, \ldots, N-1$ denotes the N-size vector of data to be transmitted. Each $S_k, k = 0, \ldots, N-1$ represents a symbol from an M-ary signal constellation (MQAM, MPSK,...), directly mapped from a bit-stream, to be transmitted at the k-th sub-carrier with frequency $f_k = k\Delta_f, k = 0, \ldots, N-1$. Usually there is one additional modulation step to translate the set of sub-carriers to a higher center frequency [22].

The orthogonality property between the sub-carriers allows the receiver to demodulate the OFDM signal in a simple way. In order to demodulate the data carried by a sub-carrier j, the received signal is mixed with a local oscillator with the same frequency f_j and integrated over the duration of the signal, T_{sym}. The operation expressed by (2.6) gives the desired output $S_k, k = 0, \ldots, N-1$, after dividing by T_{sym}. For all the other sub-carriers, the integral output is zero because the frequency difference with $k \neq j$, produces an integer number of cycles within the integration interval, which results in zero [13].

$$\begin{aligned} \int_0^{T_{sym}} s(t) e^{-j2\pi f_j t} dt &= \int_0^{T_{sym}} \sum_{k=0}^{N-1} S_k e^{j2\pi f_k t} e^{-j2\pi f_j t} dt = \\ &= \sum_{k=0}^{N-1} S_k \int_0^{T_{sym}} e^{j2\pi (f_k - f_j) t} dt = S_k T_{sym}. \end{aligned} \tag{2.6}$$

Nevertheless, such approach of generating and detecting the transmitted MC signal would result in a very expensive transmitter and receiver because it would have a high number of oscillators [13]. Furthermore, this approach would require very

accurate modulators and demodulators since any deviation on the carrier's frequencies would result in an incorrect signal detection. Therefore, in order to correctly demodulate an OFDM signal, time and frequency synchronization is necessary, as illustrated by (2.5) and (2.6). If not met, ICI will result [13].

The discrete version of an OFDM symbol is generated by sampling (2.5). By letting $t = nT_{smp}$, where T_{smp} is the sample interval and considering that the subcarriers are uniformly spaced in the frequency domain by $\Delta_f = \frac{1}{T_{sym}} = \frac{1}{NT_s} = \frac{1}{NT_{smp}}$, i.e., $f_k = k\Delta_f, k = 0, \ldots, N-1$, the digital OFDM signal in transmitter output is

$$s_n = s[n] = s(nT_{smp}) = \sum_{k=0}^{N-1} S_k e^{j2\pi f_k nT_{smp}} = \sum_{k=0}^{N-1} S_k e^{\frac{j2\pi nk}{N}}, n = 0, ..., N-1. \quad (2.7)$$

The complex baseband OFDM symbol, denoted by (2.7), can be defined by a formula that consists on an N-point inverse discrete fourier transform (IDFT), except for the multiplying constant $\frac{1}{N}$. Therefore, the OFDM transmitter can be implemented by this transform, which, in turn, can be efficiently implemented by the IFFT when N is a power of two, providing a reduction on the number of complex multiplications from N^2 to $\frac{N}{2}\log_2(N)$ [13].

In similar fashion, the demodulation of the digital OFDM received signal, at the receiver, preceding the integration operation can be expressed by

$$x_n = x[n] = x(nT_{smp}) = \sum_{k=0}^{N-1} S_k e^{-\frac{j2\pi nk}{N}}. \quad (2.8)$$

Therefore, the OFDM receiver can be implemented by the discrete fourier transform (DFT) transform, which can be efficiently implemented by the FFT algorithm.

2.4.2 Disadvantages of OFDM

Although OFDM is a mature technique, it has limited spectral and power efficiency. This section provides a discussion on its disadvantages.

Cyclic-prefix/Guard interval needed

Due to the different time delays on reception, ISI may occur between two consecutive OFDM symbols where the last part of a symbol adds with the first part of the next symbol. Therefore, to completely eliminate ISI a guard interval of T_g (N_g samples) is inserted at the beginning of each OFDM symbol. The length of the guard must be greater than the delay spread of the wireless channel [22]. This guard interval can be formed of null samples (also known as a ZP), which lower the power needed for transmission at the expense of introduced ICI [25]. Nonetheless, the preferred guard interval is a cyclic extension (also known as CP) of the current

OFDM symbol since this still enables the implementation of a simple receiver based on the FFT. A CP consists on an exact copy of final $N_g = N_{cp}$ samples of the current symbol.

Hence, a CP-OFDM signal has a total length of $N_{CP-OFDM} = N_{cp} + N$ and can be expressed based on (2.7) by

$$s_{CP-OFDM}[n] = \begin{cases} s[n-N+N_{cp}], & 0 \leq n \leq N_{cp} \\ s[n], & N_{cp} < n < N+N_{cp} \end{cases} . \tag{2.9}$$

Although the use of a CP per OFDM symbol eliminates ISI, it also reduces the effective throughput of the CP-OFDM system as well as its spectral efficiency, since the duration of the CP often represents a considerable percentage of the period of the symbol (which can reach up to 10%- 25%) [1,5,9]. Another aspect is related to the power wasted to transmit the CP, which reduces the power efficiency of OFDM transceivers.

Spectrum

An OFDM symbol with a rectangular configuration, $s[n], n = 0, \ldots, N-1$, can be expressed by

$$s[n] = \sum_{k=0}^{N-1} S_k w[n] e^{\frac{j2\pi kn}{N}}, \tag{2.10}$$

where S_k represents a symbol from an M-ary constellation and $w[n], n = 0, \ldots, N-1$ is a unitary rectangular window that limits the length of the modulated signal.

The high amplitude of OFDM's spectrum outside the allocated bandwidth is created by the sharp transitions of the rectangular pulse/window used in the signal generation, whose spectrum is a *sinc*. This way, the PSD of OFDM signal is made of a superposition sum of *sinc* shaped spectra, each one associated to a sub-carrier and centered in the corresponding frequency, f_k.

These lateral lobes, of considerable amplitude add together giving rise to considerable OOB emissions, producing a decrease in the spectral efficiency of the system since they cause interference on any other signal's spectrum placed at near frequencies.

Peak to Average Power Ratio

OFDM systems are also conditioned by the ratio of high peak power *vs.* average power ratio (PAPR), which grows proportionally to the number of sub-carriers employed on the transmission. This high PAPR results from the large fluctuations of the OFDM signal's envelope and it's associated to a decrease of the amplification efficiency [5, 26]. Such a high PAPR demands a large dynamic range in the

power amplifier of the transmitter. The linear amplifier must as thus, operate with a large output backoff to accommodate such a large dynamic range signals linearly [19] and avoid amplifier's saturation. In the non-linear region, the amplifier saturates meaning it cannot produce any higher output voltage regardless of the input voltage, distorting the signal [22].

The PAPR of a continuous time domain signal, $x(t)$, is expressed by

$$PAPR(x(t)) = 10\log_{10}\left(\frac{max[x(t)x^*(t)]}{E[x(t)x^*(t)]}\right)dB, \tag{2.11}$$

where $x^*(t)$ corresponds to the conjugate of $x(t)$ and the $E[.]$ operator represents the mathematical expectation or mean value.

By analysing the OFDM signal definition in (2.10), if we assume $S_k = 1$ for any $k = 0,\ldots,N-1$, the peak power value of the signal is $max[s[n]s^*[n]] = N^2$ and the mean square value of the signal is $E[s[n]s^*[n]] = N$. For that reason, the maximum PAPR value for an OFDM symbol with N sub-carriers occurs when each sub-carrier is modulated with the same symbol constellation and is equal to N. The most common method to evaluate the symbol-based PAPR of a transmitted signal is to obtain its complementary cumulative distribution function (CCDF). In this case, this function provides an indication of the probability of that signal's envelope exceeding a certain PAPR threshold [26] and can be expressed by

$$CCDF(PAPR(s[n])) = Prob\{PAPR(s[n]) > \zeta\}, \tag{2.12}$$

where $PAPR(s[n])$ is the PAPR of the OFDM symbol and ζ denotes the PAPR threshold.

Therefore, the probability of attaining the maximum PAPR value is very low, since the modulated data is random and uncorrelated. However, it can be concluded that the PAPR of an OFDM signal tends to grow when the number of sub-carriers, N, increases. Intuitively, by making use of smaller size FFTs (equivalent to the number of sub-carriers, N), a reduction on PAPR can be accomplished [9, 18].

2.4.3 Equalization

The received CP-OFDM signals that went through frequency selective fading channels can be recovered through equalization by a simple one-tap frequency domain equalizer (FDE). If the CP is chosen to be long enough so that all the interference between adjacent OFDM symbols, due to the multipath, occurs within this interval, the received signal, Y_k, at each sub-carrier $k = 0,\ldots,N-1$, after discarding the CP, can be expressed as

$$Y_k = S_k H_k + \eta_k, \tag{2.13}$$

where H_k denotes the channel's frequency response at k-th sub-carrier and η_k represents the complex additive white gaussian noise (AWGN) sample with variance $E\left[|\eta_k|^2\right]$, at that sub-carrier. In order to estimate the transmitted signal, $\hat{S}_k, k = 0,\ldots,N-1$, the equalizer multiplies the received signal by a coefficient at each sub-carrier k, F_k, as follows

$$\hat{S}_k = F_k Y_k. \tag{2.14}$$

Zero-Forcing Equalizer

The zero-forcing (ZF) equalizer simply eliminates the channel effect by inverting the channel frequency response and forces the frequency selective-faded signals back to flat-faded ones defining $F_k = \frac{H_k^*}{|H_k|^2} = \frac{1}{H_k}, k = 0,\ldots,N-1$ [19], where H_k^* represents the complex conjugate of the channel's frequency response. Therefore, the estimated signal is given by

$$\hat{S}_k = \frac{S_k H_k}{H_k} + \frac{\eta_k}{H_k} = S_k + \frac{\eta_k}{H_k}. \tag{2.15}$$

However, (2.15) shows that the noise associated to the sub-carriers that lay inside a deep fade region, i.e. when $H_k \to 0$, is greatly enhanced.

Minimum Mean Square Error Equalizer

The MMSE equalizer, as the name suggest, minimizes the mean square error of the received signal by determining the equalizer coefficient that satisfies $min\left\{E\left[\hat{S}_k - S_k\right]\right\}, k = 0,\ldots,N-1,$, taking the noise into account. This results in

$$F_k = \frac{H_k^*}{|H_k|^2 + \frac{1}{\gamma}} \tag{2.16}$$

where γ denotes the signal-to-noise ratio (SNR) ratio. Therefore, the estimated signal is given by

$$\hat{S}_k = \frac{S_k H_k H_k^*}{|H_k|^2 + \frac{1}{\gamma}} + \frac{\eta_k H_k^*}{|H_k|^2 + \frac{1}{\gamma}} = \frac{S_k |H_k|^2}{|H_k|^2 + \frac{1}{\gamma}} + \frac{\eta_k H_k^*}{|H_k|^2 + \frac{1}{\gamma}}. \tag{2.17}$$

Equation (2.17) suggest that the, in high-SNR scenarios, the MMSE equalizer performance approaches the ZF equalizer. In addition, in low-SNR cases, the component $\frac{1}{\gamma}$ dominates over $|H_k|^2$ and the second term of the equation related to noise tends to be low, thus, resolving the noise enhancement problem.

3

Block Windowed Burst OFDM methods

Contents

In this chapter the theoretical concepts of hybrid modulation techniques, such as BWB-OFDM and TIBWB-OFDM, are introduced.

3.1 BWB-OFDM

The BWB-OFDM transmission technique [2] was proposed in order to allow, on the one hand, a better spectral efficiency, by employing transmitted signals with a PSD as compact as filtered-OFDM schemes [16] and, on the other hand, a better power efficiency when compared to conventional CP-OFDM schemes. The new scheme grants the possibility to reach a compromise between higher data rate and spectrum confinement by removing the need of a CP. However, this transmission scheme expects to maintain the same complexity and the same advantages of standard CP-OFDM scheme, especially regarding the orthogonality between sub-carriers, allowing simple FDE. The greater spectral efficiency is obtained by increasing the spectral confinement of the signal transmitted, when compared to CP-OFDM schemes, by using windowing techniques. This is achieved by maintaining the same transmission rate and the number of sub-carriers. Another way of granting a greater spectral efficiency is to increase the transmission rate and maintaining the same spectral characteristics of the CP-OFDM scheme, keeping the same symbol's rectangular configuration [2, 9]. The increase in power efficiency is obtained by concatenating a number of OFDM symbols, to which a single prefix of zeros is added, thereby eliminating the CP. Besides, the windowing operation keeps the individual symbol's energy constant. In CP-OFDM schemes, the OFDM symbol's power is increased after the CP insertion leading to a loss in the power efficiency $\varepsilon = \frac{N}{N_{cp}+N}$, where N_{cp} is the CP length [2].

The BWB-OFDM transmitter, presented in figure 3.1[1], is built on the filtered-OFDM schemes [2]. The modulated data symbols, $S_k, k = 0, \ldots, N-1$ at the k-th sub-carrier, are usually generated by direct mapping of a bit-stream, b, where channel coding and bit-interleaving is applied into a selected signal constellation to improve the BER performance when transmitting through TD channels by detecting and correcting burst of errors. By leveraging on the IFFT algorithm, the high rate data stream is split into N lower rate sub-streams that are transmitted in parallel, spectrally spaced by $\frac{1}{N}$, over overlapping sub-bands, with each one modulating one sub-carrier belonging to a set of N orthogonal sub-carriers [2]. The complex envelope of a baseband OFDM symbol is given by (2.10).

The PSD of the transmitted signal can be enhanced by applying windowing techniques instead of using filtering techniques. The BWB-OFDM transmitter applies

[1] Reprinted with permission of the authors.

a cyclic extension to the conventional OFDM symbol and replaces the rectangular window with a roll-off dependent window, known as SRRC. This symmetric window multiplies with the samples of the signal, granting a reduction in the frequency side lobes. The greater the roll-off, the lesser the amplitude of the lateral lobes that are obtained in the spectrum, resulting in greater spectral confinement (as represented in figure 3.2[1]) but at the same time, increasing the length of the symbols in time domain.

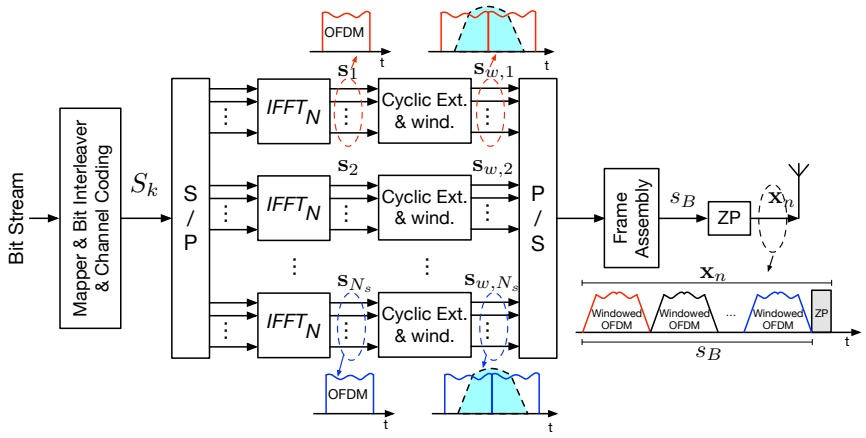

Figure 3.1: Diagram of the BWB-OFDM transmitter [1].

The conventional OFDM symbols/blocks are converted to a single BWB-OFDM symbol/mega-block. Hence, a BWB-OFDM symbol results from the concatenation of a set of cyclic extended and time domain windowed OFDM symbols.

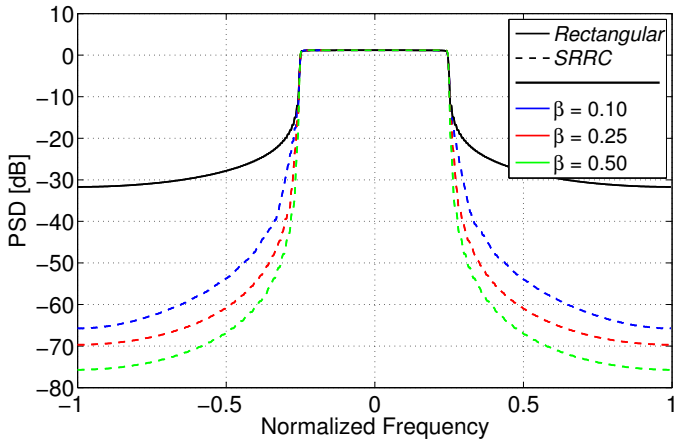

Figure 3.2: PSD of the BWB-OFDM transmitted signal as a function of the window roll-off, highlighting the obtained spectral confinement [2].

Knowing that the length of the conventional OFDM symbols is N (number of sub-carriers), subsequent of the cyclic extension and windowing operations, the

length of each new windowed OFDM symbols is extended to $N_{symb} = N(1+\beta)$, after discarding the tailing zeros from the windowing operation in the time domain, where β represents the roll-off of the window. In order to accommodate multipath propagation delay effect, inherent to TD wireless channels, a time guard interval is added at the end of the block. For this purpose, a single ZP of length N_{zp} is added to the mega-block, ensuring that N_{zp} is longer than the channel's delay spread. Hence, a BWB-OFDM mega-block has a total length of $N_x = N_s N(1+\beta)+N_{zp} = N_{symb}N_s + N_{zp}$.

Considering that $s_{w_i}[n], i = 1,...,N_s$ are the N_s OFDM symbols resulting from these operations, a BWB-OFDM symbol/mega-block, before ZP insertion, which is expressed by $s_w[n], n = 0,\ldots,N_{symb}N_s - 1$, can be described as sum of juxtaposed windowed OFDM with a delay proportional to N_{symb} and can be expressed through

$$s_w[n] = \sum_{i=1}^{N_s} s_{w_i}\left[n-(i-1)N_{symb}\right], \tag{3.1}$$

whose spectrum can be deduced by applying the discrete time fourier transform (DTFT) to (3.1)

$$S_w\left(e^{jw}\right) = DTFT\left(s_w[n]\right) = \sum_{i=1}^{N_s} S_{w_i}\left(e^{jw}\right) e^{-jw(i-1)N_{symb}}, \tag{3.2}$$

where $S_{w_i}\left(e^{jw}\right)$ represents the DTFT of the OFDM symbols resulting from the operations previously mentioned.

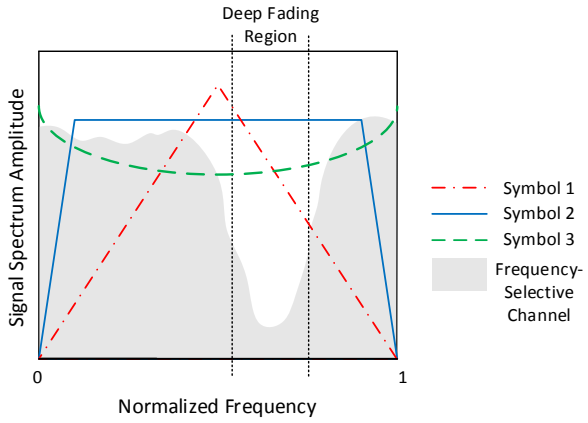

Figure 3.3: Example of the BWB-OFDM symbol's amplitude spectrum [1].

Due to the BWB-OFDM signal's spectrum characteristics, it is easy to presume that in case a deep in-band fade occurs in a frequency selective channel, the modulated data is corrupted and cannot be easily recovered. In other words, the detection

of the transmitted signal is heavily conditioned by the frequency response of the channel since the spectral data that modulate a specific set of sub-carriers that lay inside the deep fade regions are completely destroyed. Hence, this system has the same drawbacks of an OFDM scheme when transmitting over hostile channel conditions causing performance degradation since the signal spectrum of the transmitted BWB-OFDM mega-block simply consists on an overlapped and phase-shifted spectrum of all N_s windowed OFDM symbols, as represented in figure 3.3[1], where $N_s = 3$ [9].

At the reception, emphasis is put in the equalization procedure that is performed in the frequency domain (FDE), treating the received signal, i.e. the N_s consecutive windowed OFDM symbols, as a block-based SC transmission, which makes the BWB-OFDM a technique of hybrid modulation.

3.2 TIBWB-OFDM

In order to solve the problem of high sensitivity to deep fading, a MC technique, termed Time-Interleaved Block Windowed Burst Orthogonal Frequency Division Multiplexing (TIBWB-OFDM), was recently developed allowing the signal to be resilient against deep in-band fades [9]. This modulation technique performs a time-interleave operation between the samples of the various OFDM sub-symbols that make up the BWB-OFDM mega-block. In practice, such an operation corresponds, at the level of each individual OFDM symbol component, to the temporal expansion of its samples and, as such, the compression and repetition of its spectrum along with the allocated bandwidth of the BWB-OFDM symbol. Thus, this operation causes the replication of the spectral data over the available bandwidth, occupied by the BWB-OFDM signal, creating a diversity effect in the frequency domain thus increasing the robustness of the method against deep fading of the communication channel [1, 9]. It can be concluded that the occurrence of deep fades is now less burdensome, since the affected data are now replicated in other regions of the spectrum and the corrupted data affected by the deep fade is not completely lost but just degraded. Thus, it can still be recovered from the remaining unaffected replicas that contains the same information [9]. It should be noted that the TIBWB-OFDM technique retains all the advantages of the BWB-OFDM technique without adding complexity to the transceiver.

The process of constructing the TIBWB-OFDM symbol (i.e. the transmitter) is shown in figure 3.4[1] and is described in more detail in the next section, followed by the description of the receiver system shown in figure 3.5[1].

For the sake of better understanding the construction of the TIBWB-OFDM

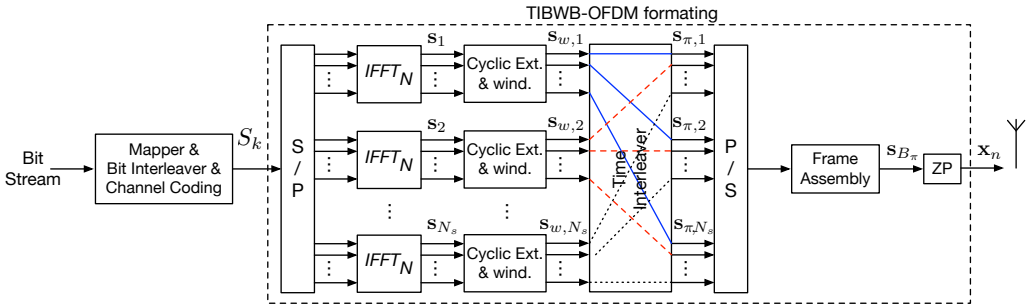

Figure 3.4: Diagram of the TIBWB-OFDM transmitter [1].

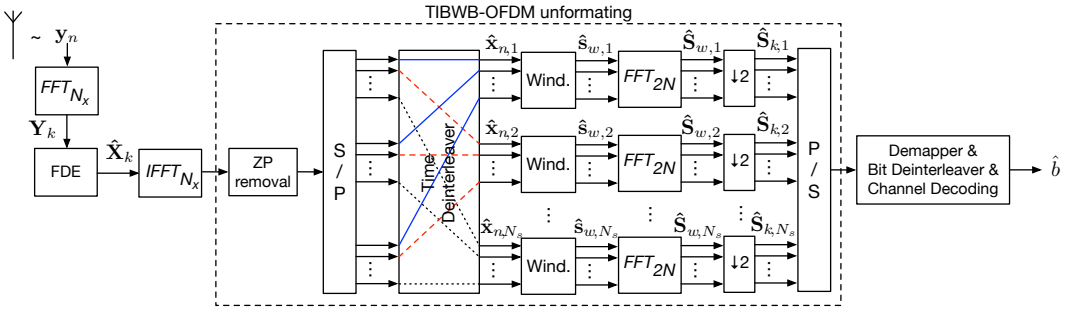

Figure 3.5: Diagram of the TIBWB-OFDM receiver [1].

symbols, we can consider one symbol $s_{w_i}[n], i \in \{1,\ldots,N_s\}$ of the original set of N_s OFDM symbols that compose the BWB-OFDM symbol after the cyclic extension and windowing operations with length N_{symb}. We can define a new symbol, resulting from the expansion of $s_{w_i}[n]$ by a factor N_s, by

$$s_{e_i}[n] = \begin{cases} s_{w_i}\left[\frac{n}{N_s}\right], & \text{if } n \bmod N_s = 0 \\ 0, & \text{if otherwise} \end{cases}, \tag{3.3}$$

for $n = 0,1,...,N_sN_{symb}-1$.

It should be noted that there is no loss of data with the application of this operation and that the signal's energy resulting from the expansion operation is equal to the energy of the original signal, since the operation is temporarily translated into a simple addition of zeros gaps between the samples of the original signal, which will be filled by the samples of the other windowed OFDM symbols [1].

Thus, a TIBWB-OFDM symbol results from a juxtaposition sum of the expanded symbols, $s_{e_i}[n]$, with unitary time delay between consecutive symbols, filling the zeros inserted through the expansion process, between not-null samples, with the samples belonging to the other sub-symbols, and can be expressed through [1]

$$s_\pi[n] = \sum_{i=1}^{N_s} s_{e_i}[n-(i-1)], \tag{3.4}$$

whose spectrum results in

$$S_\pi\left(e^{jw}\right) = DTFT\left(s_\pi[n]\right) = \sum_{i=1}^{N_s} S_{e_i}\left(e^{jw}\right) e^{-jw(i-1)}, \tag{3.5}$$

where $S_{e_i}\left(e^{jw}\right)$ represents the DTFT of the expanded symbol i, $s_{e_i}[n]$.

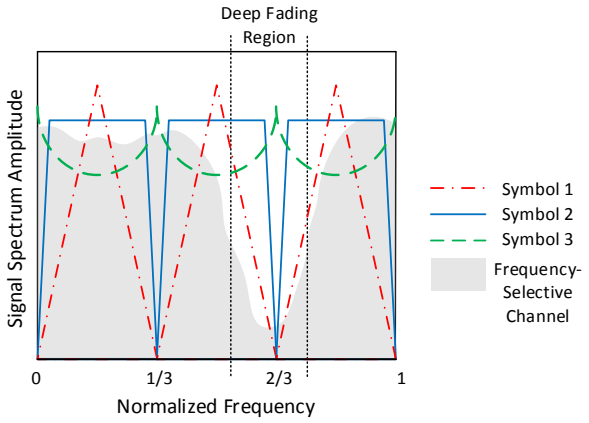

Figure 3.6: Example of the TIBWB-OFDM symbol's amplitude spectrum [1].

As expected, the resulting spectrum still remains an overlap of each of the individual spectra associated with each symbol $s_{w_i}[n], i = 1,...,N_s$, however, due to temporal expansion, the spectrum of these symbols are now compressed by a factor of $\frac{1}{N_s}$ and replicated N_s times in the frequency domain, as shown in figure 3.6[1], where $N_s = 3$.

3.2.1 TIBWB-OFDM Transmitter

The TIBWB-OFDM transmitter is built based on the BWB-OFDM transmitter [2]. The only difference relates to the block representing the time-interleave operation applied to the OFDM symbols after the cyclic extension and windowing operations.

The N_s OFDM symbols compounded by N carriers, that is, $S_{k_i}, k = 0,...,N-1$ with $i = 1,\ldots,N_s$ [9] are generated through an N-sized IDFT, performed by the IFFT algorithm, and are given by

$$s_{n_i} = s_i[n] = \sum_{k=0}^{N-1} S_{k_i} w[n] e^{\frac{j2\pi kn}{N}}, \tag{3.6}$$

where $n = 0,\ldots,N-1$ and $w[n]$ is a unitary rectangular pulse with length N. As previously mentioned, in order to construct a BWB-OFDM symbol, the cyclic extension and windowing operations must be applied to each one of the N_s OFDM

symbol, to perform spectral shaping [9]. In this way, the unitary rectangular pulse $w[n]$ is replaced by an SRRC window, expressed by

$$h_{\text{SRRC}}[n] = \begin{cases} 1, & |n| \leq \frac{N}{2}(1-\beta) \\ \cos\left(\frac{\pi}{4\beta}\left[\frac{2n}{N} - (1-\beta)\right]\right), & \frac{N}{2}(1-\beta) \leq |n| \leq \frac{N}{2}(1+\beta) \\ 0, & |n| \geq \frac{N}{2}(1+\beta) \end{cases}, \tag{3.7}$$

where $n = -N, ..., N$ and β denotes the window roll-off. Consequently, the new N_s windowed symbol are generated, expressed by

$$\mathbf{s_{w_i}} = [\mathbf{s_i}|\mathbf{s_i}]_{1\times 2N} \odot \mathbf{h_{SRRC}}_{1\times 2N}, \tag{3.8}$$

where the operator $\odot$ represents a point-wise Hadamard multiplication. The tailing zeros from the referred operation are, then, discarded and $\mathbf{s_{w_i}}$ represents a vector whose length becomes $N_{symb} = N(1+\beta)$.

The simple time domain juxtaposition of the component OFDM symbols forms a BWB-OFDM [2] and can be expressed in the time domain as (3.1) or in vector form by

$$\mathbf{s_w} = \left[\mathbf{s}_{w_1}|\mathbf{s}_{w_2}|\cdots|\mathbf{s}_{w_{N_s}}\right] . \tag{3.9}$$

TIBWB-OFDM technique adds robustness to BWB-OFDM against deep in-band fades (prone to happen in wireless broadband communications), by performing a time domain interleaving operation, with period N_s, of the samples of block $\mathbf{s_w}$ [1, 9], resulting in a set of N_s interleaved symbols, denoted by $s_{\pi_i}[n], i = 1, \ldots, N_s$. The interleaved block vector is given by

$$\mathbf{s}_\pi = \Pi^{(N_s)}\mathbf{s_w}, \tag{3.10}$$

where $\Pi^{(N_s)}$ is the time-interleave matrix with period N_s of size $N_{\text{symb}} \times N_{\text{symb}}$, where the c-th column has a "one" at row $\lfloor \frac{c}{N_s} \rfloor + \left(cN_{\text{symb}} \mod N_{\text{symb}}N_s\right)$ [11].

Equation (3.10) relates with (3.4) since each of one of the interleaved symbols, $s_{\pi_i}[n]$, is concatenated to generate a single mega-block consisting of N_s interleaved symbols, forming a TIBWB-OFDM symbol, $s_\pi[n], n = 0, \ldots, N_B - 1$, where $N_B = N_{symb}N_s$. This can be written, in vector form, through

$$\mathbf{s}_\pi = [s_\pi[0], \cdots, s_\pi[N_B-1]] = \left[\mathbf{s}_{\pi_1}|\mathbf{s}_{\pi_2}|\cdots|\mathbf{s}_{\pi_{N_s}}\right]_{1\times N_B} = \left[\mathbf{s_{w_1}}\mathbf{s_{w_2}}\cdots\mathbf{s_{w_{N_s}}}\right]\Pi^{(N_s)} \tag{3.11}$$

TIBWB-OFDM block construction ends by appending a single guard interval (ZP), of length N_{zp} to $\mathbf{s}_\pi$, inserted at the end of the mega-block (TIBWB-OFDM symbol) in order to deal with frequency selective multipath channel's delay spread.

Thus, the transmitted TIBWB-OFDM symbol, $x[n], n = 0, \ldots N_x - 1$, is given by the vector

$$\mathbf{x_n} = \left[\mathbf{s}_\pi | 0_{1\times N_{zp}}\right]_{1\times N_x}, \tag{3.12}$$

where $0_{(1\times N_{zp})}$ represents a null vector (ZP) of dimension N_{zp}. The total length of the transmitted mega-block is, then, $N_x = N_B + N_{zp}$.

3.2.2 TIBWB-OFDM Receiver

The main role of the TIBWB-OFDM receiver, shown in figure 3.5, is to equalize the received signal and perform the time-deinterleave and matched filtering operations. The latter is intended to compensate for interference between adjacent sub-carriers (ICI), prior to the bit-deinterleaving and channel decoding operations [9].

The received signal, denoted as $y_n = y[n], n = 0, \ldots, N_x - 1$, is converted to the frequency domain by means of a long N_x-sized DFT, resulting $Y_k = DFT(y_n), k = 0, \ldots, N_x - 1$ [9]. Assuming that the ISI, arising from multipath fading, is eliminated by the use of the ZP, Y_k can be written through (2.13) where $X_k = DFT_{N_x}(x_n)$ denotes the transmitted signal, in this case.

As settled in the previous chapter, linear FDE of the signal is performed in the receiver. This process can make use of a ZF equalizer or relying on a more efficient FDE technique that results from the application of the MMSE method.

The estimated signal, $\hat{X}_k, k = 0, \ldots N_x - 1$, is then converted to the time domain after applying an IDFT of size N_x, and, eventually, the guard interval (ZP) is removed, following the time-deinterleave operation. This operation is applied to the resulting signal and is complementary to the operation applied in the transmitter, obtaining the separated symbols $\hat{x}_{n_i} = \hat{x}_i[n], i = 1, \ldots, N_s$, each one with length $N_{symb} = N(1+\beta)$. In order to employ the same window (matched filtering), it is necessary to add a certain number of zeros to each symbol, so that their length reach $2N$. Then, the matched filtering operation is performed as follows

$$\hat{\mathbf{s}}_{\mathbf{w_i}} = \hat{\mathbf{x}}_{\mathbf{n_i}} \odot \mathbf{h}_{\mathbf{SRRC}1\times 2N}. \tag{3.13}$$

Afterwards, in order to obtain an estimation of the original OFDM symbols, $\hat{S}_{k_i}, k = 0, \ldots N-1, i = 1, \ldots, N_s$ the estimated sub-symbols, $\hat{s}_{n_{w_i}} = \hat{s}_{w_i}[n], n = 0, \ldots, 2N-1$, are converted back to the frequency domain, $\hat{S}_{k_{w_i}} = \hat{S}w_i[k], k = 0, \ldots, 2N-1, i = 1, \ldots, N_s$, through a $2N$-size DFT and downsampled by 2 [9], resulting in

$$\hat{S}_{k_i} = \hat{S}_{w_i}[2k]_{1\times 2N}. \tag{3.14}$$

Finally, the de-mapping, bit-deinterleaving and channel decoding operations, complementary to those used in the transmission process, are applied to the estimated symbols $\hat{S}_{k_i}$ to obtain an estimate of the original binary sequence, $\hat{b}$.

3.3 TIBWB-OFDM with IB-DFE

Although the two linear frequency domain equalizers, previously described in section 2.4.3, provide a satisfying performance in reversing the distortion incurred the channel, the performance is still far from the match filter bound (MFB) [27]. In block-based SC transmissions category, where the BWB-OFDM/TIBWB-OFDM transceiver scheme fits, in order to tackle the ISI or inter-block interference (IBI), arising from the multipath effects, a more suited non-linear equalization technique can outperform the conventional linear equalizers [1]. This equalization technique is known as IB-DFE [28, 29].

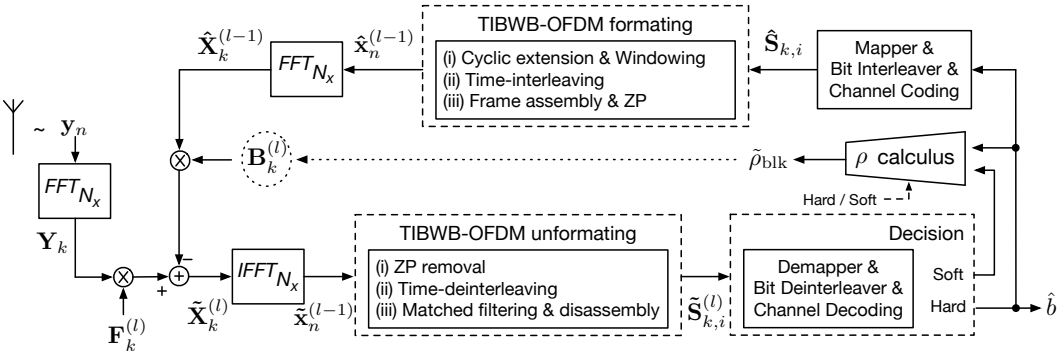

Figure 3.7: Diagram of the TIBWB-OFDM receiver with Turbo IB-DFE [1].

Figure 3.7[1] depicts the IB-DFE equalizer schematic for a TIBWB-OFDM receiver. This iterative frequency domain equalizer is compounded by two filters. On the one hand, the filter in the feedforward (FF) path acts as a conventional FDE aiming to reduce the precursors of the channel impulse response, assuming perfect channel knowledge. On the other hand, the filter in the feedback (FB) path tries to cancel the remaining ISI or IBI due to postcursors from the previous estimation [1, 30].

The equalizer processes the received signal block, $Y_k, k = 0, \ldots, N_x - 1$ as whole and produces at the output, for each iteration l, a frequency domain block serving as an estimation of the equalized TIBWB-OFDM symbol, $\tilde{X}_k^l, k = 0, \ldots, N_x - 1$, which can be written as

$$\tilde{X}_k^l = F_k^l Y_k - B_k^l \hat{X}_k^{l-1}, \tag{3.15}$$

where F_k^l and $B_k^l, k = 0, \ldots, N_x - 1$ are the frequency domain coefficients of the FF and FB filters, respectively. Besides, $\hat{X}_k^{l-1}$ represents the DFT of the estimated

block $\hat{x}_n^{l-1}, n = 0, \ldots, N_x - 1$ after the decision device, denoting the *hard* or *soft* FB estimation of $\tilde{x}_n^{l-1}$, i.e., the TIBWB-OFDM estimated symbol from the previous $(l-1)$ FDE iteration. In order to maximize the overall SNR the optimal FF and FB filter coefficients are, respectively [1, 31]

$$F_k^l = \frac{\kappa H_k^*}{\frac{1}{\gamma} + \left(1 - \rho_{blk}^{l-1} |H_k|^2\right)}, \tag{3.16}$$

and

$$B_k^l = \rho_{blk}^{l-1} \left(F_k^l H_k - 1\right), \tag{3.17}$$

where γ represents the SNR, κ is a normalized constant selected to guarantee that $\frac{1}{N}\sum_{k=0}^{N-1} F_k^l H_k = 1$ and ρ_{blk} is a correlation factor that measures the block-wise reliability of the $\hat{x}_n^{l-1}$ estimates from the previous iteration, employed in the FB loop. Therefore, ρ_{blk} measures the reliability between $\tilde{X}_k^l$, at the output of the FF filter and $\hat{X}_k^l$, the estimated signal at the output of the decision device [30]. At the first iteration of the IB-DFE $\rho_{blk} = 0$ and the equalizer can be classified as a simple MMSE equalizer since the FB filter has only null coefficients. The reliability ρ_{blk} constitutes a key parameter for the good performance of the IB-DFE receiver and is defined in time and frequency domains as

$$\rho_{blk}^{l-1} = \frac{E\left[\hat{x}_n^{l-1} x_n\right]}{E\left[|x_n|^2\right]} = \frac{E\left[\hat{X}_k^{l-1} X_k\right]}{E\left[|X_k|^2\right]}. \tag{3.18}$$

Although the exact computation of ρ_{blk} depends on the TIBWB-OFDM transmitted signal x_n (which in fact is the aim of the equalization procedure), a good approximation can be computed as [1, 29]

$$\rho_{blk}^{l-1} = \frac{E\left[\hat{x}_n^{l-1} \tilde{x}_n^{l-1}\right]}{E\left[|\tilde{x}_n^{l-1}|^2\right]}, \tag{3.19}$$

where $\tilde{x}_n^{l-1}$ is the signal obtained at the output of the FF filter. In the FB loop, a decision device is included. Its purpose is to provide block estimates as best as it can in order to guarantee a good measure of the block reliability, since the inaccurate data estimation affect the ρ_{blk} accuracy, affecting the overall performance [1]. In a TIBWB-OFDM receiver employing IB-DFE, after unformatting the equalized mega-block, as described in section 3.2.2, the decision device acts, producing either a *soft* or *hard decision*.

3.3.1 IB-DFE with *hard decisions*

After unformatting the TIBWB-OFDM symbol the OFDM sub-symbols, denoted by $\tilde{S}_{k_i}, k = 0, \ldots, N-1, i = 1, \ldots, N_s$ are estimated. A *hard decision* is, then,

taken on each one of these blocks, generating the *hard symbols* $\hat{S}_{k_i}, k = 0,\ldots,N-1, i = 1,\ldots,N_s$ by choosing the constellation symbol (among the M possible candidates), based on the minimum distance criteria [30]. Afterwards, the resulting bit-stream obtained from the *hard symbols* takes the role of the original data and is used to format the *original* TIBWB-OFDM mega-block, as described in section 3.2.1, and compute the correlation factor, ρ_{blk}.

However, *soft decisions* can improve the accuracy of the IB-DFE block-wise reliability factor $\tilde{\rho}_{blk}$ computation over (3.19) [30]. When channel coding is employed, soft-decoding can be performed over $\tilde{S}_{k_i}$, on the channel decoder output. Therefore, either by leveraging on the soft-information contained in $\tilde{S}_{k_i}$, or after soft-decoding $\tilde{S}_{k_i}$, a better *hard decision* can be taken to generate $\hat{S}_{k_i}$. The inclusion of the channel decoder in the IB-DFE loop, a technique known Turbo IB-DFE, can improve the performance of the equalizer operation [1].

3.3.2 IB-DFE with *soft decisions* and channel coding

To improve the performance, the *block-wise averages* are replaced by *symbol averages*, meaning that, now, the FB input is $\hat{S}_{k_i} = DFT(\hat{s}_{n_i})$, where $\hat{s}_{n_i}$ denotes the average symbol value conditioned to the FDE output of the previous iteration [30, 31].

If the original OFDM symbol sample values directly come from a normalized quadrature phase shift keying (QPSK) constellations (i.e., $S_{k_i} = \beta_0 + j\beta_1 = \pm 1 \pm j$) with Gray mapping it is easy to show that the log-likelihood ratio (LLR) information of the *in-phase bit*, b_0, and *quadrature bit*, b_1, based on the received $\tilde{S}_{k_i}$ is given, respectively, by [1]

$$\lambda_{k_i}^{b_0} = \log\left(\frac{Prob\left\{b_0 = 0|\tilde{S}_{k_i}\right\}}{Prob\{b_0 = 1|\tilde{S}_{k_i}\}}\right) = \frac{4Re\left\{\tilde{S}_{k_i}\right\}}{\sigma_\eta^2}, \tag{3.20}$$

and

$$\lambda_{k_i}^{b_1} = \log\left(\frac{Prob\left\{b_1 = 0|\tilde{S}_{k_i}\right\}}{Prob\left\{b_1 = 1|\tilde{S}_{k_i}\right\}}\right) = \frac{4Im\left\{\tilde{S}_{k_i}\right\}}{\sigma_\eta^2}, \tag{3.21}$$

where σ_η^2 represents the variance of the complex noise plus the residual interference at FF filter output. The *hard decisions* of both bits are defined by the signs of (3.20) and (3.21), respectively [30].

The average bit values resulting from soft demodulation can, thus, be computed as

$$\bar{\beta}_0 = Prob\{b_0 = 0\} - Prob\{b_0 = 1\} = tanh\left(\frac{\lambda_{k_i}^{b_0}}{2}\right), \tag{3.22}$$

and

$$\bar{\beta}_1 = Prob\{b_1 = 0\} - Prob\{b_1 = 1\} = tanh\left(\frac{\lambda_{k_i}^{b_1}}{2}\right), \tag{3.23}$$

Therefore, the LLR values provide the *soft decisions* of both the *in-phase* and *quadrature* bits and the reliabilities of these average bits are, respectively, given by

$$\rho_{k_i}^{b_0} = |\bar{\beta}_0| = tanh\left(\frac{|\lambda_{k_i}^{b_0}|}{2}\right), \tag{3.24}$$

and

$$\rho_{k_i}^{b_1} = |\bar{\beta}_1| = tanh\left(\frac{|\lambda_{k_i}^{b_1}|}{2}\right). \tag{3.25}$$

The block-wise reliability factor of an IB-DFE receiver employing *soft decisions* [1, 31], for a TIBWB-OFDM system, $\tilde{\rho}_{blk}$, can be expressed by

$$\tilde{\rho}_{blk} = \frac{1}{2}\sum_{i=1}^{N_s}\sum_{k=0}^{N-1}\left(\rho_{k_i}^{b_0} + \rho_{k_i}^{b_1}\right). \tag{3.26}$$

A correct estimation of σ_η^2 is a key factor for an accurate estimation of reliable LLR through (3.20) and (3.21) and an accurate computation of $\tilde{\rho}_{blk}$, which depends on transceiver scheme. In a conventional IB-DFE receiver the LLR values are computed on a symbol-by-symbol basis. Alternatively, the Turbo-IB-DFE employs the channel decoder outputs instead of the uncoded *soft decisions* in the FB loop. Therefore, the main difference between conventional IB-DFE and Turbo-IB-DFE is in the decision device [31]. This way, when a coded bit-stream is transmitted, the estimation of σ_η^2 also influences the performance of the soft decoder, which, in turn, degrades the LLRs estimations and, consequently, provides an inaccurate estimation of $\tilde{\rho}_{blk}$.

Instead of computing σ_η^2 at each IB-DFE iteration (which adds considerable complexity to the system), for the TIBWB-OFDM case, the σ_η^2 is estimated at the first IB-DFE iteration by performing kind of average on the SNR, γ, along the signal bandwidth, avoiding the unrealistic enhancement of σ_η^2 due to deep fades [1]. Thus, σ_η^2 is estimated as

$$\sigma_\eta^2 = \frac{\varepsilon_s}{N_x}\sum_{k=0}^{N_x-1}\frac{1}{1+\gamma|H_k|^2}, \tag{3.27}$$

where ε_s denotes the power transmitted per modulated symbol ($\varepsilon_s = 2$ for a QPSK modulation). When using this estimation, the IB-DFE algorithms converges to the expected result, showing no performance loss, after just a few iterations, when compared to a genie receiver that computes the exact value of σ_η^2, given by, $\sigma_\eta^2 = E\left[|\tilde{X}_k^l - X_k|\right]$ [1].

4

Time Interleaved Block Windowed Burst OFDM with Time Overlapping

Contents

The concept of a new waveform, arising from the TIBWB-OFDM technique optimization, is introduced in this chapter, in which a partial overlap of the windowed OFDM sub-symbols is allowed and a new equalizer is defined. Many studies have already included the concept of overlapping or other similar operation that generate interference within the data structure, at time and/or frequency domains, in order to improve spectral efficiency of the transmission scheme [32–34]. An increased complexity in the receiver is necessary to identify and deal with self-created interference in the transmitted signal and maintain an acceptable performance in wireless channels [34–36].

The TIBWB-OFDM waveform as presented in [1] claims several advantages to conventional CP-OFDM along with being easily employed in MIMO systems compared to other waveforms [11, 18]. The use of ZP improves power efficiency [2], since no power is wasted on its transmission. A spectral efficiency gain is also claimed by the use of SRRC windowing, that improves the spectral confinement and reduces OOB emissions of the OFDM-based blocks. Although spectral confinement increases for higher window's roll-off, the length $N_s N_{\text{symb}}{=}N_s N\,(1{+}\beta)$ of the TIBWB-OFDM block increases proportionally, due to the juxtaposition of the component symbols. This implies a reduction of symbol rate, which limits spectral efficiency gains. Also the overall average power of the TIBWB-OFDM block is reduced thus implying an increased of the transmitted PAPR which limits achievable power efficiency gains.

If we consider an OFDM symbol with the same length as a TIBWB-OFDM mega-block discarding the ZP, that is $N_{OFDM} = N_x - N_{zp} = N_s N\,(1+\beta)$ $= N_s N_{symb} = N_B$, one could expect to get a higher PAPR than the TIBWB-OFDM transmitted signal since the IFFT operation is performed with a larger number of points. However, this might not be true owing to the windowing operation. This operation consists of a point-wise time domain product between the selected window and the cyclically extended OFDM symbol. The window employed corresponds to an SRRC, which is equivalent to a rectangular window when the roll-off is equal to 0. In this case, the PAPR of the TIBWB-OFDM signal is, indeed, reduced, because the window has no effect in regard to the temporal amplitude of the signal. In other words, the window does not affect the average power, neither the maximum power of the signal since the TIBWB-OFDM symbol simply consists of N_s OFDM symbols, each one having N sub-carriers. Hence, by employing smaller size FFTs, the probability of getting a high PAPR lessens. Nevertheless, this situation is not optimal taking into consideration that by using a rectangular window there is no spectral confinement and, therefore, the spectral efficiency is not improved. In fact,

in this particular case, the spectrum of the transmitted signal simply consists of a superimpose spectrum of all N_s OFDM symbols and, as a consequence, will have the same drawbacks of OFDM concerning spectrum leakage that can cause ICI [2].

Besides that, when $\beta > 0$ is used to achieve greater spectral confinement, the length of the TIBWB-OFDM block grows, as already explained, and thus two options can be taken. If the original symbol transmission rate is kept constant, the required bandwidth for transmission must increase. For better understanding, taken as example the construction of two TIBWB-OFDM waveforms, A and B, with $\beta_A > 0$ and $\beta_B = 0$, the length of the TIBWB-OFDM blocks relates by $N_{B_A} = N_{B_B}(1+\beta)$. If we have as constraint the original symbol transmission rate $1/T_s$, the time waste on transmitting blocks A and B should be the same, meaning that the N_{B_A} samples of block A should be transmitted $(1+\beta)$ times faster than the samples from block B. Thus, this means that the minimum required bandwidth (according to Nyquist theory) should relate as $B_A = B_B(1+\beta)$. On the contrary, if the available bandwidth is a constraint, the transmission rate achievable by waveform A is $(1+\beta)$ times slower than the achievable with waveform B.

In order to address both the issues presented by the TIBWB-OFDM scheme and achieve an improved spectral efficiency by avoiding the temporal expansion of the signal, an alternative packing of the windowed OFDM component blocks of the TIBWB-OFDM symbol is proposed, by allowing a partial overlap between adjacent windowed OFDM symbols, in the time domain, as shown in figure 4.1.

The next sections present the details on the TIBWB-OFDM with WTO transmitter and receiver. The TIBWB-OFDM with WTO transceiver architecture is presented in figure 4.2.

4.1 TIBWB-OFDM with WTO Transmitter

The way this new waveform is created is based on the operations performed on the BWB-OFDM and TIBWB-OFDM transmitters [2, 9], followed by an overlapping procedure. This packing follows the windowing procedure given by (3.8), while preceding the time interleaving procedure (3.10), described in the previous chapter.

First, the coded and bit-interleaved bit-stream is mapped onto symbols originating from an M-ary constellation, which are loaded onto N_s sets of sub-carriers, $n_i = 0, ..., N-1$ where $i = 1, \ldots, N_s$, according to (2.10). Channel coding and bit-interleave operations allow to minimize burst of bit errors.

Afterwards, the N_s OFDM symbols are cyclic extended and windowed forming the windowed OFDM symbols, $s_{w_i}, i = 1, ..., N_s$, which can be expressed by (3.8)

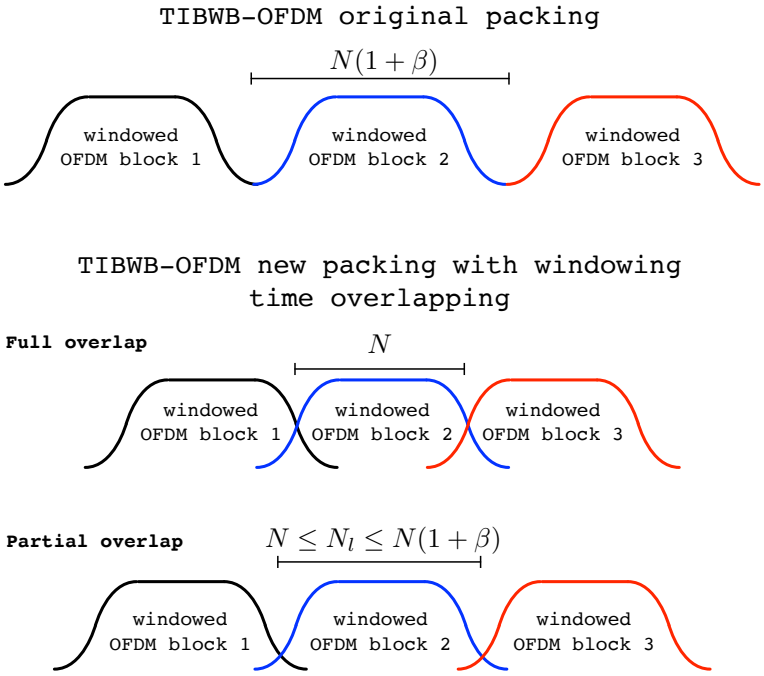

Figure 4.1: New packing proposal using windowing time overlapping for high efficient TIBWB-OFDM waveform.

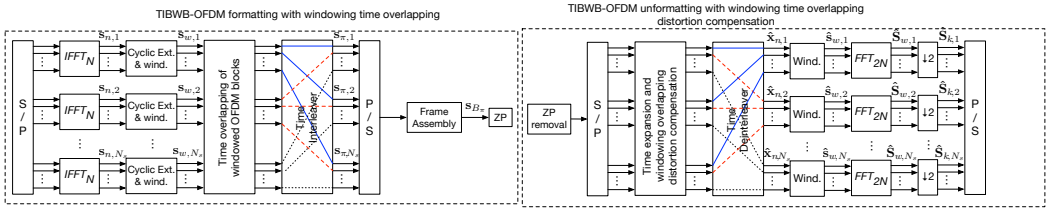

Figure 4.2: TIBWB-OFDM with WTO transceiver architecture.

for each i. The windowing operation is performed using the window defined in (3.7).

Then, after discarding the tailing zeros, the BWB-OFDM mega-block is obtained through (3.1). At this point, the overlapping operation is applied. Each one of those cyclic extended and windowed OFDM symbols, $s_{w_i}, i = 1, ..., N_s$, is overlapped with the adjacent sub-symbols, that is, the last samples of the current sub-symbol are added, in the time domain, with the first samples of the next sub-symbol. The new BWB-OFDM with WTO symbol/mega-block has a different configuration and, thus, instead of juxtaposing the symbols as given by (3.1), windowed OFDM

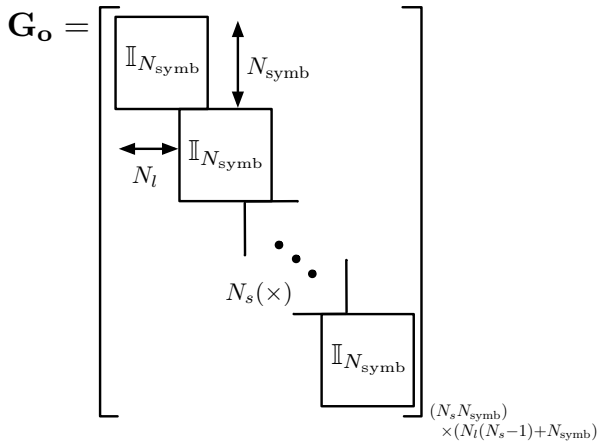

Figure 4.3: Matrix structure for packing with time overlapping. $\mathbb{I}_{N_{\text{symb}}}$ denotes an identity matrix of dimensions $N_{\text{symb}} \times N_{\text{symb}}$.

blocks are partially overlapped with overlap signal samples being given by

$$s_{wo}[n] = \sum_{i=1}^{N_s} s_{w_i}[n-(i-1)N_l] \quad \text{and } N \leq N_l \leq N_{\text{symb}} \,. \tag{4.1}$$

or in vector form by

$$\mathbf{s_{wo}} = \mathbf{s_w}\mathbf{G_o} \,, \tag{4.2}$$

where N_l represents the first overlapped sample from each block. The equality stands for the TIBWB-OFDM case without overlap. $\mathbf{G_o}$ is a rectangular matrix that group OFDM component blocks with overlapping, having the structure presented in figure 4.3. For the TIBWB-OFDM case without overlapping, $\mathbf{G_o}$ is a $N_s N_{symb} \times N_s N_{symb}$ square matrix.

Figure 4.1 presents the concept of the overlapping operation between adjacent sub-symbols and a comparison of prior art TIBWB-OFDM block construction, in the new proposed block format with windowing time overlapping.

The spectrum of (4.1) can be expressed as

$$S_{wo}\left(e^{jw}\right) = \sum_{i=1}^{N_s} S_{w_i}\left(e^{jw}\right) e^{-jw(i-1)N_l}. \tag{4.3}$$

Therefore, taking into consideration the same spectrum usage, this waveform allows to transmit with a higher rate and, in this case, the power spectrum of the new BWB-OFDM with WTO mega-block is similar to the non-overlapped one, since it contains the superimposition of the spectrum of each windowed OFDM symbol.

The remaining steps for the construction of the TIBWB-OFDM follows as described in section 3.2.1, with time-interleaving being performed according to (3.10)

where $\mathbf{s_w}$ vector is replaced by $\mathbf{s_{wo}}$, and ZP being appended; as stated before, time-interleaving grants for robustness against deep fades in broadband wireless channels, making more effective the use of frequency domain equalizers [1, 11], while ZP is used for preventing ISI.

This way, the new waveform has intentionally introduced interference between the N_s blocks that shape the BWB-OFDM mega-block where the number of overlapped samples, N_{os} is dynamic and can be regulated through $N_{os} = N_{symb} - N_l$. The overall TIBWB-OFDM with WTO block (excluding ZP) has a total length of $N_{OB} = N_l\,(N_s - 1) + N_{\text{symb}}$. When setting N_l=N this results in the minimum block length $N_{OB} = N\,(N_s + \beta)$, thus meaning there is no temporal extension compared to packing N_s conventional OFDM blocks with rectangular windowing (please note that $\beta < 1$). Since the packed windowed OFDM blocks are independent, although it happens some spectral regrowth resulting from the partial time overlapping, this is minimum, with the new proposed waveform still achieving considerable spectrum confinement compared to conventional OFDM. The new TIBWB-OFDM with windowing time interleaving can deliver as so very high spectral efficiency. The packing with time overlapping has also as consequence the increase of the average power of the transmitted signal, and thus a reduction on the signal's PAPR; note that, since only the tails of the windowed OFDM symbols overlap, the increase (in average) of the peak power of the TIBWB-OFDM block is minimum. Thus, the proposed technique enables also a considerable improvement in power efficiency.

4.2 TIBWB-OFDM with WTO Receiver

Although the proposed TIBWB-OFDM new packing method enables a highly efficient spectral and power transmission, these are achieved at the expense of introduced interference between consecutive sub-blocks, as can be easily concluded from figure 4.1. As so, the TIBWB-OFDM with WTO receiver must entail two equalization steps. The receiver architecture must be composed at first by a linear (or non-linear) equalizer at frequency domain to cancel channel impairments, followed by a time domain linear (or non-linear) equalizer of the type forward and backward successive cancellation, employed to cancel out windowing time overlapping distortion.

4.2.1 Frequency Domain Equalization

TIBWB-OFDM is seen as a hybrid modulation technique [1, 11], where the received packed block can be seen as of a block-based SC transmission type, and it is equalized as a whole in the frequency domain. Both, linear or iterative frequency

domain equalizers can be employed [1, 11].

Following the same analysis, if the ZP added to the transmitted signal is longer than the channel's impulse response, the received signal at frequency domain, $Y_k, k = 0, \ldots, N_x - 1$, with $N_x = N_{zp} + N_{OB} = N_{zp} + N_l (N_s - 1) + N_{symb}$ can be expressed as a function of the DFT of the transmitted signal, $S_k, k = 0, \ldots, N_x - 1$ as (2.13).

In order to get an estimate of the transmitted signal, $\hat{S}_k, k = 0, \ldots, N_x - 1$ the received signal is equalized in the frequency domain, which can be performed by the equalization method MMSE [1] as expressed by (2.17) or by the IB-DFE described in section 3.3 from the previous chapter.

Afterwards, the estimated signal is converted to time domain, $\hat{s}_n = \hat{s}[n], n = 0, ..., N_x - 1$, through a N_x-sized IFFT so its ZP can be removed. Then, the time-deinterleave operation is applied on the time domain signal. This operation reorders the signal so that it can be reverted to its original sequence, based on the number of blocks, N_s.

4.2.2 Time Domain Equalization

At this point, after applying the FDE and time-deinterleave operations to the received signal, an estimate of the BWB-OFDM with WTO signal is obtained. In order to get the original BWB-OFDM signal, prior to the overlapping operation, it is necessary to develop another equalization algorithm to cancel its effect. These equalization algorithms are developed in time domain and aim to obtain an estimate of the N_s windowed and extended OFDM symbols, $\hat{s}_{w_i}, i = 1, ..., N_s$ with length $N_{symb} = N(1 + \beta)$. After performing this time domain equalization, the detection of the OFDM component blocks follows the procedure described in the previous chapter or in [1, 2]. For that, it is necessary to add an equal number of zeros to each symbol, N_{zb}, in order to increase its length up to $2N$ to enable the match filtering operation (same window) based on (3.7). This operation is performed in an overlapping approach, similar to the overlapping operation described in the transmitter, resulting in the sub-symbols estimates, after discarding the tailing zeros from the point-wise multiplication with the window, followed by an DFT of each sub-block to recover individual OFDM symbols, basically following the procedure of the transmitter of figure 3.4 in reverse order.

These time domain equalization algorithms can be developed as ZF or MMSE channel cancellation methods, although, in this case, the channel can be perceived as the product of both windows used in the transmitter and the receiver, i.e., a RRC, where $h_{RRC}[n] = h^2_{SRRC}[n]$. The cancellation method is possible due to the cyclic extension operation performed in the transmitter and illustrated in figure 4.4[1]. The

principles of the forward and backward successive interference cancellation method to cancel out windowing time overlapping distortion are presented in figure 4.5.

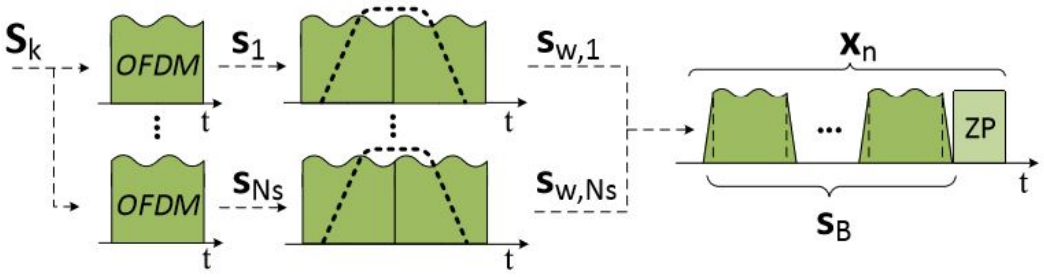

Figure 4.4: Windowing and cyclic extension operations [2].

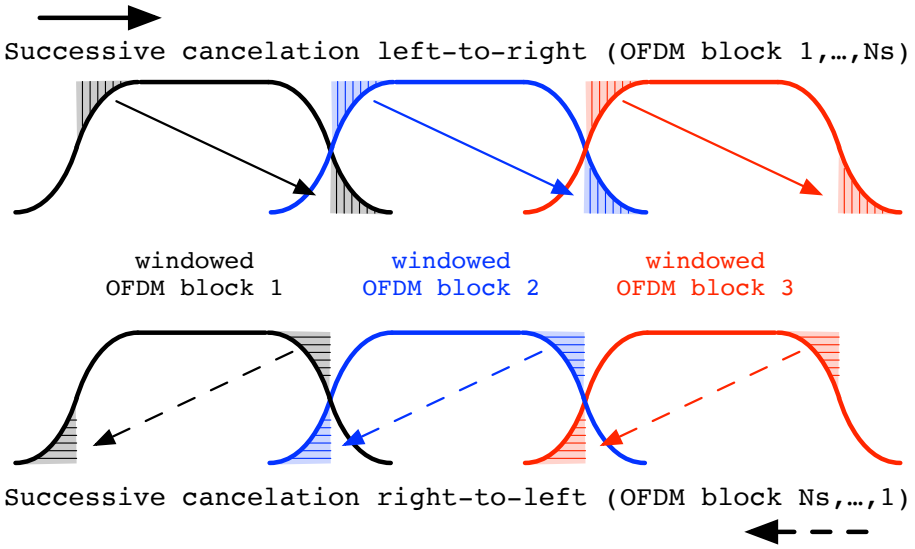

Figure 4.5: Time domain equalization algorithm interference cancellation concept.

The i-th cyclic extended and windowed OFDM symbol of BWB-OFDM block will be represented as

$$\begin{aligned}\mathbf{s}_{w_i} = [&s_{0_i}h_{-Y},\ s_{1_i}h_{-Y+1},\cdots,\\ &s_{Y-1_i}h_{-1},\ s_{Y_i}h_0,\ s_{Y+1_i}h_1,\cdots,s_{N_{symb}-1_i}h_{Y-1}].\end{aligned} \tag{4.4}$$

where for the sake of simplicity h denotes the h_{SRRC} window [1], defined in (3.7), $X = \frac{N_l}{N}\frac{N}{2}(1-\beta)$ and $Y = \frac{N}{2}(1+\beta)$.

[1] The tailing zeros from the square root raised cosine are removed.

The correspondent symbol after WTO at transmitter is given by

$$\begin{aligned}\mathbf{s}_{wo_i} &= [s_{wo_{i,-Y}}, s_{wo_{i,-Y+1}}, \cdots, s_{wo_{i,-1}} s_{wo_{i,0}} s_{wo_{i,1}}, \cdots, s_{wo_{i,Y-1}}] \\ &= [s_{0_i} h_{-Y} + s_{N_{l_{i-1}}} h_X, \cdots, s_{Y-1_i} h_{-1},\ s_{Y_i} h_0, \cdots, \\ &\quad s_{N_{l_i}} h_X + s_{0_{i+1}} h_{-Y}, \cdots, \\ &\quad s_{N_{symb}-1_i} h_{Y-1} + s_{N_{\text{symb}}-N_{l_{i+1}}} h_{-X}]\end{aligned} \tag{4.5}$$

4.2.3 ZF Cancellation Method

After the match filter operation, the interference cancellation algorithms are applied to the received signal. Considering the first symbol $\hat{s}_{w,1}$ and following the cyclic extension operation, it is known that the same data is replicated in the symbol, although weighted with different windowing factors. Thus, in an noise-free scenario, it is possible to retrieve the information entirely. However, in this case, the second symbol is distorted since it contains interference due to the partial overlap with the tail of the first symbol. The following equation represents the vectors of the first and second received symbols in a noise-free environment.

$$\begin{aligned}\hat{\mathbf{s}}_{w_1} &= [\hat{s}_{w_{1,-Y}} \hat{s}_{w_{1,-Y+1}}, \cdots, \hat{s}_{w_{1,-1}} \hat{s}_{w_{1,0}} \hat{s}_{w_{1,1}}, \cdots, \hat{s}_{w_{1,Y-1}}] \\ &= [s_{0_1} h_{-Y}^2, \cdots, s_{Y-1_1} h_{-1}^2,\ s_{Y_1} h_0^2, \cdots, \\ &\quad s_{N_{l_1}} h_X^2 + s_{0_2} h_X h_{-Y}, \cdots, \\ &\quad s_{N_{symb}-1_1} h_{Y-1}^2 + s_{N_{\text{symb}}-N_{l_2}} h_{Y-1} h_{-X}]\end{aligned} \tag{4.6}$$

$$\begin{aligned}\hat{\mathbf{s}}_{w_2} &= [\hat{s}_{w_{2,-Y}} \hat{s}_{w_{2,-Y+1}}, \cdots, \hat{s}_{w_{2,-1}} \hat{s}_{w_{2,0}} \hat{s}_{w_{2,1}}, \cdots, \hat{s}_{w_{2,Y-1}}] \\ &= [s_{0_2} h_{-Y}^2 + s_{N_{l_1}} h_X h_{-Y}, \cdots, s_{Y-1_2} h_{-1}^2,\ s_{Y_2} h_0^2, \cdots, \\ &\quad s_{N_{l_2}} h_X^2 + s_{0_3} h_X h_{-Y}, \cdots, \\ &\quad s_{N_{symb}-1_2} h_{Y-1}^2 + s_{N_{\text{symb}}-N_{l_3}} h_{Y-1} h_{-X}]\end{aligned} \tag{4.7}$$

The first replica of the first received symbol has no interference from any other symbol, thus, leveraging on the window knowledge, it is possible to estimate the interference caused by the second symbol in the first symbol. By using both the Hadamard multiplication and division operations on the samples from the first symbol's first replica, it is possible to retrieve the data sent on the second replica of the same symbol, that is causing interference with the first replica of the second symbol, as illustrated by figure 4.5. Afterwards, by subtracting the interfered portion of the first symbol's second replica with the samples from the first replica of the second symbol, the original data can be recovered. The samples of the distorted second symbol are given by $\hat{s}_{w_2,j}$, where $j = -\frac{N}{2}(1-\beta), \cdots, \frac{N}{2}(1-\beta)$. If we consider a sample at indexes $j = -\frac{N}{2}, \cdots, -\frac{N}{2}(1-\beta)$, the original sample can be recovered

through

$$\hat{s}^{I}_{w_2,j} = \hat{s}_{w_2,j} - h^2_{(j+N_l)} \frac{\hat{s}_{w_1,j}}{h^2_j} \tag{4.8}$$

This procedure is iterative, allowing to estimate the distortion introduced in a symbol i, $i = 1,...,N_s$, due to the symbol $i-1$, i.e.,

$$\hat{s}^{I}_{w_i,j} = \hat{s}_{w_i,j} - h^2_{(j+N_l)} \frac{\hat{s}_{w_i-1,j}}{h^2_j} \tag{4.9}$$

In similar fashion, we can perform the cancellation in the backward direction, as shown in 4.5. In this case, samples $j = \frac{N}{2}(1-\beta), \cdots, \frac{N}{2}$ from penultimate symbol are distorted since it contains interference from the left tail of the last symbol. Therefore, it is also possible to estimate the interference caused by the last symbol in the penultimate symbol, following similar analysis. This process is iterative, allowing to estimate the distortion introduced in a symbol i, $i = N_s,...,1$, due to the symbol $i+1$.

4.2.4 MMSE cancellation method

This method is similar to the previous one, however, the calculation of the interference values and partial estimations of the symbols take into account the SNR. Instead of simply using the Hadamard division, we apply a second Hadamard product with the window samples and, later, a Hadamard division that includes the SNR, γ. The forward and backward cancellation method are defined by equation

$$\hat{s}^{I}_{w_i,j} = \hat{s}_{w_i,j} - h^2_{(j+N_l)} \hat{s}_{w_i-1,j} \frac{h^2_j}{\left(h^2_j\right)^2 + \frac{1}{\gamma}} \tag{4.10}$$

where j takes the respective values for each method, previously defined.

Thus, this time domain cancellation algorithm is similar to the usual MMSE FDE algorithm, intending not only to cancel the window's effect but also to minimize the error due to AWGN.

The next sections present the main results regarding the PAPR, the BER performance and the saving in spectrum achieved by the new TIBWB-OFDM with WTO waveform.

4.3 TIBWB-OFDM with WTO Receiver with Linear Equalizers Results

The first receiver embodiment was considered for a single input single output (SISO) channel. Its architecture is represented in figure 4.6. This receiver

architecture consists on a linear equalizer at frequency domain to cancel channel impairments, while a time domain linear equalizer of the type forward and backward successive cancellation is employed to cancel out windowing time overlapping distortion.

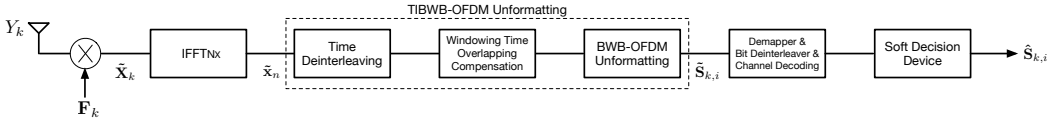

Figure 4.6: TIBWB-OFDM with WTO receiver with a linear equalizer in both frequency and time domains.

4.3.1 PAPR Issue

The following simulations aim to compare the PAPR of the TIBWB-OFDM waveforms with and without the symbol overlap operation, as a function of the amount of overlapping samples, which depends on N_l and the window roll-off, β. In addition, the PAPR of an OFDM signal with the same length as the TIBWB-OFDM signal, that is, $N_{OFDM} = NN_s(1+\beta)$, was calculated. In all the simulations it was considered $N = 64$ sub-carriers, $N_s = 16$ blocks and QPSK modulation under a Gray coding rule.

PAPR as function of time overlapping

By keeping the window roll-off set at $\beta = 0.5$, $\beta = 0.25$ and $\beta = 0.1$ and by varying the number of overlapping samples between adjacent symbols (N_{os}), through N_l, the PAPR's CCDF of the OFDM, TIBWB-OFDM and TIBWB-OFDM with WTO transmitted signals were plotted for different values of N_l.

As illustrated by figures 4.7, 4.8 and 4.9 it can be concluded that by introducing the overlapping operation, the new waveform has lower PAPR values when compared to the non-overlapped waveform, since $\mu = \frac{N}{N_l}$ represents the ratio between the number of sub-carriers, N, and the first overlapped sample of the sub-block, N_l. In addition, the PAPR decreases with increasing number of overlapping samples, i.e., lowering N_l. As previously stated, the PAPR also depends on the window roll-off, decreasing as the roll-off decreases.

PAPR as function of the window roll-off

Alternatively, in order to corroborate the last statement, another simulation was performed. In this case, by keeping N_l fixed at $N_l = 64$, i.e., $\mu = 1$, and by changing the window roll-off, β, the PAPR of the TIBWB-OFDM and TIBWB-OFDM with

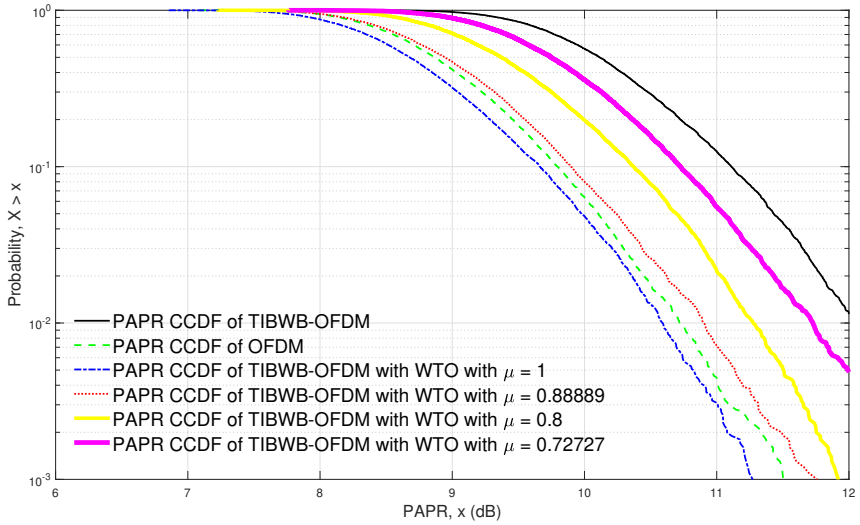

Figure 4.7: PAPR's CCDF of the OFDM, TIBWB-OFDM with and without WTO transmitted signals for $\beta = 0.5$.

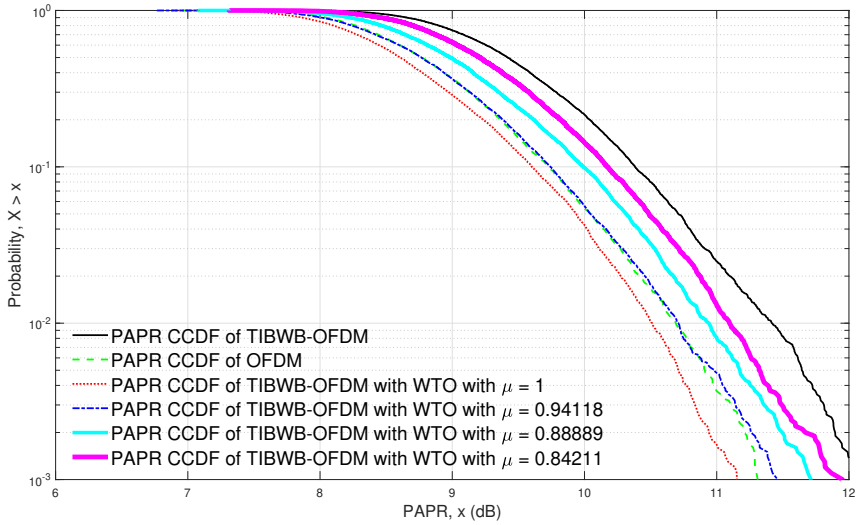

Figure 4.8: PAPR's CCDF of the OFDM, TIBWB-OFDM with and without WTO transmitted signals for $\beta = 0.25$.

WTO transmitted signals, for which its $CCDF = 10^{-3}$, were plotted for different values of β.

Figure 4.10 shows that the PAPR values are almost independent of the window roll-off for the overlapped waveform whereas the PAPR values of the non-overlapped waveform tend to grow with increasing roll-off.

4.3.2 BER performance

The following simulations aim to evaluate and compare the BER performances results concerning the TIBWB-OFDM waveforms with and without the symbol

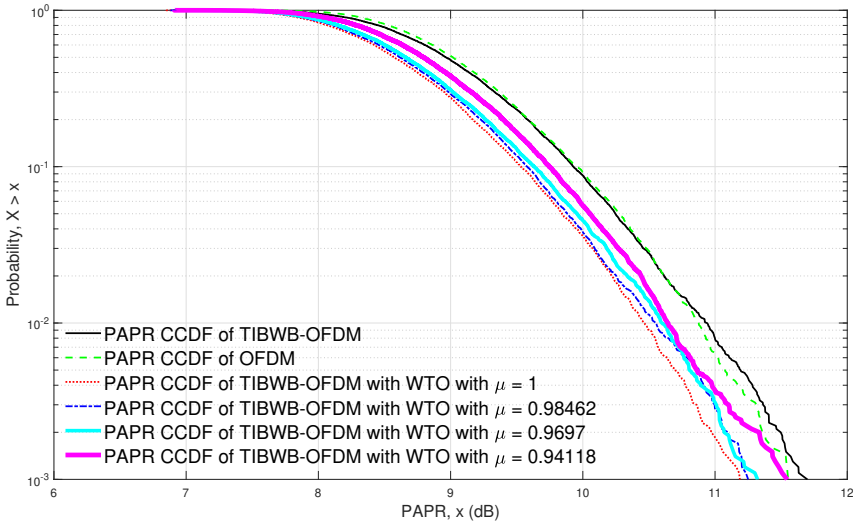

Figure 4.9: PAPR's CCDF of the OFDM, TIBWB-OFDM with and without WTO transmitted signals for $\beta = 0.1$.

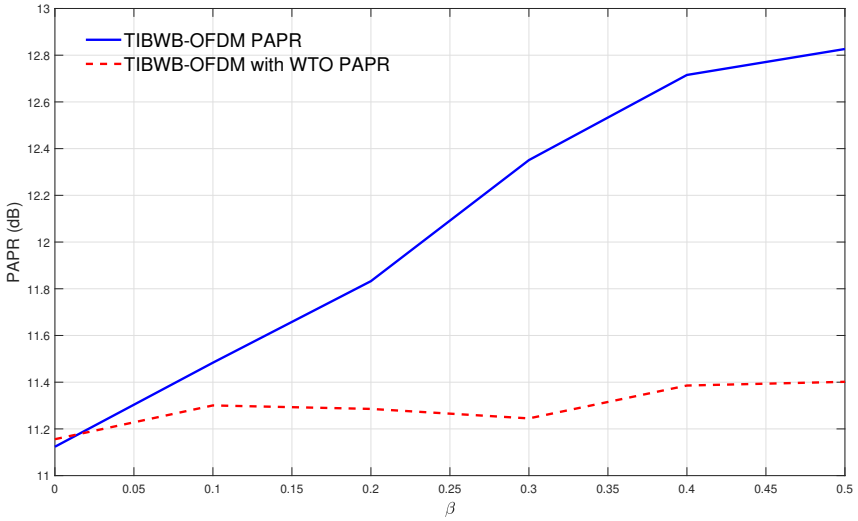

Figure 4.10: PAPR of TIBWB-OFDM with and without WTO at $CCDF = 10^{-3}$ as function of the window roll-off, β.

overlap operation (for the sake of comparisons, it was also considered conventional OFDM/CP-OFDM schemes), over two channel types: an AWGN channel and a severely TD channel with 32 symbol-spaced multipath components with uncorrelated Rayleigh fading. Perfect synchronization and channel estimation are assumed at the receiver. In addition, these simulations also present the BER performances of the TIBWB-OFDM with WTO and the standard TIBWB-OFDM as a function of the window roll-off, β and highlight the role of the proposed receiver. The number of sub-carriers for the TIBWB-OFDM waveforms is $N = 64$ and the number of blocks is $N_s = 16$. Moreover, the overlapping operation is performed with $N_l = N$. Con-

sequently, in the AWGN channel the TIBWB-OFDM with WTO transmitted mega-block has a total length of $N_{OB} = N_l\,(N_s - 1) + N_{symb} = 1056$, while the standard TIBWB-OFDM transmitted mega-block has a total length of $N_B = N_s N_{symb} = 1536$. QPSK constellations with a Gray coding rule are applied. To cope with a TD channel, a ZP of length $N_{zp} = 32$ is added to both signals, leading to overall blocks with length $N_x = 1088$ and $N_{x2} = 1568$, respectively. The OFDM transmitted symbol has a length of $N_{OFDM} = N_x$ or $N_{OFDM} = N_x + N_{cp}$ for the AWGN channel and TD channel, respectively. Similarly, the CP has a length of $N_{cp} = \frac{N}{2} = 32$. Unless otherwise stated, channel coding is employed using a $(128, 64)$ short low-density parity-check (LDPC) code and bit-interleaving is applied over 10 consecutive coded words. The following results concern the use of a MMSE FDE receiver to cope with channel impairments.

TIBWB-OFDM *vs* TIBWB-OFDM with WTO in a receiver without interference cancellation

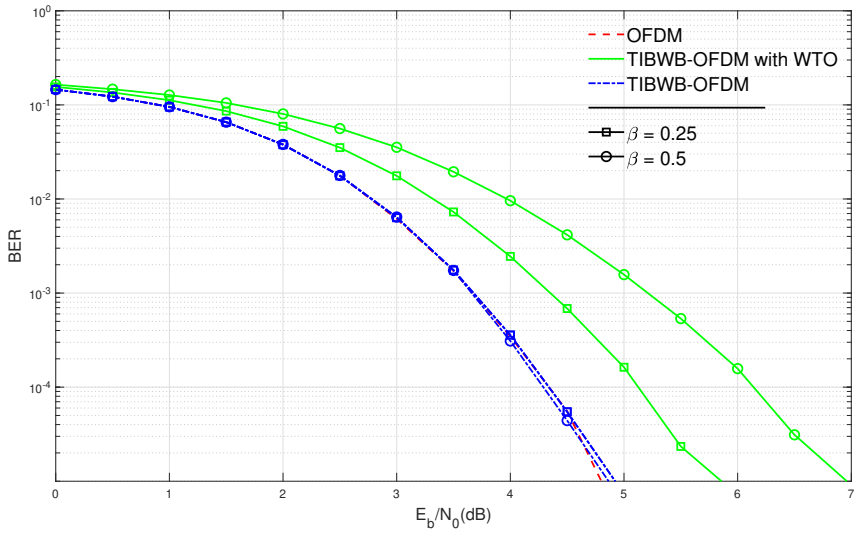

Figure 4.11: BER results for OFDM , TIBWB-OFDM with and without WTO over an AWGN channel as a function of β employing the no-cancellation receiver.

Figures 4.11 and 4.12 show, respectively, the BER performance for OFDM and TIBWB-OFDM with and without WTO when the receiver does not employ the overlapping cancellation operation. Clearly, although the window roll-off, β, has no effect on the BER performance concerning the TIBWB-OFDM technique, it plays an important role on the TIBWB-OFDM with WTO case. This can be explained by recognizing that a higher window roll-off means that the TIBWB-OFDM blocks grow larger which results in a greater number of interfering samples in time domain, since $N_l = N = 64$ is kept constant in all simulations. Also, the performance of the

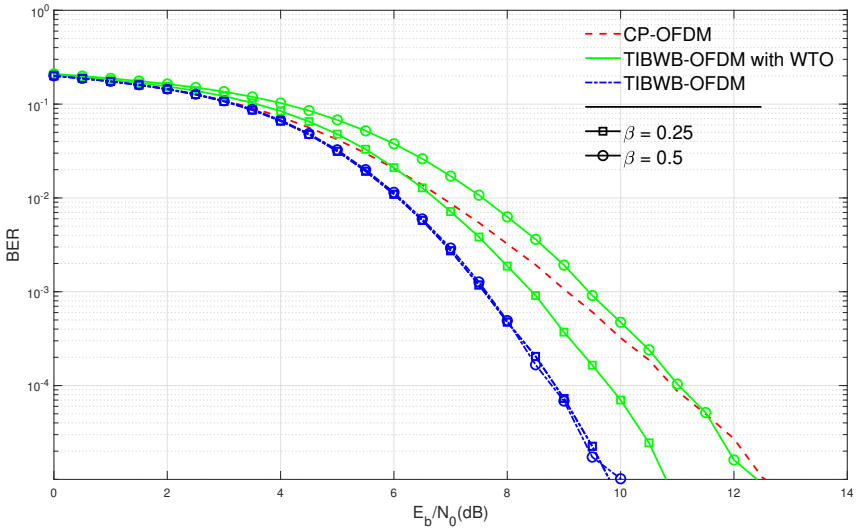

Figure 4.12: BER results for OFDM, TIBWB-OFDM with and without WTO over a TD channel as a function of β employing the no-cancellation receiver.

TIBWB-OFDM technique is identical to the conventional OFDM when transmitting in an AWGN channel. It also can be observed that, even without the cancellation operation, the BER performance of the TIBWB-OFDM with WTO tends to be better than the CP-OFDM, in the TD channel, which is due to the time-interleave operation that creates a kind of diversity effect.

TIBWB-OFDM with WTO MMSE *vs* ZF receiver *vs* no-cancellation receiver

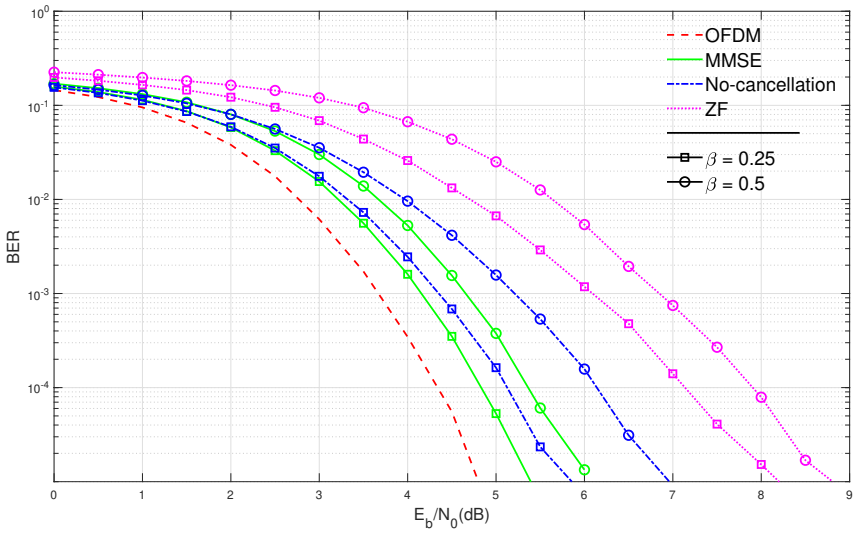

Figure 4.13: BER results for TIBWB-OFDM with WTO over an AWGN channel as a function of β employing a MMSE, ZF and a no-cancellation receiver.

Figure 4.13 compares the BER performance over the same AWGN channel for OFDM and the new TIBWB-OFDM with WTO while employing three different

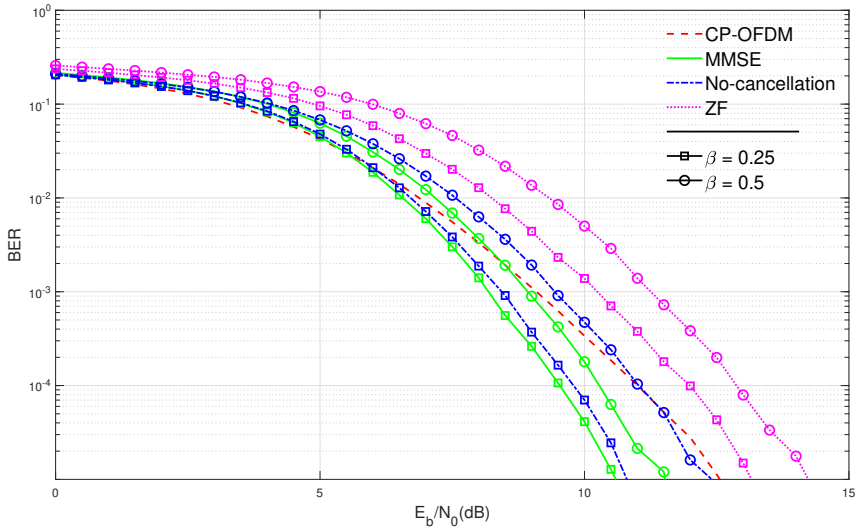

Figure 4.14: BER results for TIBWB-OFDM with WTO over a TD channel as a function of β employing a MMSE, ZF and a no-cancellation receiver.

receivers: the time domain ZF cancellation method; the time domain MMSE cancellation operation; and the case without cancellation. Figure 4.14 presents similar results, regarding a TD channel. Clearly, both figures show that, when channel coding is applied, the ZF cancellation method has a performance that is even worse than the classic TIBWB-OFDM receiver (without the time domain equalization operation), with a degradation of about $2dB$. However, for the MMSE cancellation, the receiver shows a slight performance gain (less than $1dB$ when comparing with the no-cancellation receiver) than the no-cancellation receiver, regardless of the window roll-off factor.

TIBWB-OFDM with WTO MMSE *vs* ZF *vs* genie *vs* no-cancellation receiver

Figures 4.15 and 4.16 present the TIBWB-OFDM BER performances, while applying the overlapping operation for different window roll-offs (0.25 and 0.5), with the previous receivers, as well as for the case with perfect reconstruction (PR), i.e., a genie receiver where there is an ideal cancellation of the symbols tail's effects and the interference resulting from this process is perfectly eliminated. It can be seen, in both figures, that the receiver with a MMSE cancellation is the one with better performance with results that are the closest to the ideal receiver for both channel types (only $1dB$ or less from the case with perfect cancellation).

TIBWB-OFDM with WTO sub-blocks

Figures 4.17 and 4.18 present the BER results for some sub-blocks (first, seventh, thirteenth and sixteenth) that make up the TIBWB-OFDM with WTO received signal in both channel types, for $\beta = 0.5$ and $\beta = 0.25$, in a scenario with uncoded

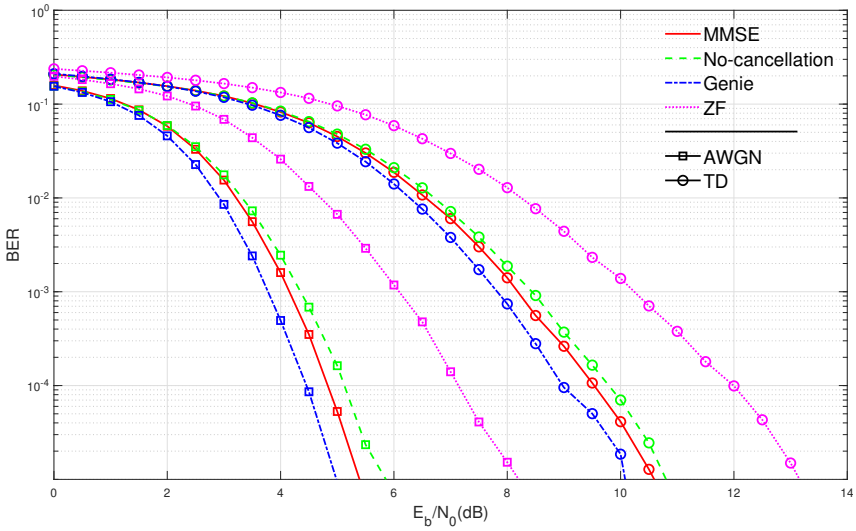

Figure 4.15: BER results for TIBWB-OFDM with WTO employing a MMSE, ZF, genie and a no-cancellation receiver for $\beta = 0.25$.

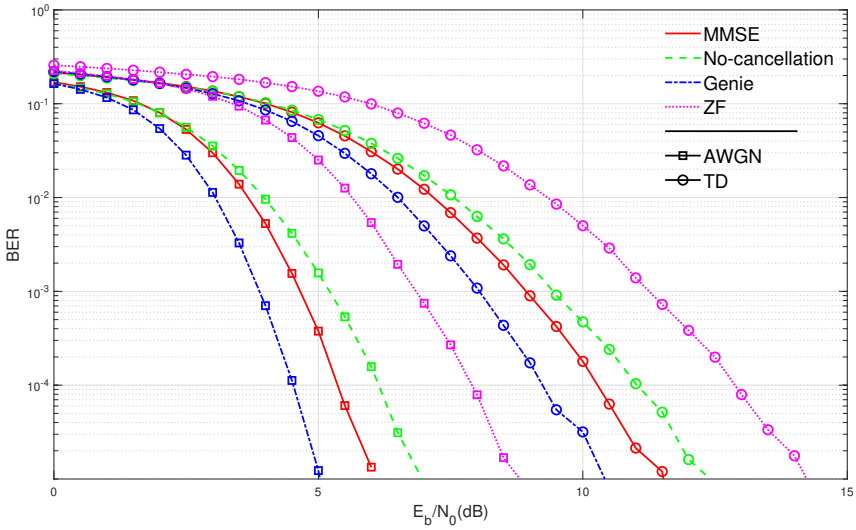

Figure 4.16: BER results for TIBWB-OFDM with WTO employing a MMSE, ZF, genie and a no-cancellation receiver for $\beta = 0.5$.

transmission and where the time domain MMSE interference cancellation algorithm is applied to the received overlapped signal. In both figures, it is clear the successive cancellation between each sub-block's tail. Regardless of the roll-off, it can be noticed that the first and the last sub-blocks have better performance than the remaining blocks (i.e. the ones in the middle). This can be explained by the fact that the edge sub-blocks (first and last) have half the number of interfering samples than the remaining blocks. Furthermore, the estimation of each sub-block is used to reconstruct the next sub-block through a backward and a forward iterative process, as mentioned previously. Hence, the error propagation is also a concern in this

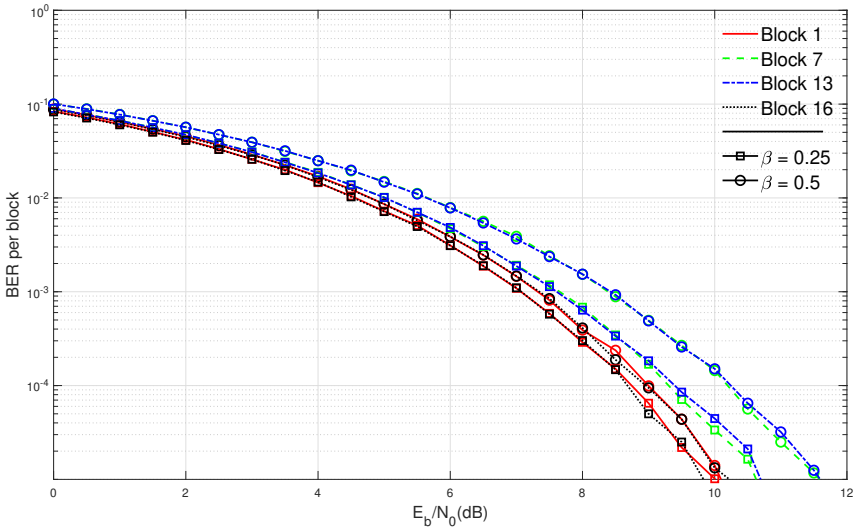

Figure 4.17: BER results for some TIBWB-OFDM's with WTO sub-blocks using a MMSE receiver in an AWGN channel.

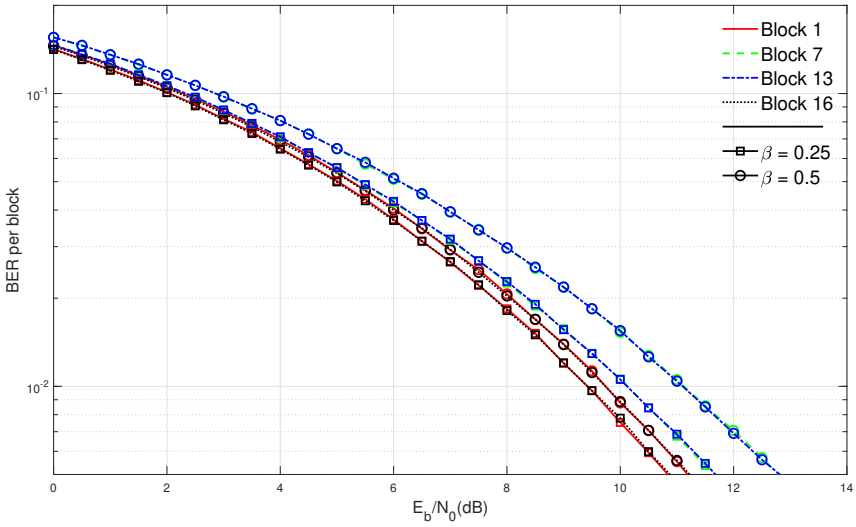

Figure 4.18: BER results for some TIBWB-OFDM's with WTO sub-blocks using a MMSE receiver in a TD channel.

transmission scheme.

4.4 TIBWB-OFDM with WTO Receiver with Iterative Frequency Domain Equalizer Results

A second embodiment of the TIBWB-OFDM with WTO receiver consists on an iterative equalizer at frequency domain, of the type IB-DFE, maximum ratio combining (MRC) or equal gain combining (EGC) [11] employed to cancel the channel impairments, while a time domain linear equalizer of the type forward and backward successive cancellation is employed to cancel out windowing time over-

lapping distortion. A sketch of this receiver is presented in figure 4.19.

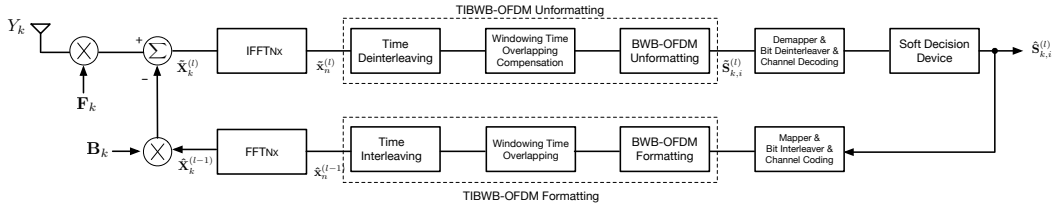

Figure 4.19: TIBWB-OFDM with WTO receiver with frequency domain iterative equalizer and time domain linear equalizer.

The next simulations present the set of results, for SISO case, concerning the employment of the Turbo-IB-DFE principle on the TIBWB-OFDM with and without WTO receivers, for the transmission scenario over the TD channel previously mentioned with channel coding and bit-interleaving applied over 21 consecutive coded words. In these simulations it was considered $N = 64$ sub-carriers, $N_s = 42$ blocks, QPSK modulation under a Gray coding rule, a SRRC window with $\beta = 0.5$ and $\beta = 0.25$ and the overlapping operation is performed with $N_l = N$ for the TIBWB-OFDM with WTO case. These simulations aim to compare the BER performance of the TIBWB-OFDM with WTO transmission under the MMSE criteria and the first 4 iterations of the TIBWB-OFDM with WTO transmission with an IB-DFE receiver. In addition, it would be useful to analyze and compare the performance of both receivers provided by the use of the Turbo IB-DFE technique, while transmitting a coded sequence of TIBWB-OFDM symbols, with and without the overlapping operation between its adjacent sub-symbols. Two situations for the computation of the IB-DFE block-wise reliability ρ_{blk} are studied.

4.4.1 IB-DFE with *hard decisions*

Figure 4.20 presents the TIBWB-OFDM with WTO BER performances for $\beta = 0.5$ and $\beta = 0.25$, using the ρ_{blk} approximation employing the input $\tilde{x}_n$ and output $\hat{x}_n$ of the *hard decision* device. Figure 4.21 allows to compare this performance with the BER performance for the TIBWB-OFDM case.

When employing the IB-DFE with *hard decisions*, the TIBWB-OFDM mega-block is unformatted and each constellation symbol loaded in each sub-carrier of the OFDM original symbols is estimated through the minimum distance criteria. This estimation is performed by a decision device and, then, it is used to format the presumably original TIBWB-OFDM mega-block, compute the correlation factor through (3.19) and the filter coefficients through (3.16) and (3.17).

Both figures show that the proposed TIBWB-OFDM with and without WTO

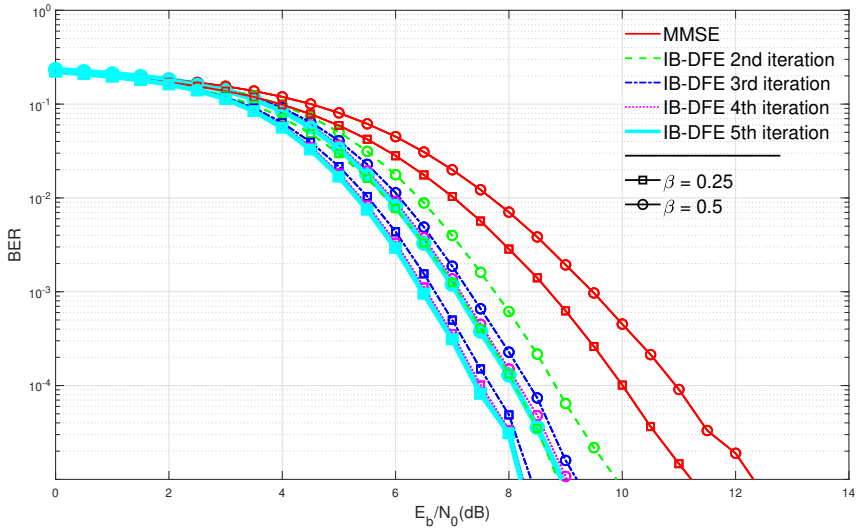

Figure 4.20: BER performance for TIBWB-OFDM with WTO employing the IB-DFE receiver with *hard decisions*, for $\beta = 0.5$ and $\beta = 0.25$.

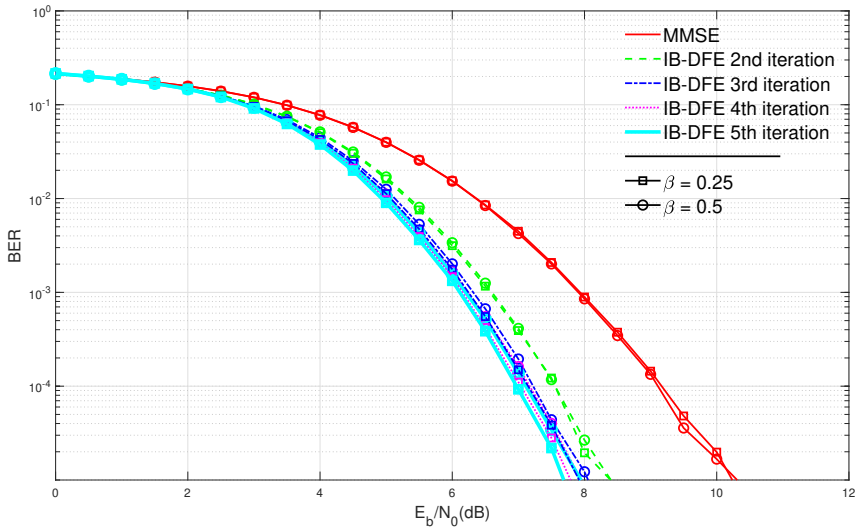

Figure 4.21: BER performance for TIBWB-OFDM employing the IB-DFE receiver with *hard decisions*, for $\beta = 0.5$ and $\beta = 0.25$.

IB-DFE receiver with *hard decisions*, when transmitting a coded sequence, has an improvement (around $1.7dB$ for the overlapped waveform and $2.3dB$ for the TIBWB-OFDM case) in BER performance over the TIBWB-OFDM with and without WTO MMSE criteria, with just two iterations of the IB-DFE algorithm. Besides, in both transmission scenarios, the IB-DFE receiver can deal with occurring deep fades with small error propagation and shows some evolution from iteration to iteration [1, 30]. However, it is clear that this evolution is much more pronounced for the TIBWB-OFDM with WTO transmission since each iteration allows a better estimate of the transmitted signal. This can be understood keeping in mind that each

iteration provides a better reconstruction of the transmitted TIBWB-OFDM signal, cancelling the effect of the overlapping operation between the adjacent sub-blocks, by applying iteratively the time domain interference cancellation algorithm to the received signal. These simulations also show that, although the TIBWB-OFDM IB-DFE receiver can achieve a determined BER with just a few iterations, it is possible for the TIBWB-OFDM with WTO IB-DFE receiver to almost match its BER performance with a few more iterations. For this case, we observe that at the 1-st iteration (MMSE receiver) the TIBWB-OFDM receiver outperforms the TIBWB-OFDM with WTO receiver by a large margin, where the bulk of gain is about $0.8dB$ and $1.6dB$, when $\beta = 0.25$ and $\beta = 0.5$, respectively. Nevertheless, at the 5-th iteration of the IB-DFE algorithm, the TIBWB-OFDM receiver has a gain around $0.3dB$, for the $\beta = 0.25$ case and around $0.9dB$ for the $\beta = 0.5$ case, when compared to the TIBWB-OFDM with WTO receiver. Finally, we can reinforce the idea that although the window roll-off, β, has no influence on the BER performance concerning the TIBWB-OFDM technique, it has a huge impact on the TIBWB-OFDM with WTO BER performance since a higher roll-off corresponds to a large number of overlapped samples, considering that $N_{os} = N_{symb} - N_l = N(1+\beta) - N_l$.

4.4.2 IB-DFE with *soft decisions*

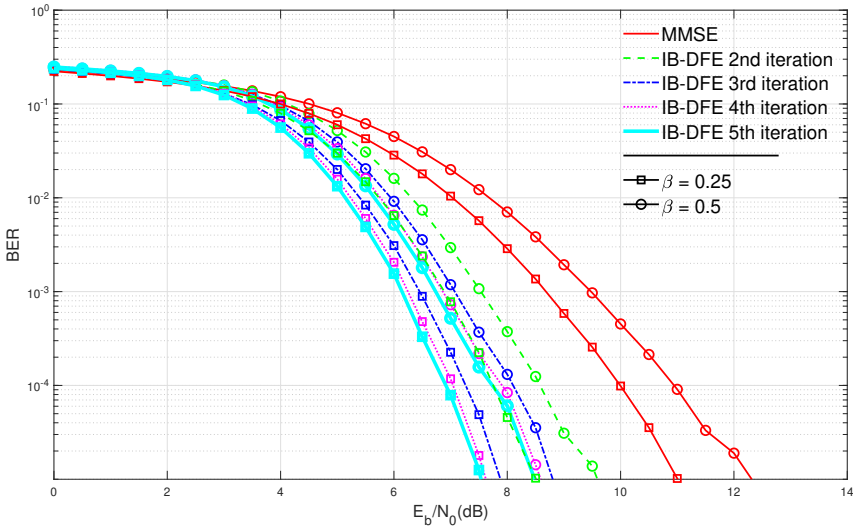

Figure 4.22: BER performance for TIBWB-OFDM with WTO employing the IB-DFE receiver with *soft decisions*, for $\beta = 0.5$ and $\beta = 0.25$.

Figures 4.22 and 4.23 present, respectively, the TIBWB-OFDM with and without WTO BER performances for $\beta = 0.5$ and $\beta = 0.25$, using the proposed block-wise *soft* reliability factor $\tilde{\rho}_{blk}$.

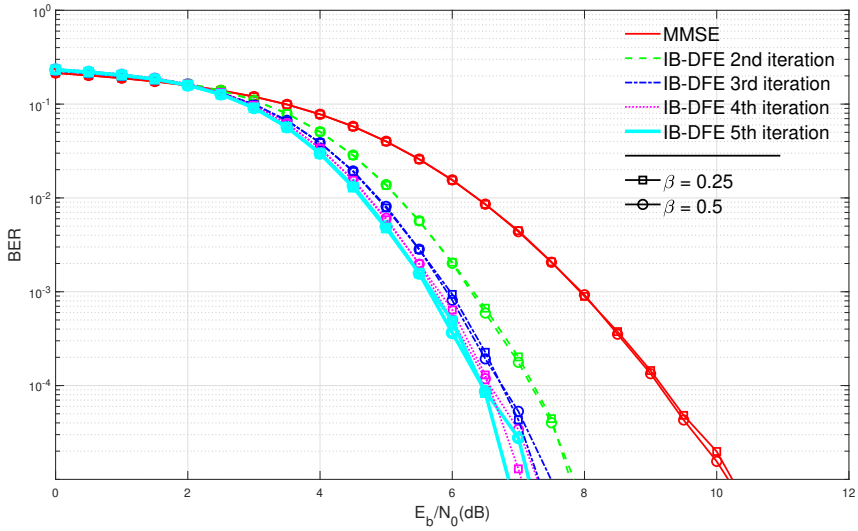

Figure 4.23: BER performance for TIBWB-OFDM employing the IB-DFE receiver with *soft decisions*, for $\beta = 0.5$ and $\beta = 0.25$.

When employing the Turbo-IB-DFE with *soft decisions*, both systems are expected to improve in BER performance. This is done by including a coder/decoder and a bit-interleaver/bit-deinterleaver on the FB loop and calculating the average bit values through (3.22) and (3.23). Unlike the IB-DFE with *hard decisions* that employs a decision device, estimating the transmitted symbol/bit based on the minimum distance criteria, the Turbo-IB-DFE with *soft decisions* calculates the LLR of the transmitted bits, through (3.24) and (3.25), allowing a better estimate of the original bit-stream and, consequently, the reliability factor, ρ_{blk}, through (3.26). This procedure helps to obtain a better measurement of the residual interference and reduces the errors caused by occurring deep fades [30]. Both figures show that the proposed TIBWB-OFDM with and without WTO IB-DFE receiver with *soft decisions*, when transmitting a coded sequence, has a considerable gain in BER performance over the TIBWB-OFDM with and without WTO receivers employing the IB-DFE technique with *hard decisions*. The BER performance gain of the TIBWB-OFDM with WTO receiver, employing the *soft* IB-DFE technique, is more noticeable through each iteration, when compared to the receiver employing the *hard* IB-DFE technique. The bulk of gain at $BER = 10^{-3}$ is about $0.25dB$ for the 2-nd iteration, $0.23dB$ for the 3-rd, $0.28dB$ for the 4-th and $0.36dB$ for the 5-th iterations, when $\beta = 0.5$ and about $0.23dB$ for the 2-nd iteration, $0.24dB$ for the 3-rd, $0.31dB$ for the 4-th and $0.36dB$ for the 5-th iterations, when $\beta = 0.25$. The BER performance improvement of the TIBWB-OFDM receiver, employing the *soft* IB-DFE technique, is also improved in each iteration, when compared to the receiver employing the *hard* IB-DFE technique. The bulk of gain is roughly $0.3dB$

for all the iterations, when $\beta = 0.5$ and $\beta = 0.25$.

4.5 TIBWB-OFDM with WTO Receiver with Iterative Time Domain Equalizer Results

In this section, a third embodiment of the TIBWB-OFDM with WTO receiver is presented.

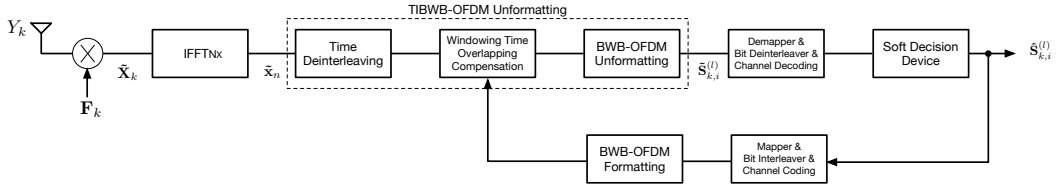

Figure 4.24: TIBWB-OFDM with WTO receiver with frequency domain linear equalizer and time domain iterative equalizer.

It relies on a linear equalizer at frequency domain, such as MMSE or ZF, to reverse channel effects, while an iterative interference cancellation time domain equalizer (IIC-TDE) is employed to eliminate the overlapping distortion. The time domain equalizer performed in the first stage consists on a forward and backward successive cancellation, such as the MMSE or ZF cancellation operations, previously described, while in the following stages uses the prior estimated TIBWB-OFDM signal. A sketch of this receiver is presented in figure 4.24.

The next simulations present the set of results, for SISO case, concerning the employment of this receiver with non-iterative MMSE FDE. In the first iteration a MMSE successive cancellation algorithm is also employed. These simulations aim to evaluate the BER performance of the TIBWB-OFDM with WTO transmission scheme while applying the IIC-TDE algorithm with 3 iterations and comparing it with the TIBWB-OFDM scenario.

In the previous section, it was stated that the BER evolution was more pronounced for the TIBWB-OFDM with WTO transmission since each iteration allowed a better estimate of the transmitted signal by applying iteratively the time domain equalizer to the received signal. In this receiver, instead of applying iteratively the time domain equalizer to the received signal, each iteration (except the first one) performs the time domain equalization algorithm assuming that the prior estimated signal is the one that allows a perfect reconstruction of the distorted signal. Figure 4.25 displays the gains in BER performance achieved by employing the IIC-TDE in the TIBWB-OFDM with WTO receiver. The TIBWB-OFDM with WTO IIC-TDE receiver can almost achieve the BER performance of the TIBWB-OFDM with just 3

IIC-TDE iterations. For this case, we observe that at the 1-st iteration (MMSE time domain equalizer) the TIBWB-OFDM receiver outperforms the TIBWB-OFDM with WTO receiver by a relatively large margin, where the bulk of gain is about $1dB$ and $1.7dB$, when $\beta = 0.25$ and $\beta = 0.5$, respectively. Nonetheless, at the 3-rd iteration of the IIC-TDE algorithm, the TIBWB-OFDM receiver has a gain of around $0.3dB$, for the $\beta = 0.25$ case and around $0.6dB$ for the $\beta = 0.5$ case, when compared to the TIBWB-OFDM with WTO receiver. These results suggest that this receiver, when combined with the IB-DFE algorithm, can achieve a better performance, when compared to the case where only the IB-DFE is employed at the TIBWB-OFDM with WTO receiver.

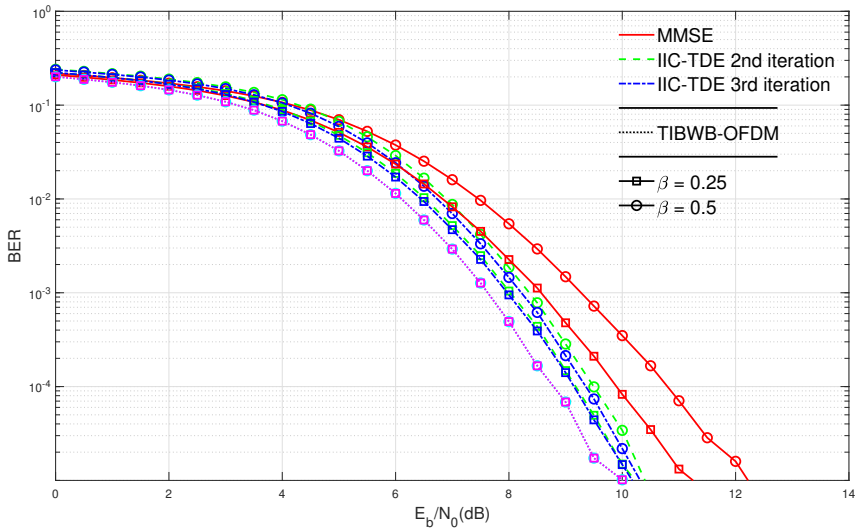

Figure 4.25: BER performance for TIBWB-OFDM with and without WTO receiver employing the IIC-TDE algorithm, for $\beta = 0.5$ and $\beta = 0.25$.

4.6 TIBWB-OFDM with WTO Receiver with Iterative Equalizers Results

In this section, a last embodiment of the TIBWB-OFDM with WTO receiver is discussed. It consists on a combination of both previously presented receivers, wherein an iterative equalizer at frequency domain, of the type IB-DFE, MRC or EGC and a IIC-TDE are employed. A sketch of this receiver is presented in figure 4.26.

The produced graphics present the set of results, for SISO channel, concerning the employment of this receiver. All simulation parameters were kept constant. These simulations aim to evaluate the BER performance of the TIBWB-OFDM with WTO transmission scheme when both the IB-DFE and IIC-TDE algorithms

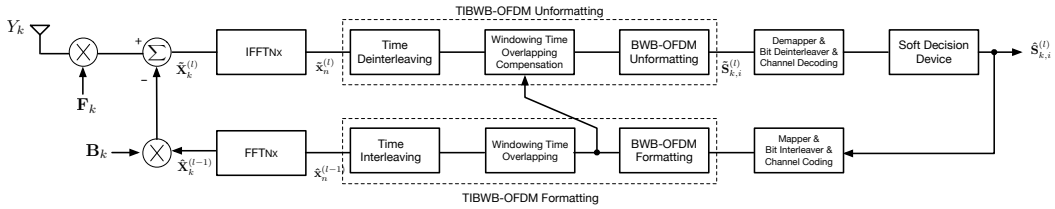

Figure 4.26: TIBWB-OFDM with WTO receiver with frequency domain and time domain iterative equalizers.

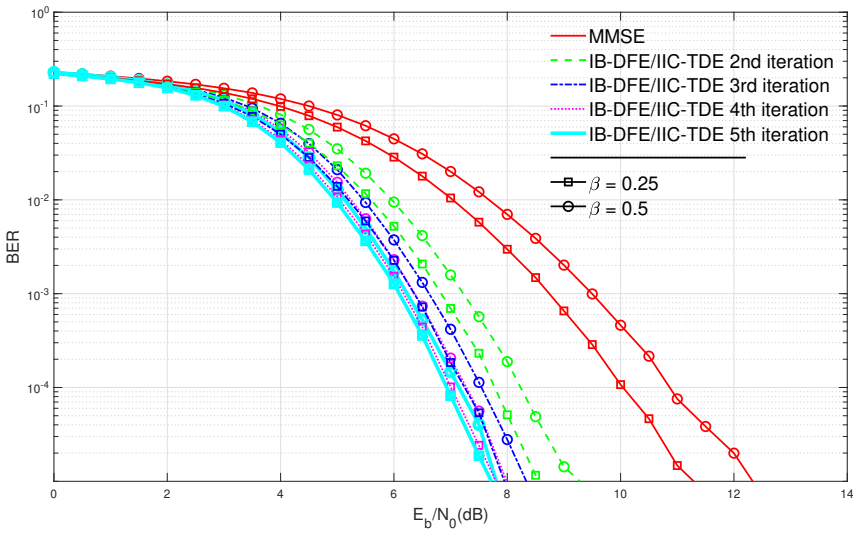

Figure 4.27: BER performance for TIBWB-OFDM with WTO receiver employing both the IB-DFE and IIC-TDE algorithms with *hard decisions*, for $\beta = 0.5$ and $\beta = 0.25$.

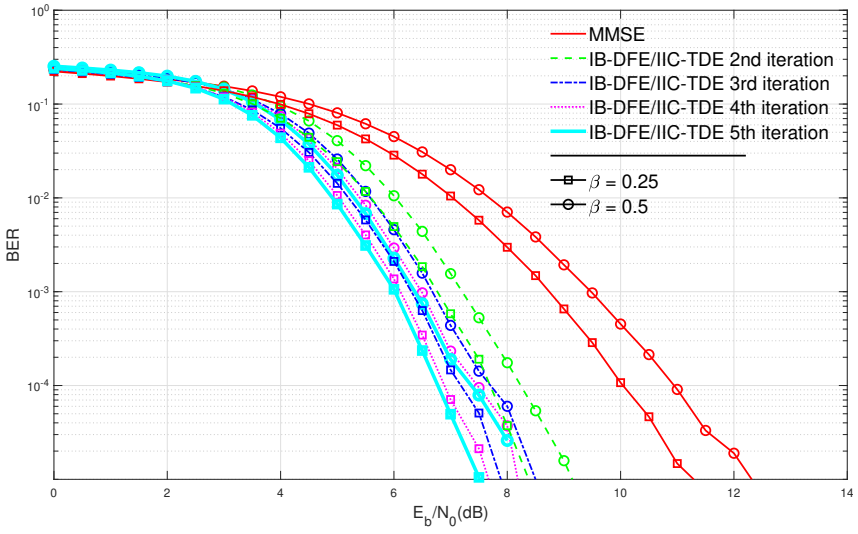

Figure 4.28: BER performance for TIBWB-OFDM with WTO receiver employing both the IB-DFE and IIC-TDE algorithms with *soft decisions*, for $\beta = 0.5$ and $\beta = 0.25$.

with 5 iterations are applied. The same two situations for the computation of the IB-DFE block-wise reliability ρ_{blk} were considered.

Both figures show a combination of the BER performance from the two previous presented receiver. It is clear that the gains in BER performance tends to improve per IB-DFE iteration, being more noticeable for the IB-DFE case with *soft decisions*. Additionally, along each IB-DFE iteration, the BER results improve per IIC-TDE iteration. This iterative process allows achieving a better performance, when compared to both previous cases:

- IB-DFE, where the FDE only deals with the channel impairments.
- IIC-TDE, where the time domain equalizer only deals with the time overlapping interference.

We observe that at the 5-th iteration the TIBWB-OFDM IB-DFE receiver with *hard decisions* (figure 4.21) has yet a considerable gain over the TIBWB-OFDM with WTO IB-DFE receiver with *hard decisions* (figure 4.20), where the bulk of gain is roughly around $0.3dB$ and $0.9dB$, when $\beta = 0.25$ and $\beta = 0.5$, respectively. However at the 5-th iteration the BER performances of both TIBWB-OFDM IB-DFE receiver with *hard decisions* and TIBWB-OFDM with WTO IIC-TDE/IB-DFE receiver with *hard decisions* (figure 4.27) are almost similar when $\beta = 0.25$. When $\beta = 0.5$ the first receiver outperforms the second one and the bulk of gain is around $0.05dB$.

It also can be concluded that at the 5-th iteration the TIBWB-OFDM IB-DFE receiver with *soft decisions* (figure 4.23) has a significant gain over the TIBWB-OFDM with WTO IB-DFE receiver with *soft decisions* (figure 4.22), where the bulk of gain is around $0.45dB$ and $1dB$, when $\beta = 0.25$ and $\beta = 0.5$, respectively. However at the 5-th iteration the TIBWB-OFDM IB-DFE receiver with *soft decisions* has smaller gains when compared to the TIBWB-OFDM with WTO IIC-TDE/IB-DFE receiver with *soft decisions* (figure 4.28), where the bulk of gain is around $0.3dB$ and $0.65dB$, when $\beta = 0.25$ and $\beta = 0.5$, respectively. Therefore, this receiver embodiment is the one that presents the best BER results and exhibits the same complexity as the IB-DFE receiver, since the signal reconstruction performed in the FB loop also enables to cancel the time domain interference resulting from the overlapping operation.

4.7 Spectrum Saving

As mentioned earlier in this chapter, one concern about the standard TIBWB-OFDM technique is the increase in the sub-symbol's length. In fact, larger blocks

lead to higher sensibility to both carrier frequency offset (CFO) and Doppler effects. These phenomena occur in frequency dispersive (FD) channels, also known as time selective channels, where the user mobility is taken into account. Therefore, taking as reference the channel coherence time, the admissible maximum Doppler drifts or any residual CFO are reduced by a factor equal to the ratio of the TIBWB-OFDM block duration, i.e., N_x, and the conventional OFDM block duration which is $N(1+\beta)$ [1]. The TIBWB-OFDM with WTO transmission scheme can be modelled not to produce an increase in the symbol's length. This way, the TIBWB-OFDM with WTO waveform allows a spectrum saving, compared to the TIBWB-OFDM waveform, which is proportional to the temporal growth of the OFDM-based blocks. The temporal extension of the sub-blocks are proportional to roll-off, β and can be observed by figures 4.29 where $\beta = 0.5$ and 4.30 where $\beta = 0.25$.

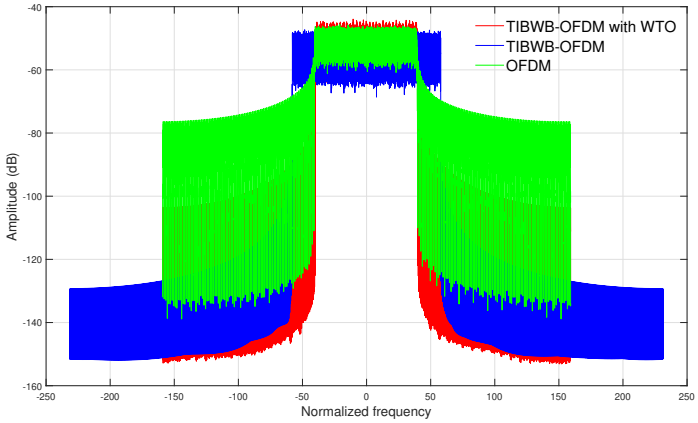

Figure 4.29: Power spectrum of OFDM and TIBWB-OFDM with and without WTO with $N_l = 64$, for $\beta = 0.5$.

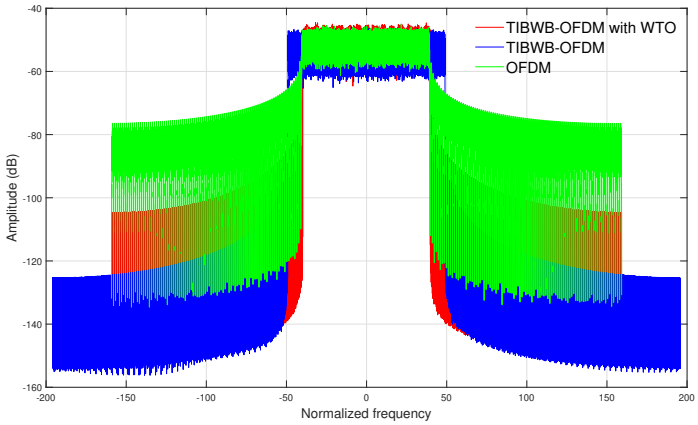

Figure 4.30: Power spectrum of OFDM and TIBWB-OFDM with and without WTO with $N_l = 64$, for $\beta = 0.25$.

5

Conclusions

Contents

This thesis addressed a modified version of the TIBWB-OFDM signal by allowing a partial time domain overlap between the adjacent OFDM-based sub-symbols that compose the overall signal, termed TIBWB-OFDM with WTO.

This new waveform eases deterioration in the signal's PAPR, produced by the windowing operation performed in the TIBWB-OFDM transmitter. This is done through the overlapping operation that attenuates the effect of the windowing operation.

The PAPR of the transmitted signal was evaluated for both TIBWB-OFDM with and without WTO scenarios by calculating its CCDF. It could be seen that the PAPR achieved for the classic TIBWB-OFDM case was heavily dependent of the roll-off employed in the windowing operation. Otherwise, the PAPR obtained in the TIBWB-OFDM with WTO was almost independent of the roll-off value. Besides, the probability of getting a high PAPR tends to decline when the number of overlapped samples in the signal increases by lowering N_l.

Furthermore, this new waveform allows achieving an increased spectral efficiency since it eliminates the signal temporal expansion, as verified in the TIBWB-OFDM case. However, this transmission scheme introduces interference between the data sent by consecutive sub-symbols, bringing the necessity of developing interfering cancellation algorithms, in time domain, to enhance the BER performance of the current receiver. BER results were observed for two window roll-off values in order to evaluate its impact. It can be concluded that a larger roll-off produces worse results, keeping N_l constant, since it increases the degree of signal distortion.

Under MMSE FDE and channel coding, the MMSE non-iterative interference cancellation time domain equalizer was the one that showed the best BER results when transmitting both in an AWGN channel and a TD channel, outperforming the receiver with no interference cancellation. The BER performance was also appraised for different receiver embodiments consisting of non-iterative and iterative equalization algorithms to cancel both channel impairments, at frequency domain (FDE) and interference resulting from the overlapping operation, at time domain. The BER performance was greatly improved when the IB-DFE algorithm was included in the TIBWB-OFDM with WTO receiver and when the IIC-TDE was employed, the BER results almost matched the ones from TIBWB-OFDM. Finally a combination of the two iterative receivers was tested, exhibiting the best overall performance.

5.1 Future Work

Although some interesting results were achieved with the inclusion of the non-iterative and iterative frequency and time domain equalizers in the TIBWB-OFDM with WTO receiver, all simulations were performed for the SISO case and the channel was considered perfectly estimated. Moreover, perfect synchronization between the transmitter and receiver was assumed. Therefore, one of the future work suggestions is the universal software radio peripheral (USRP)-based development of the TIBWB-OFDM with WTO transmission scheme in a more realistic and practical scenario. Since the signal temporal expansion is now avoided, it is straightforward to adapt both the 4G LTE or the new 5G New Radio radio interfaces resource grid for the TIBWB-OFDM with WTO transmission. Another interesting future work sugesstion involves the study of the same transmission scheme but expanding the system regarding a MIMO implementation.

Bibliography

[1] T. Fernandes, A. Pereira, M. Gomes, V. Silva, and R. Dinis, "A new hybrid multicarrier transmission technique with iterative frequency domain detection," *Physical Communication*, vol. 27, pp. 7 – 16, 2018.

[2] J. Nunes, P. Bento, M. Gomes, R. Dinis, and V. Silva, "Block-windowed burst OFDM: a high-efficiency multicarrier technique," *Electronics Letters*, vol. 50, no. 23, pp. 1757–1759, 2014.

[3] X. Lin, J. Li, R. Baldemair, T. Cheng, S. Parkvall, D. Larsson, H. Koorapaty, M. Frenne, S. Falahati, A. Grövlen, and K. Werner, "5G New Radio: Unveiling the Essentials of the Next Generation Wireless Access Technology," *CoRR*, 2018.

[4] A. Osseiran, F. Boccardi, V. Braun, K. Kusume, P. Marsch, M. Maternia, O. Queseth, M. Schellmann, H. Schotten, H. Taoka, H. Tullberg, M. A. Uusitalo, B. Timus, and M. Fallgren, "Scenarios for 5G mobile and wireless communications: the vision of the METIS project," *IEEE Communications Magazine*, vol. 52, no. 5, pp. 26–35, May 2014.

[5] "5G Waveform Candidates," Rohde & Schwarz, Tech. Rep., 06 2016. [Online]. Available: https://www.rohde-schwarz.com/nl/applications/5g-waveform-candidates-application-note_56280-267585.html

[6] X. Zhang, L. Chen, J. Qiu, and J. Abdoli, "On the Waveform for 5G," *IEEE Communications Magazine*, vol. 54, pp. 74–80, 11 2016.

[7] A. A. Zaidi, J. Luo, R. Gerzaguet, A. Wolfgang, R. J. Weiler, J. Vihriala, T. Svensson, Y. Qi, H. Halbauer, Z. Zhao, P. Zetterberg, and H. Miao, "A Preliminary Study on Waveform Candidates for 5G Mobile Radio Communications above 6 GHz," in *2016 IEEE 83rd Vehicular Technology Conference (VTC Spring)*, May 2016, pp. 1–6.

[8] "Study on scenarios and requirements for next generation access technologies," 3rd Generation Partnership Project, Tech. Rep., 03 2017. [Online]. Available: https://portal.3gpp.org/desktopmodules/Specifications/SpecificationDetails.aspx?specificationId=2996

[9] T. Fernandes, M. Gomes, V. Silva, and R. Dinis, "Time-Interleaved Block-Windowed Burst OFDM," in *2016 IEEE 84th Vehicular Technology Conference (VTC-Fall)*, Sep. 2016, pp. 1–5.

[10] R. Hadani, S. Rakib, M. Tsatsanis, A. Monk, A. J. Goldsmith, A. F. Molisch, and R. Calderbank, "Orthogonal Time Frequency Space Modulation," in *2017 IEEE Wireless Communications and Networking Conference (WCNC)*, March 2017, pp. 1–6.

[11] A. Pereira, P. Bento, M. Gomes, R. Dinis, and V. Silva, "TIBWB-OFDM: A Promising Modulation Technique for MIMO 5G Transmissions," in *2018 IEEE 88th Vehicular Technology Conference (VTC-Fall)*, Aug 2018, pp. 1–5.

[12] P. Demestichas, A. Georgakopoulos, D. Karvounas, K. Tsagkaris, V. Stavroulaki, J. Lu, C. Xiong, and J. Yao, "5G on the Horizon: Key Challenges for the Radio-Access Network," *IEEE Vehicular Technology Magazine*, vol. 8, no. 3, pp. 47–53, Sep. 2013.

[13] R. v. Nee and R. Prasad, *OFDM for Wireless Multimedia Communications*, 1st ed. Norwood, MA, USA: Artech House, Inc., 2000.

[14] F. Schaich, "Filterbank based multi carrier transmission (FBMC) — evolving OFDM: FBMC in the context of WiMAX," in *2010 European Wireless Conference (EW)*, April 2010, pp. 1051–1058.

[15] G. Fettweis, M. Krondorf, and S. Bittner, "GFDM - Generalized Frequency Division Multiplexing," in *VTC Spring 2009 - IEEE 69th Vehicular Technology Conference*, April 2009, pp. 1–4.

[16] X. Zhang, M. Jia, L. Chen, J. Ma, and J. Qiu, "Filtered-OFDM - Enabler for Flexible Waveform in the 5th Generation Cellular Networks," in *2015 IEEE Global Communications Conference (GLOBECOM)*, Dec 2015, pp. 1–6.

[17] I. Darwazeh, H. Ghannam, and T. Xu, "The First 15 Years of SEFDM: A Brief Survey," in *2018 11th International Symposium on Communication Systems, Networks Digital Signal Processing (CSNDSP)*, 2018.

[18] A. Pereira, P. Bento, M. Gomes, R. Dinis, and V. Silva, "MIMO Time-Interleaved Block Windowed Burst OFDM with Iterative Frequency Domain Equalization," in *2018 15th International Symposium on Wireless Communication Systems (ISWCS)*, Aug 2018, pp. 1–6.

[19] T.-D. Chiueh and P.-Y. Tsai, *OFDM Baseband Receiver Design for Wireless Communications*. Wiley Publishing, 2007.

[20] T. Rappaport, *Wireless Communications: Principles and Practice*, 2nd ed. Upper Saddle River, NJ, USA: Prentice Hall PTR, 2001.

[21] H. Zarrinkoub, *Understanding LTE with MATLAB: From Mathematical Modeling to Simulation and Prototyping*, 1st ed. Wiley Publishing, 2014.

[22] W. Stallings and C. Beard, *Wireless Communication Networks and Systems*. Pearson, 2016.

[23] M. Rice, *Digital Communications: A Discrete-time Approach*. Pearson/Prentice Hall, 2009.

[24] J. Anatory, N. Theethayi, R. Thottappillil, M. M. Kissaka, and N. H. Mvungi, "Broadband Power-Line Communications: The Channel Capacity Analysis," *IEEE Transactions on Power Delivery*, vol. 23, no. 1, pp. 164–170, Jan 2008.

[25] T. van Waterschoot, V. Le Nir, J. Duplicy, and M. Moonen, "Analytical Expressions for the Power Spectral Density of CP-OFDM and ZP-OFDM Signals," *IEEE Signal Processing Letters*, vol. 17, no. 4, pp. 371–374, April 2010.

[26] Y. Rahmatallah and S. Mohan, "Peak-To-Average Power Ratio Reduction in OFDM Systems: A Survey And Taxonomy," *IEEE Communications Surveys Tutorials*, vol. 15, no. 4, pp. 1567–1592, Fourth 2013.

[27] N. Souto, R. Dinis, A. Correia, and C. Reis, "Interference-Aware Iterative Block Decision Feedback Equalizer for Single-Carrier Transmission," *IEEE Transactions on Vehicular Technology*, vol. 64, no. 7, pp. 3316–3321, July 2015.

[28] N. Benvenuto, R. Dinis, D. Falconer, and S. Tomasin, "Single Carrier Modulation With Nonlinear Frequency Domain Equalization: An Idea Whose Time Has Come—Again," *Proceedings of the IEEE*, vol. 98, no. 1, pp. 69–96, Jan 2010.

[29] N. Benvenuto and S. Tomasin, "Iterative design and detection of a DFE in the frequency domain," *IEEE Transactions on Communications*, vol. 53, no. 11, pp. 1867–1875, Nov 2005.

[30] T. G. S. Fernandes, "Time-Interleaved BWB-OFDM with Iterative FDE," Master's thesis, Universidade de Coimbra, Coimbra, Portugal, 2015.

[31] R. Dinis, P. Montezuma, N. Souto, and J. Silva, "Iterative Frequency-Domain Equalization for general constellations," in *2010 IEEE Sarnoff Symposium*, April 2010, pp. 1–5.

[32] W. Ozan, K. Jamieson, and I. Darwazeh, "Truncating and oversampling OFDM signals in white Gaussian noise channels," in *2016 10th International Symposium on Communication Systems, Networks and Digital Signal Processing (CSNDSP)*, July 2016, pp. 1–6.

[33] J. Fan, S. Guo, X. Zhou, Y. Ren, G. Y. Li, and X. Chen, "Faster-Than-Nyquist Signaling: An Overview," *IEEE Access*, vol. 5, pp. 1925–1940, 2017.

[34] I. Kanaras, A. Chorti, M. R. D. Rodrigues, and I. Darwazeh, "Spectrally Efficient FDM Signals: Bandwidth Gain at the Expense of Receiver Complexity," in *2009 IEEE International Conference on Communications*, June 2009, pp. 1–6.

[35] T. Xu and I. Darwazeh, "Experimental Validations on Self Interference Cancelled Non-Orthogonal SEFDM Signals," in *2018 IEEE 87th Vehicular Technology Conference (VTC Spring)*, June 2018, pp. 1–5.

[36] T. A. Kumar, "A Robust Multiuser Detection Based Scheme for Crosstalk Mitigation in DMT VDSL with Non-Gaussian Noise," in *2009 International Conference on Signal Acquisition and Processing*, April 2009, pp. 234–238.

Appendix I

26º Seminário RTCM 24 January 2019, Coimbra Portugal

Testbed implementation of TIBWB-OFDM within LTE frame structure

Filipe Conceição(Univ. Coimbra - Portugal)
Marco Gomes (Univ. Coimbra - Portugal)
Vítor Silva (Univ. Coimbra - Portugal)

instituto de telecomunicações

Outline

- Introduction
- MIMO TIBWB-OFDM
  - TIBWB-OFDM Principle
  - MIMO TIBWB-OFDM
  - LTE Physical Layer
- Implementation
- Conclusions

Introduction

- 5G wireless networks must be able to meet the requirements imposed by the ever increasing demand in capacity, while guaranteeing robustness, reliability and spectral efficiency.

  - Multiple-Input Multiple-Output (MIMO)
  - New Spectral and Power Efficient Waveforms

Introduction

- MIMO employs **multiple antennas** at both the **transmitter** and **receiver**, meeting the **capacity requirement** and enabling significant performance improvements, namely in terms of **spectral efficiency** through **Spatial Multiplexing (SM)**.

- OFDM is a mature technique that allows an **efficient equalisation** and the removal of MIMO inter-stream interference, providing **spectral efficiency** and **robustness** against frequency selective fading.

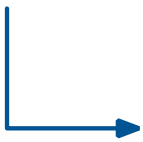

However, it comes with several **drawbacks:**

- Severe **out-of-band (OOB) radiation**
- **High peak-to-average power ratio (PAPR)**
- A **loss** in **spectral** and **power efficiency** (due to the use of the **cyclic prefix**)

Introduction

- Alternative OFDM-based techniques have been proposed to overcome the limitations imposed by OFDM, achieving a superior spectral efficiency.

  → Time-Interleaved Block Windowed Burst-OFDM (TIBWB-OFDM) (Sharing properties of OFDM-type and Block-based single carrier-type)

  - Low OOB emissions
  - Spectral and power efficiency
  - Easily combined with MIMO systems
  - Prompts the use of iterative frequency domain equalizers

MIMO TIBWB-OFDM
TIBWB-OFDM Waveform

- Hybrid Block Transmission Technique
  - **Transmitter side:** Windowed OFDM transmission
  - **Receiver Side:** Single carrier-type transmission with **SC-FDE (Single Carrier – Frequency Domain Equalization)**.
- **TIBWB-OFDM** packs together several **windowed small size OFDM-based blocks**, with a **zero padding (ZP)** guard interval appended at the end.

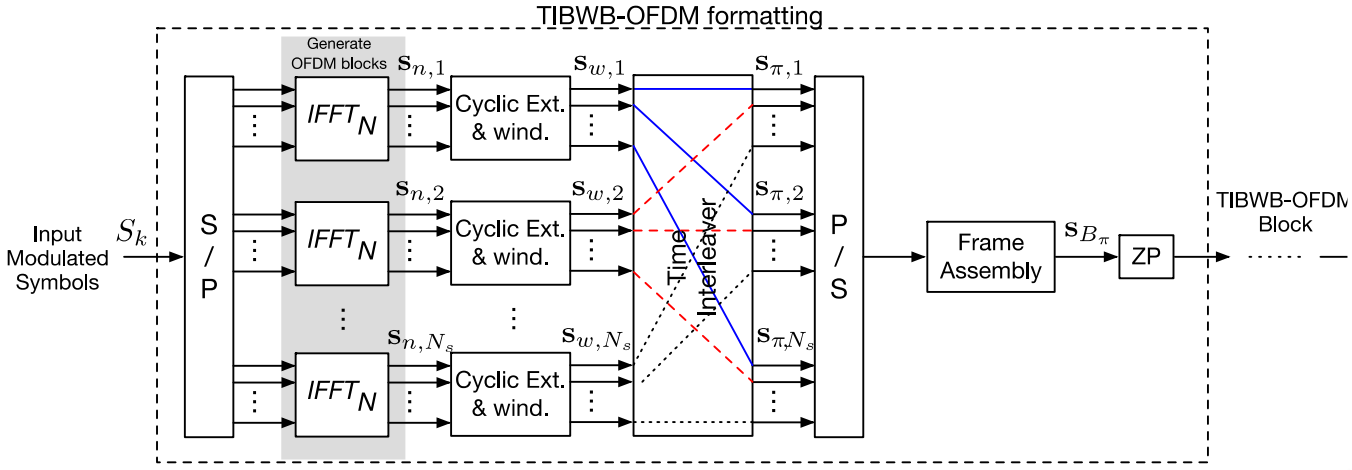

MIMO TIBWB-OFDM
TIBWB-OFDM Waveform

- Time domain square root raised cosine (SRRC) window profile
  --> superior spectrum confinement or higher data rate.
- Small size FFTs -> PAPR reduction
- Zero Padding -> Power efficiency

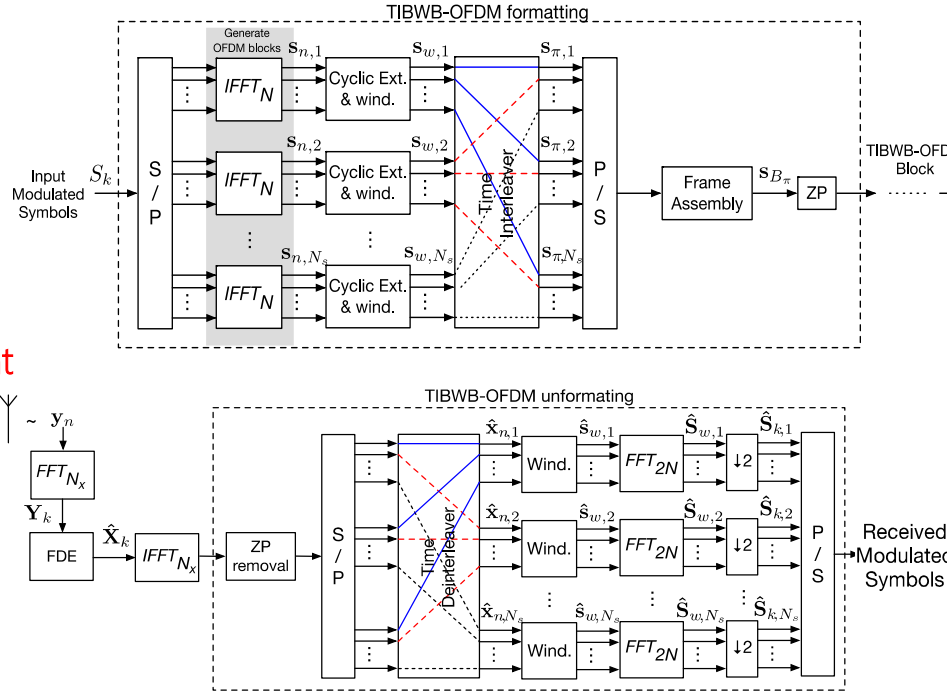

TIBWB-OFDM Block length:

$$N_x = N_s N(1+\beta) + N_{ZP}$$

Size of the windowed symbols $S_{w,i}$

TIBWB-OFDM Formatting	TIBWB-OFDM Unformatting
(i) Cyclic Extension & Windowing (ii) Time-Interleaving (iii) Frame Assembly & ZP	(i) ZP removal (ii) Time-Deinterleaving (iii) Matched filtering & Disassembly

MIMO TIBWB-OFDM
TIBWB-OFDM Waveform

The Time Interleaving Approach creates a sort of diversity effect in the frequency domain

- If the **spectral content** inside the deed fading region **is affected,** that **information is lost**

It is still possible to **recover part of it from the remaining unaffected regions** containing the same information.

- **Waveform** able to **deal with hostile channel conditions** (with deep fades of the frequency selective channel)

Signal spectrum of the transmitted block composed by three OFDM symbols

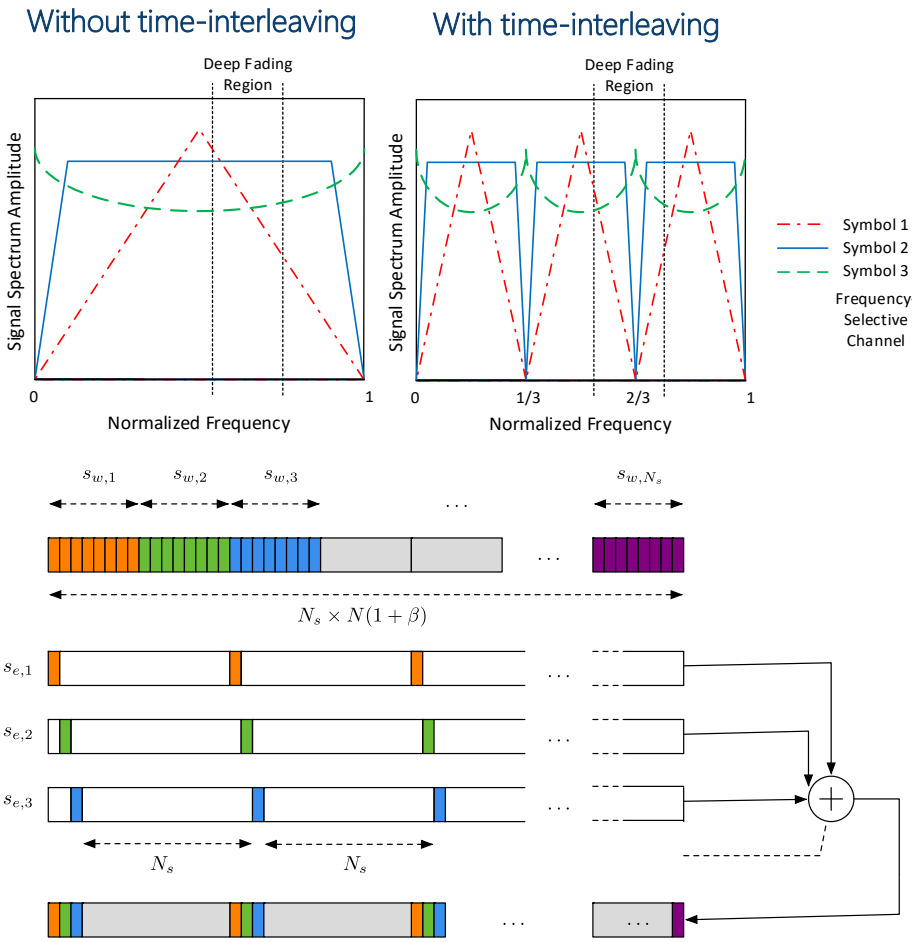

LTE Physical Layer
Allocation of Bandwidth

- Formed by the concatenation of **resource blocks.**
- Each **resource block** consists of 12 **subcarriers**.
- The **subcarriers** are separated by 15 kHz.
- Total bandwidth of a **resource block** is 180 kHz.
- Transmission bandwidth configurations from 6 to 110 resource blocks.
- Channel bandwidth ranging from 1.4 to 20 MHz.

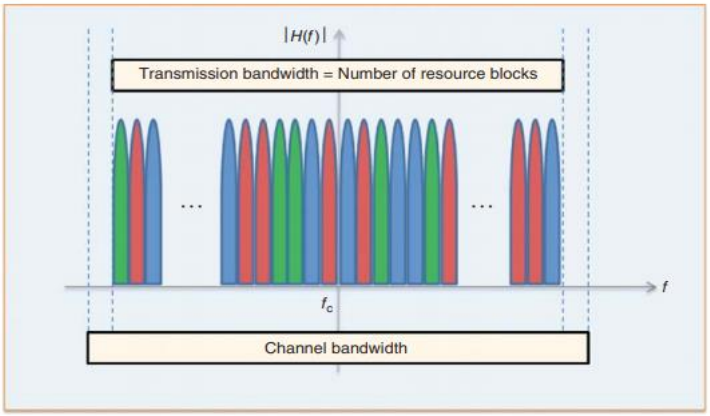

LTE Physical Layer
Time Framing

In the time domain, LTE organizes the transmission as a sequence of radio **frames of length 10 ms.**

Each frame is then subdivided into **10 subframes of length 1 ms.**

Each subframe is composed of two **slots of length 0.5 ms each.**

Each slot consists of a number of OFDM symbols, either 7 or 6, depending on whether a normal or extended cyclic prefix is used, resulting in **14 or 12 OFDM symbols per subframe**.

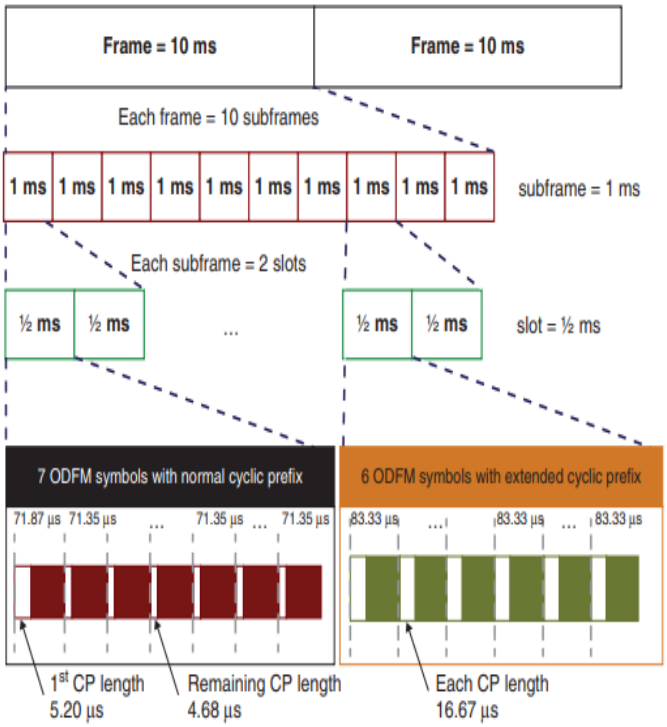

LTE Physical Layer
Time – Frequency Representation

There is an alternative way to represent the transmission of a LTE signal which consists of a time-frequency representation, called a **downlink resource grid**.

Each one of the modulated complex values, called **physical resource elements** is mapped on a time-frequency **resource grid,** in which the x-axis indicates the OFDM symbol to which it belongs in time and the y-axis represents the OFDM subcarrier to which it belongs in frequency.

One **resource element** is placed at the intersection of an OFDM symbol and a subcarrier.

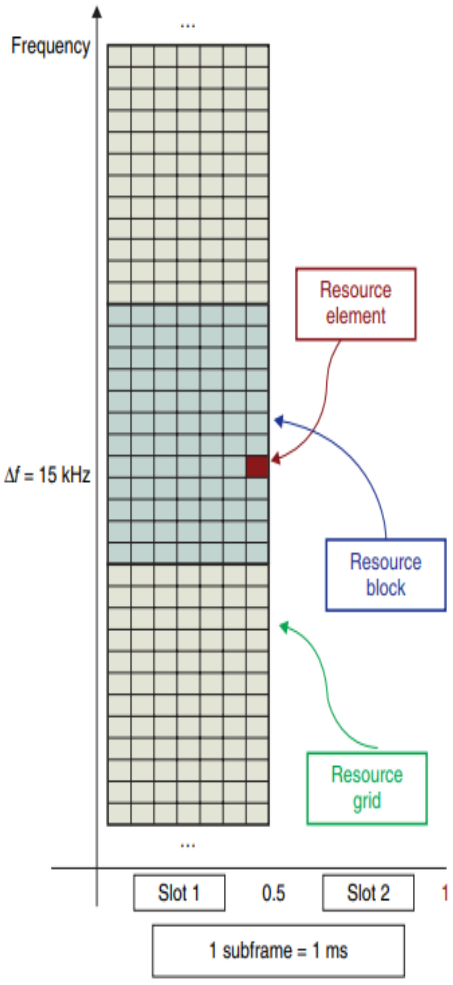

LTE Physical Layer
Resource Grid Content

Each **resource element** in the **resource grid** contains the modulated symbol of either user data, reference or synchronization signal or it can also contain control information originating from various higher-layer channels.

A variety of physical signals, including **reference and synchronization signals**, are transmitted in the shared physical channels. Physical signals are mapped to a specific **resource element** in the **resource grid**.

Downlink reference signals, such as the cell specific reference signals, support the channel estimation functionality needed to equalize and demodulate the control and data information.

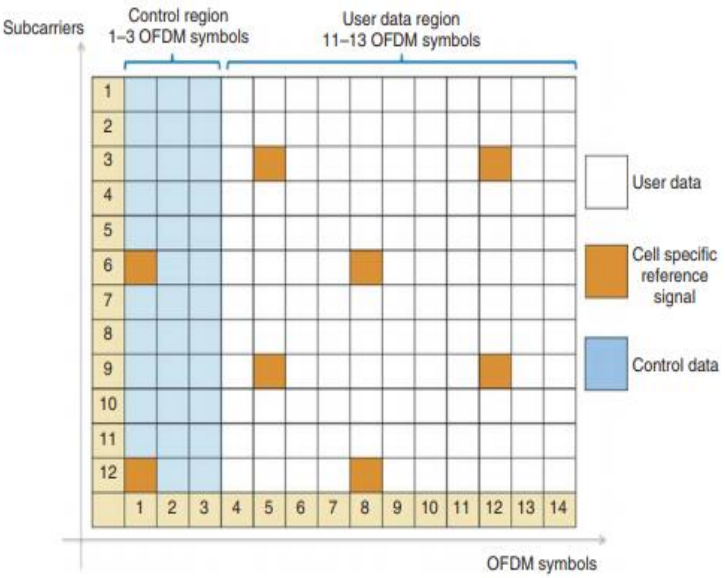

LTE Physical Layer
Resource Grid Content

PSCH (Primary Synchronization Channel)
SSCH (Secondary Synchronization Channel)
RS (cell-specific Reference Signal) for selected Tx antenna port

Downlink synchronization signals include the detection of frame boundaries, determination of the number of antennas, initial cell search, neighbor cell search and handover. Two synchronization signals are available in the LTE: the Primary Synchronization Signal (PSS) and the Secondary Synchronization Signal (SSS).

Both the PSS and the SSS are transmitted as 72 subcarriers located around the DC subcarrier.

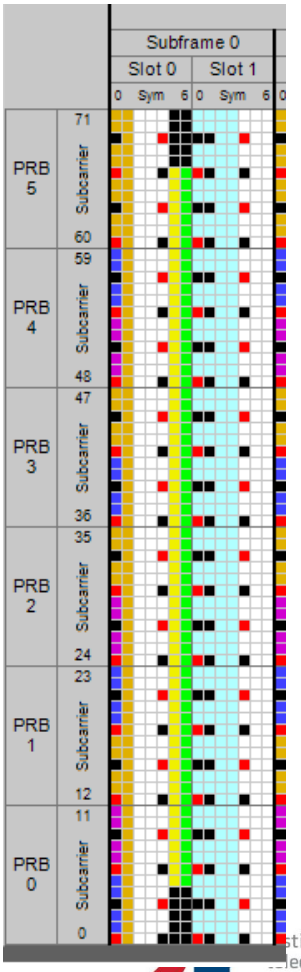

Implementation

- MIMO transmission with N_T=2 and N_R = 2.
- LTE signal:
  - 8 frames, 80 subframes, 160 slots
  - 1120 OFDM symbols
- OFDM symbols:
  - 6 resource blocks
  - Number of Useful Subcarriers N = 72
  - Number of FFT points NFFT = 128
  - Cyclic Prefix (CP) NCP = 10 for the first symbol in every slot and NCP = 9 for the remaining ones.
  - Quadrature Phase Shift Keying (QPSK) Modulation
- TI-BWB case:
  - N_s=4 OFDM-based blocks of size NFFT = 32 with only N = 18 useful subcarriers.
  - SRRC windowing with roll-off β=0.5
  - TI-BWB block length N_x = 2688 (N_{ZP} is included in the non-useful subcarriers)

Implementation

Power spectrum of an OFDM symbol transmitted in both the antennas.

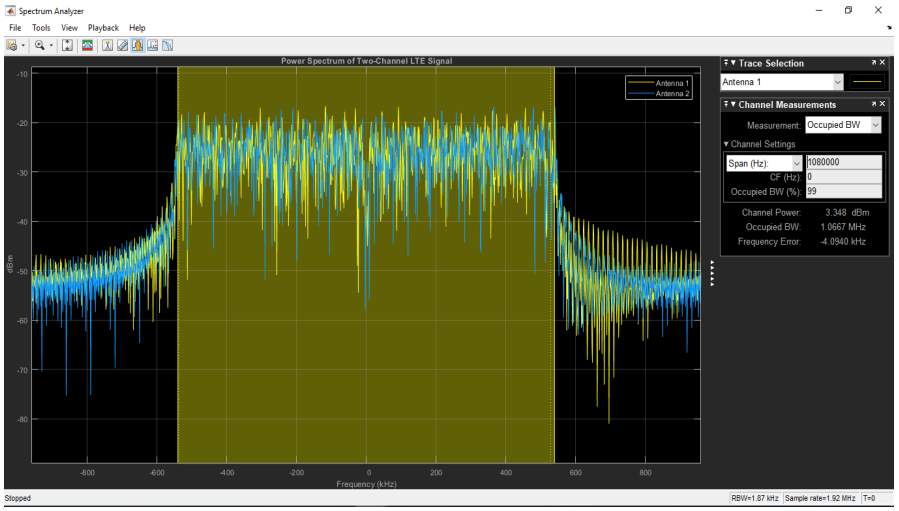

Power spectrum of the constructed TIBWB-OFDM symbol transmitted in both the antennas.

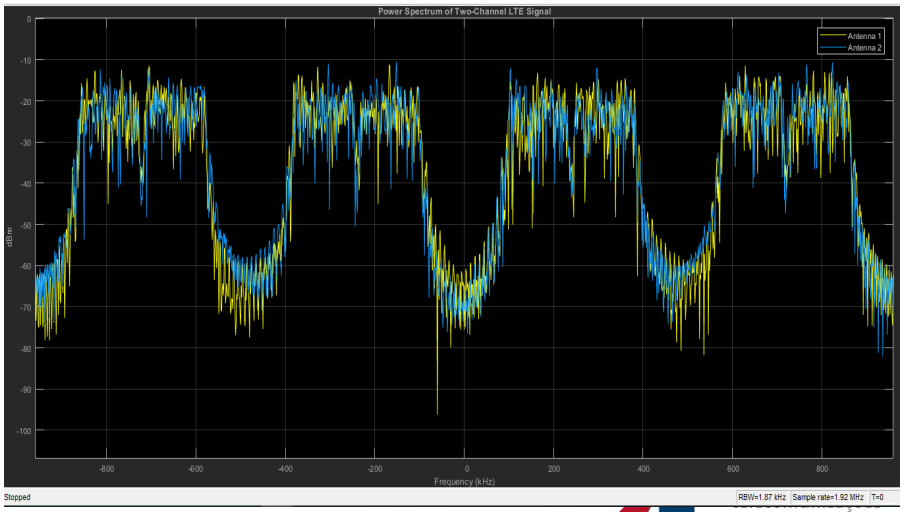

Implementation

It was necessary to maintain the same structure of the **resource grid** so that the receiver can receive and decode the information correctly.

In other words, the physical channels of the resource grid that carry the **reference and the synchronization physical signals must be sent on the pre-defined subcarriers relative to the original resource grid**, which is based on the transmission of conventional OFDM symbols.

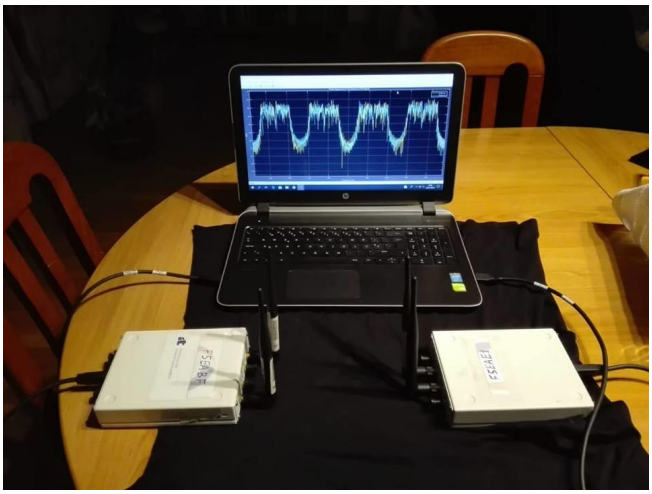

It was necessary to adapt the **process of constructing the TIBWB-OFDM symbols** based on the time-frequency representation of a LTE signal.

Implementation

Therefore, the first approach used in this work was the configuration **of the first 14 symbols sent in each frame, which represents the first subframe, as conventional OFDM symbols** and the **remaining ones as TIBWB-OFDM symbols.**

Also, note that TIBWB-OFDM symbols have a larger number of samples than the original OFDM symbols due to the application of the cyclic extension and windowing operations. Consequently, it was introduced a **zero pad in the conventional OFDM symbols** so that they appear with the same length as the TIBWB-OFDM symbols.

However, the new created frames are now 14 ms long, due to the process of constructing the TIBWB-OFDM symbols.

Implementation

In order to reduce the number of OFDM symbols needed for transmission, we reallocated the **resource elements** that represent the the cell-specific reference signals. This can be done because the black dots represent unused subcarriers.

With this approach we assume that only the **first symbol transmitted in each slot of the first subframe** needs to be an OFDM symbol. However, the **sixth and seventh symbols of the first slot must be OFDM symbols** because they carry the synchronization signals and therefore, it is necessary to maintain their structure.

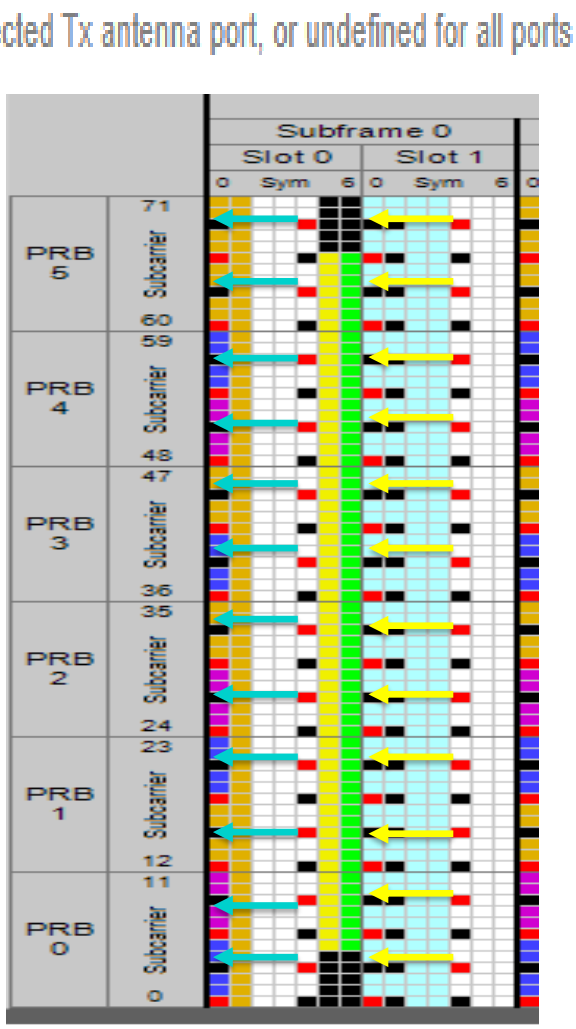

Conclusions

- TIBWB-OFDM presents always superior gains both in terms of power consumption and efficient spectral usage, when compared with OFDM. Additionally, it can easily be combined with MIMO systems.

- Nonetheless, the structure of a LTE signal and the way the information is organized in both time and frequency (resource grid) is not flexible enough to simply allow the replacement of the OFDM symbols by the TIBWB-OFDM symbols.

- Thus, would be interesting to study about the frame structure and the resource grid of the 5G New Radio in order to conclude if a better implementation of the proposed TIBWB-OFDM technique is possible.

INSTITUIÇÕES ASSOCIADAS

TÉCNICO LISBOA

universidade de aveiro

U C

Universidade de Coimbra

PT Inovação

nsn Nokia Solutions Network

UNIVERSIDADE DA BEIRA INTERIOR
Covilhã | Portugal

U.PORTO

ISCTE IUL
Instituto Universitário de Lisboa

IPL
instituto politécnico de leiria

Thank you!

Filipe Conceição

Kindly supported by:

FCT
Fundação para a Ciência e a Tecnologia
MINISTÉRIO DA CIÊNCIA, TECNOLOGIA E ENSINO SUPERIOR

UID/EEA/50008/2013

instituto de telecomunicações

B

Appendix II

Time Overlapping TIBWB-OFDM Symbols for Peak-To-Average Power Ratio Reduction

Filipe Conceição[1,3], Marco Gomes[1], Vítor Silva[1] and Rui Dinis[2]
1 Instituto de Telecomunicações and Department of Electrical and Computer Engineering,
University of Coimbra, 3030-290 Coimbra, Portugal
2 Instituto de Telecomunicações and FCT-UNL, 2829-512 Caparica, Portugal
3 filipe.conceicao@co.it.pt

***Abstract*—The Time-Interleaved Block Windowed Burst Orthogonal Frequency Division Multiplexing (TIBWB-OFDM) waveform enables to achieve greater confinement in the signal spectrum that improves with the increase of the window roll-off since the out-of-band (OOB) radiation drops. However, the TIBWB-OFDM block length grows temporarily, which corresponds to a decrease of the transmission rate, limiting the increase in the spectral efficiency of the system. Furthermore, the windowing operation is responsible for the reduction in the average power of the signal, which, in turn, depends on the value of the window roll-off. As a consequence, the Peak-to-Average Power Ratio (PAPR) of the TIBWB-OFDM signal tends to grow as the roll-off increases. Therefore, this work proposes an alternative method concerning the TIBWB-OFDM symbol construction by allowing a partial overlap between adjacent windowed OFDM symbols in order to reduce PAPR.**

***Index Terms*—TIBWB-OFDM, PAPR, Overlapped-TIBWB-OFDM, spectral efficiency**

I. Introduction

Future wireless communications systems are expected to bring improvements in the way data are transmitted and the waveforms are designed. Such improvements are related to higher data rate, lower latency, and flexibility brought by the need to transmit over hostile channel conditions, as well as higher spectral and power efficiency [1]. Orthogonal Frequency Division Multiplexing (OFDM) [2] has been, since the 3rd generation (3G) of wireless communications, the preferred waveform of choice, due to its robustness to inter-symbol interference (ISI) associated with multipath channels. OFDM is a multicarrier technique that divides a high data rate stream into N parallel lower rate streams that, in turn, modulate N subcarriers. The process of OFDM modulation and demodulation can be efficiently implemented by the inverse fast Fourier transform (IFFT) operation and its reverse, the fast Fourier transform (FFT), respectively. The orthogonality between subcarriers is one of the main features of OFDM because it denies any inter-carrier interference (ICI) and allows a simple frequency domain equalization (FDE) [3]. The portion of the spectrum occupied by each stream is usually less than the coherence bandwidth of the frequency selective channel (also known as a time dispersive channel) and, therefore, the ISI in each stream is neglected. In order to eliminate interference between the N symbol streams, it is necessary to add a cyclic prefix (CP) to each OFDM symbol, which must be longer than the duration of the impulse response of the transmission channel. The CP duration often represents 10% to 25% of the OFDM symbol period, and therefore the effective throughput of useful data and the spectral efficiency of CP-OFDM systems are reduced [3],[4]. In fact, in order for a CP-OFDM system to achieve the same transmission rate of an OFDM system (without CP) the transmission rate of the useful data must be increased, which in turn increases the amount of spectrum used. In addition, due to the power wasted on CP transmission, the power efficiency of CP-OFDM transceivers is decreased [4].

Besides the restricted spectral efficiency, time domain transmitted signals in an OFDM system can have high peak values since the instantaneous amplitude of each sub-carrier that form the OFDM symbol is added by the IFFT operation. As a consequence, OFDM systems are known to have a high peak-to-average power ratio (PAPR) when compared to single-carrier systems, which grows with an increasing number of sub-carriers. Thus, an OFDM system has a limited power efficiency and requires the use of a power amplifier with a considerable back-off to ensure a distortion-free linear signal amplification [3],[4].

Thus, the development of new techniques as alternatives to OFDM, with greater spectral and power efficiency, has been the subject of many recent studies [5],[6], with several techniques being proposed as: filter-bank multicarrier [7]; generalized frequency division multiplexing (GFDM) [8]; filtered-OFDM [9]; the non-orthogonal multicarrier system termed spectrally efficient frequency division multiplexing (SEFDM) [10], which improves spectral efficiency by packing subcarriers at frequency spacing below the symbol rate, intentionally creating inter-carrier interference (ICI); and more recently the Time-Interleaved Block Windowed Burst Orthogonal Frequency Division Multiplexing (TIBWB-OFDM) technique [4].

Although the spectral confinement of the TIBWB-OFDM blocks improves with the increase of the window roll-off, since the out of band (OOB) radiation drops, the size of the TIBWB-OFDM blocks grows temporarily, which corresponds to a decrease of the transmission rate, limiting the increase in the spectral efficiency of the system. Furthermore, conclusions drawn from this work are that the windowing operation is responsible for the decrease in the average power of the signal, which, in turn, depends on the value used for the roll-off. As a

consequence, the PAPR of the TIBWB-OFDM signal tends to grow as the roll-off increases. Therefore, this work proposes an alternative method with respect to the TIBWB-OFDM symbol construction by allowing a partial overlap between adjacent windowed OFDM symbols, in the time domain. For that, it is necessary to develop equalization algorithms in the receivers capable of overriding the self-created interference resulting from this process. This new waveform would allow achieving an increased spectral efficiency since there is no temporal expansion of the signal. Furthermore, the overlapping operation diminishes the windowing attenuation effect and opposes the decrease in the average signal power. In this paper, Section II presents the TIBWB-OFDM waveform concept. Then, Section III presents the PAPR concept and describes the PAPR issues related to TIBWB-OFDM. Section IV describes the process of generating the new Overlapped-TIBWB-OFDM waveform. Section V presents the main results and finally Section VI concludes the paper.

II. TIBWB-OFDM WAVEFORM

The TIBWB-OFDM transmitter is built on the Block Windowed Burst Orthogonal Frequency Division Multiplexing (BWB-OFDM) transmitter [11], which grants greater confinement in the signal spectrum, and thus, increases the spectral efficiency by converting the OFDM symbols to BWB-OFDM symbols. The OFDM symbols are sequentially cyclically extended and windowed, in the time-domain, through a non-rectangular, roll-off dependent window (Square Root Raised Cosine - SRRC window). This process is responsible for the reduction of the OOB radiation, typically observed in OFDM systems. Each one of those windowed OFDM symbols is extended to $N_{sym} = N(1+\beta)$ samples after discarding the tailing zeros from the windowing operation in the time domain, where β represents the window roll-off. In this waveform, N_s windowed OFDM symbols or blocks are packed together and are added a single zero-pad (ZP) of length N_z, in order to deal with the multipath channel's propagation delay, thereby improving power efficiency [11]. A BWB-OFDM mega-block, s_B, can be described as a sum of juxtaposed windowed OFDM symbols, $s_{w,k}, k = 1, \ldots, N_s$, with a delay proportional to N_{sym} and can be written as:

$$s_B[n] = \sum_{k=0}^{N_s-1} s_{w,k}[n - kN_{sym}] \tag{1}$$

Hence, a BWB-OFDM mega-block has a total length of $N_x = N_s N(1+\beta) + N_z$. Moreover, since the CP attached to each transmitted symbol is eliminated, the BWB-OFDM can either achieve higher transmission rates than CP-OFDM schemes while maintaining the same spectrum or achieve better spectrum confinement maintaining the same data rate [11].

The Time-Interleaved BWB-OFDM (TIBWB-OFDM) [3],[4] technique allows the signal to be resilient against deep inband fades by compressing and replicating the original spectrum of the BWB-OFDM block in the allocated bandwidth. Fig. 1 presents the process of creating the TIBWB-OFDM mega-block. This technique generates the TIBWB-OFDM symbols by performing interleaving on the time samples of each BWB-OFDM block (from a total of N_s), which creates a diversity effect at the frequency domain, granting much better robustness against inband deep-fades [3].

III. PAPR ANALYSIS

The PAPR of a continuous-time domain signal, $x(t)$, is expressed by

$$PAPR(x(t)) = 10log_{10}(\frac{max[x(t)x^*(t)]}{E[x(t)x^*(t)]})\ [dB] \tag{2}$$

where $x^*(t)$ corresponds to the conjugate of $x(t)$. In order to maintain the orthogonality, an OFDM symbol with a rectangular configuration, $s[n], n = 0, \ldots, N-1$, is generated as a sum of N modulated sub-carriers, equally spaced in frequency by the inverse of the symbol period, i.e. $\Delta f = \frac{1}{T_s}$, where T_s represents the OFDM symbol period [12]. The discrete-time version of this signal can be expressed by

$$s[n] = \sum_{k=0}^{N-1} S_k w[n] e^{\frac{j2\pi kn}{N}} \tag{3}$$

where S_k represents a symbol from an M-ary constellation and $w[n]$ is a rectangular window.

If we assume $S_k = 1$ for any k, the peak power value of the signal is $max[s[n]s^*[n]] = N^2$ and the mean square value of the signal is $E[s[n]s^*[n]] = N$. For that reason, the maximum PAPR value for an OFDM symbol with N sub-carriers occurs when each sub-carrier is modulated with the same constellation symbol and is equal to N. The most common method to evaluate the symbol-based PAPR of a transmitted signal is to obtain its Complementary Cumulative Distribution Function (CCDF). In this case this function provides an indication of the probability of that signal's envelope exceeding a certain PAPR threshold [12] and can be expressed by:

$$CCDF(PAPR(s[n])) = Prob\{PAPR(s[n]) > \delta\} \tag{4}$$

where $PAPR(s[n])$ is the PAPR of the OFDM symbol and δ is a PAPR threshold. Therefore, the probability of attaining the maximum PAPR value is very low, since the modulated data is random and uncorrelated. However, it can be concluded that the PAPR of an OFDM signal tends to grow when the number of sub-carriers, N, increases. Intuitively, by making use of smaller size FFTs (equivalent to the number of sub-carriers, N), a reduction on PAPR can be accomplished [4].

If we consider an OFDM symbol with the same length as a TIBWB-OFDM mega-block discarding the ZP, that is $N_{OFDM} = N_x - N_z = N_s N(1+\beta) = N_s N_{sym}$, one could expect to get a higher PAPR than the TIBWB-OFDM transmitted signal since the IFFT operation is performed with a larger number of points. However, this might not be true owing to the windowing operation. This operation consists of a point-wise time domain product between the selected window

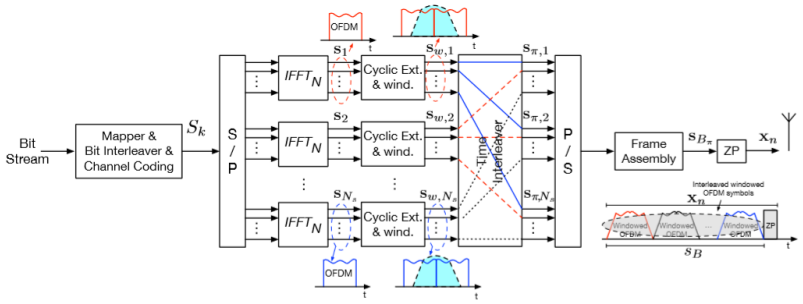

Fig. 1. TIBWB-OFDM mega-block construction [3],[4].

and the cyclically extended OFDM symbol. The window employed corresponds to an SRRC, which is equivalent to a rectangular window when the roll-off is equal to 0. In this case, the PAPR of the TIBWB-OFDM signal is, indeed, reduced, because the window has no effect in regard to the temporal amplitude of the signal. In other words, the window does not affect the average power, neither the maximum power of the signal since the TIBWB-OFDM symbol simply consists of N_s OFDM symbols, each one having N sub-carriers. Hence, by employing smaller size FFTs, the probability of getting a high PAPR lessens. Nevertheless, this situation is not optimal taking into consideration that by using a rectangular window there is no spectral confinement and, therefore, the spectral efficiency is not improved. In fact, in this particular case, the spectrum of the transmitted signal simply consists of a superimpose spectrum of all N_s OFDM symbols and, as a consequence, will have the same drawbacks of OFDM concerning spectrum leakage that can cause inter-channel interference [11].

IV. Overlapped-TIBWB-OFDM

The way this new waveform is created is based on the operations performed on the BWB/TIBWB-OFDM transmitters [11],[4], followed by an overlapping procedure. First, the coded and bit-interleaved bitstream is mapped onto symbols originating from an M-ary constellation, which are loaded onto N_s sets of sub-carriers, $n_k = 0, ..., N-1$ where $k = 1, \ldots, N_s$, according to (3). Afterwards, the BWB-OFDM mega-block is obtained according to (1). At this point, the overlapping operation is applied. Each one of those cyclic extended and windowed OFDM symbols, $s_{w,k}, k = 1, \ldots, N_s$, is overlapped with the adjacent symbols, that is, the last samples of the current symbol are added, in the time domain, with the first samples of the next symbol. The new overlapped symbol can be expressed by

$$s_{OB}[n] = \sum_{k=0}^{N_s-1} s_{w,k}[n - kN_{start}] \tag{5}$$

where $N_{start} \leq N_{sym}$ represents the first overlapped sample from the block.

Fig. 2 presents the concept of the overlapping operation between adjacent symbols.

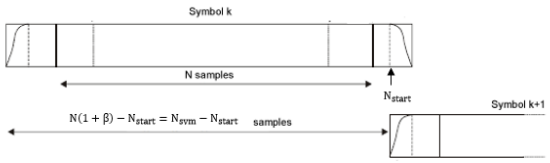

Fig. 2. BWB-OFDM mega-block with overlapped symbols.

The spectrum of (5) can be expressed as

$$S_{OB}(e^{jw}) = \sum_{k=0}^{N_s-1} S_{w,k}(e^{jw}) e^{-jwkN_{start}} \tag{6}$$

Therefore, if we consider the same spectrum usage, this waveform allows to transmit with a higher rate and the power spectrum of the new Overlapped-BWB-OFDM mega-block is similar to the non-overlapped one, since it contains the superimposition of the spectrum of each windowed OFDM symbol.

This way, the new waveform has intentionally introduced interference between the N_s blocks that shape the BWB-OFDM mega-block and, thus, the number of transmitted samples is reduced to $N_x = N_{start}(N_s - 1) + N_{sym}$. The number of overlapped samples, N_{os} is dynamic and can be regulated through $N_{os} = N_{sym} - N_{start}$. If we considered a BWB-OFDM mega-block with $N = 64$, $N_s = 4$, $\beta = 0.5$ and $N_{start} = 64$, the length of the transmitted signal reduces from $N_x = NN_s(1 + \beta) = 384$ (in the TIBWB-OFDM case) to $N_x = 288$ samples. Since we are transmitting the same data in less time, this allows an improvement of the spectral efficiency when compared to the Non-Overlapped BWB-OFDM scenario.

Furthermore, the overlapping operation creates a flatter waveform with fewer transitions, reducing the time domain window effect and, thus, opposing the decrease the average signal power and, consequently, reducing the PAPR. In this case, to generate the TIBWB-OFDM mega-block it is necessary to inquire about what is the factor used in the time-interleave operation, since in this case, the signal length may not be multiple of the number of blocks, N_s. Therefore, in order to maintain the advantages created by this technique, with respect to its robustness in time dispersive channels, the number of blocks and N_{start} must be chosen accordingly.

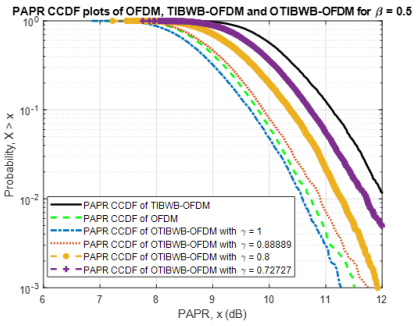

Fig. 3. PAPR's CCDF of the OFDM, TIBWB-OFDM and Overlapped-TIBWB-OFDM transmitted signals for $\beta = 0.5$.

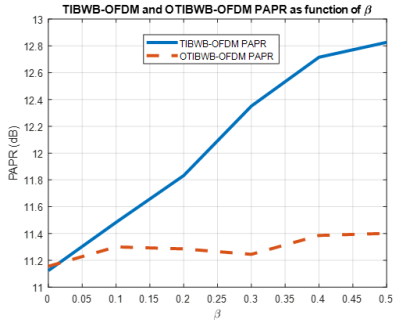

Fig. 4. PAPR of TIBWB-OFDM and Overlapped-TIBWB-OFDM for which the value of its $CCDF = 10^{-3}$ as function of the window roll-off, β.

V. Simulation Results

The following simulations aim to compare the PAPR of the TIBWB-OFDM waveforms with and without the symbol overlap operation, as a function of the amount of overlapping samples, which depends on N_{start}, and the window roll-off, β. In addition, the PAPR of an OFDM signal with the same length as the Non-Overlapped-TIBWB-OFDM, that is, $N_{OFDM} = NN_s(1+\beta)$, was calculated. In all the simulations it was considered $N = 64$ sub-carriers, $N_s = 16$ blocks and 4-QPSK modulation under a Gray coding rule.

By keeping the window roll-off set at $\beta = 0.5$ and by varying the amount of overlapping samples between adjacent symbols, N_{start}, the PAPR's CCDF of the OFDM, Non-Overlapped-TIBWB-OFDM and Overlapped-TIBWB-OFDM transmitted signals were plotted for different values of N_{start}.

As illustrated by Fig. 3, it can be concluded that by introducing the overlap operation, the new waveform has lower PAPR values compared to the non-overlapped waveform, since $\gamma = \frac{N}{N_{start}}$ represents the ratio between the number of sub-carriers, N, and the first overlapped sample, N_{start}. In addition, the PAPR decreases with increasing amount of overlapping samples, i.e., lowering N_{start}.

Alternatively, by keeping N_{start} fixed at $N_{start} = 64$, i.e., $\gamma = 1$, and by changing the window roll-off, β, the PAPR of the Non-Overlapped-TIBWB-OFDM and Overlapped-TIBWB-OFDM transmitted signals, for which its $CCDF = 10^{-3}$, were plotted for different values of β.

Fig. 4 show that the PAPR values are almost independent of the window roll-off for the overlapped waveform whereas the PAPR values of the non-overlapped waveform tend to grow with increasing roll-off.

VI. Conclusions

In this paper, a modified version of the TIBWB-OFDM signal is proposed by overlapping the adjacent sub-symbols that compose the signal, in the time domain. This new waveform eases deterioration in the PAPR of the signal produced by the TIBWB-OFDM transmitter. This is done through an overlapping operation since it attenuates the effect of the windowing operation on the calculation of this parameter, at the expense of introducing interference between the data sent by consecutive sub-symbols.

VII. Acknowledgment

This work is funded by FCT/MEC through national funds and when applicable co-funded by European Regional Development Fund (FEDER), the Competitiveness and Internationalization Operational Programme (COMPETE 2020) and Regional Operational Program of Lisbon and Financial Support National Public (FCT)(OE), under the projects UID/EEA/50008/2019 and MASSIVE5G (POCI-01-0145-FEDER-030588).

References

[1] P. Demestichas, A. Georgakopoulos, D. Karvounas, K. Tsagkaris,V. Stavroulaki, J. Lu, C. Xiong, and J. Yao, "5G on the horizon:key challenges for the radio-access network," Vehicular Technology Magazine, IEEE, vol. 8, no. 3, pp. 47–53, 2013.

[2] R.v. Nee, R. Prasad, OFDM for Wireless Multimedia Communications, Artech House, Inc., 2000.

[3] T. Fernandes, A. Pereira, M. Gomes, V. Silva, and R. Dinis, "A new hybrid multicarrier transmission technique with iterative frequency domain detection," Physical Communication, vol. 27, pp. 7–16, 2018.

[4] T. Fernandes, M. Gomes, V. Silva and R. Dinis, "Time-Interleaved Block-Windowed Burst OFDM," 2016 IEEE 84th Vehicular Technology Conference (VTC-Fall), Montreal, QC, 2016, pp. 1-5.

[5] X. Zhang, L. Chen, J. Qiu and J. Abdoli, "On the Waveform for 5G," in IEEE Communications Magazine, vol. 54, no. 11, pp. 74-80, November 2016.

[6] A. A. Zaidi et al., "A Preliminary Study on Waveform Candidates for 5G Mobile Radio Communications above 6 GHz," 2016 IEEE 83rd Vehicular Technology Conference (VTC Spring), Nanjing, 2016, pp. 1-6.

[7] F. Schaich, "Filterbank based multi carrier transmission (FBMC) — evolving OFDM: FBMC in the context of WiMAX," 2010 European Wireless Conference (EW), Lucca, 2010, pp. 1051-1058.

[8] G. Fettweis, M. Krondorf and S. Bittner, "GFDM - Generalized Frequency Division Multiplexing," VTC Spring 2009 - IEEE 69th Vehicular Technology Conference, Barcelona, 2009, pp. 1-4.

[9] X. Zhang, M. Jia, L. Chen, J. Ma and J. Qiu, "Filtered-OFDM - Enabler for Flexible Waveform in the 5th Generation Cellular Networks," 2015 IEEE Global Communications Conference (GLOBECOM), San Diego, CA, 2015, pp. 1-6.

[10] I. Kanaras, A. Chorti, M. R. D. Rodrigues and I. Darwazeh, "Spectrally Efficient FDM Signals: Bandwidth Gain at the Expense of Receiver Complexity,". Communications, 2009. ICC '09. IEEE International Conference on, Dresden, 2009, pp. 1-6.

[11] J. Nunes, P. Bento, M. Gomes, R. Dinis, and V. Silva, "Block-windowed burst OFDM: a high-efficiency multicarrier technique," Electronics Letters, vol. 50, no. 23, pp. 1757–1759, 2014.

[12] Y. Rahmatallah and S. Mohan, "Peak-To-Average Power Ratio Reduction in OFDM Systems: A Survey And Taxonomy," IEEE Communications Surveys Tutorials, vol. 15, no. 4, pp. 1567–1592, Fourth 2013.